REVISITING THE DENDROCLIMATOLOGICAL POTENTIAL OF AFROCARPUS FALCATUS, SOUTH AFRICA

Jean Baverstock

Submitted in fulfilment of the academic requirements for the degree of Master of Science in the Discipline of Environmental Science, School of Agricultural, Earth and Environmental Sciences, University of KwaZulu-Natal, Pietermaritzburg

4 February 2021

Preface

The experimental work described in this research thesis was carried out in the School of Agricultural, Earth and Environmental Sciences, University of KwaZulu-Natal, Pietermaritzburg from July 2015 to January 2021, under supervision of Prof. T.R. Hill, Dr. J.M. Finch and Prof. S. Woodborne.

The Studies represent the original work of the author and have not otherwise been submitted in any form of degree or diploma to any other University. Where use has been made of the work of others it is duly acknowledged in the text.

J Baverstock (candidate)

Prof. T.R. Hill

Dr. J.M. Finch

Prof. S. Woodborne

Frontispiece

The Natal Museum *Afrocarpus falcatus* specimen and modern trees from Karkloof, KwaZulu-Natal

Abstract

The long-lived evergreen conifer *Afrocarpus falcatus* has been shown to have dendrochronological potential, however, complex tree-ring structures have hampered further research on the species. Hall (1976) produced a classic South African tree-ring width-based rainfall record using an *Afrocarpus falcatus* museum specimen from the Karkloof Forest in KwaZulu-Natal, South Africa. Despite wide application of this palaeoclimate rainfall record, the dendroclimatological potential of this species has yet to be fully explored, nor has the associated climate environmental forcing been validated. The aim of this research was to investigate tree-growth climate relationships and to develop a modern analogue for *Afrocarpus falcatus* in the Karkloof Forests. Twenty trees were sampled from the Karkloof Forests, but due to ring-width eccentricity, only a limited number could be used to develop a ring-width and ring stable carbon isotope based mean chronology using classical methods. When tested against instrumental climate records, temperature, not rainfall, was found to be the most important variable driving tree growth. Ring $\delta^{13}C$ series were shown to be unaffected by compression and ring-width eccentricity, requiring a much smaller sample size than the ring-width analysis. Where annual rings can be correctly identified, and an adequate number of samples crossdated, ring $\delta^{13}C$ series of *Afrocarpus falcatus* can potentially provide a reliable proxy for temperature. Dendroclimatological studies of *Afrocarpus falcatus* therefore have the potential to make an important contribution in a region where reliable palaeoclimate records are limited.

Keywords *Afrocarpus falcatus;* dendroclimatology; dendrochronology; tree-ring width; carbon isotopes; South Africa

Acknowledgements

Thank you to the Department of Agriculture, Forestry and Fisheries for permission to core *Afrocarpus falcatus.*

I am very grateful to Mbona Private Nature Reserve for permission to core in the Reserve, and for your interest in this project.

Thank you, Edward Naidoo, of UCL Company (Pty) Ltd for arranging permission and access to 'The Forest', and your rainfall data.

I am also grateful to Dr. Hylton Adie for help to identify *Afrocarpus falcatus*.

To the late Pierre Olivier of Mbona who loved wood - thank you for your help with making my wooden core mounts and with the core polishing. I was so lucky to have had such skilled input right there in the forest. You would have been eager to learn the results of this thesis.

I am grateful to Dr. Grant Hall from the Mammal Research Institute, University of Pretoria, for teaching me the techniques of cellulose extraction from wholewood and to Prof. Stephan Woodborne from iThemba Labs for coordinating the carbon isotope ratio analysis.

Thank you to the National Research Foundation for the 2015 bursary funding.

Thanks Mark Horan of UKZN for the climate data used in this thesis.

To Brice Gijsbertsen, thank you for sharing your cartographic expertise (as well as your carpentry skills).

Thank you to my supervisors Prof. Trevor Hill, Dr. Jemma Finch and Prof. Stephan Woodborne for your support in the field, your coaching, guidance, and constant kind encouragement throughout!

This research was undertaken on a part time basis while I was working full time and therefore, I would like to give a special thank you to my family for putting up with my long absence from regular family life.

Finally, thank you Thandi Mtolo for your support at home, without which this research would not have been possible.

Table of Contents

List of Tables

List of Figures

List of Acronyms

American National Standards Institute (ANSI)

Auto Regression (AR)

Atmospheric correction (atm)

Auto regressive standardisation (ARSTAN)

Correlation Coefficient (CorrC)

Crossdate program (COFECHA)

Diameter at Breast Height (DBH)

Express Population Signal (EPS)

Intergovernmental Panel Climate Change (IPCC)

International Tree-Ring Data Bank (ITRDB)

Intrinsic Water Use (IWU)

Mean Inter series Correlation Value (R-BAR)

Measurement (MSMT)

Mean Sample Segment Length (MSSL)

Precipitation 0Evaporation (P-E)

Standard Deviation (SD)

Stable Isotopes (SI)

Subsample Signal Strength (SSS)

Signal (Climate) to Noise Ratio (SNR)

Student's' t Test (TTEST)

Tree-Ring Widths (TRW)

Vienna Pee Dee Belemnite (VPDB)

Regional Curve Standardisation (RCS)

List of Species

Afrocarpus falcatus

Adansonia digitata L.

Breonadia salicina

Mimusops caffra

Podocarpus latifolius

Widdringtonia cedarbergensis

CHAPTER 1: INTRODUCTION

The current global climate change crisis is not a single hemispheric concern and the limited understanding of the southern hemisphere's past climate is a serious drawback for global climate models (Villalba, 2000). The planning and execution of resource deployment to mitigate the effects of climate change relies, among other factors, strongly on the Intergovernmental Project on Climate Change (IPCC) future climate projections. The research work being undertaken by climate modelling groups forms the basis of the IPCC (IPCC, 2013). Climate projections rely on a long-term understanding of the climate system to help build and validate models, and these data can only be derived from the field of palaeoclimatology. Palaeoclimatologists, in turn, rely on environmental proxy measurements derived from natural archives that extend beyond the timescales of meteorological recordings. These environmental proxies include glaciological (ice cores), geological (marine sediments), biological (pollen, tree rings, corals) and historical sources (written records and phenological records) (Bradley, 2015). In dendrochronology annual growth rings are assigned calendar years (Fritts, 1976). Chronological variations in tree- ring widths are a valuable source of climatic information used by dendroclimatologists to investigate present and past climates (Hughes, 2002). Tree-ring proxies have been shown to yield continuous, annually resolved climate reconstructions (Jones et al., 2009). High-resolution tree-ring chronologies continue to contribute significantly to the IPCC Working Group I (Physical Science Basis) assessments, although, at a regional scale, proxy-based climate reconstruction is still limited from many parts of the world, including Africa (Bradley, 2015; Gebrekirstos et al., 2014; Hughes, 2002; Jones et al., 2009; Martinelli, 2004; Villalba, 2000).

Complicated tree-ring structures of tropical and subtropical trees obstructed the earlier development of dendroclimatic research on the African continent (Gebrekirstos et al., 2014). At first, the lack of seasonal growing cycles in tropical trees prohibited the application of classical dendroclimatology methods for climate reconstruction (Gebrekirstos et al., 2014). Technological advancement and the development of new methods to detect seasonal variation in tree rings (e.g. dendrometer measurements and intra-annual stable isotope ratio measurements) are being used to overcome the initial problem of tropical non-distinct anatomical ring boundaries (Gebrekirstos et al., 2014; Pearl et al., 2020). In subtropical South Africa, warm temperate conditions are experienced with distinct seasons. Dendroclimatology investigations started up in the late 1970's on long-lived tree species (between 500 and 1000 years would be considered long-lived in South Africa) using *Afrocarpus falcatus, Podocarpus latifolius* and *Widdringtonia cedarbergensis.* Classical methods were employed to analyse ring widths from these two species, but with low success (Curtis et al., 1978; February and Stock, 1999, 1998; McNaughton and Tyson, 1979). That there is only one tree-ring width study (Die

Bos *Widdringtonia cedarbergensis*; Dunwiddie and LaMarche, 1980) from South Africa in the open access International Tree-Ring Data Bank (ITRDB) (https://www.ncdc.noaa.gov/data-access/paleoclimatology-data/datasets/tree-ring) confirms this. February and Stock (1998) strongly discouraged further research on *Podocarpus* in South Africa because of complicated tree-ring width structure and missing tree-rings which could only be identified through complete cross-section analysis. Incremental coring on *Podocarpus* was thus believed to be an impossible sampling strategy and has never been done for a tree-ring width dendroclimatic study in South Africa. More recently, stable isotope (SI) tree-ring studies in South Africa have had more success because the trees sampled grew in open-canopy environments and had less complicated tree-ring structures. Two separate *Adansonia digitata L*. tree-ring stable isotope studies have contributed a long regional chronology from the northern summer rainfall area of South Africa to the ITRDB (Woodborne et al., 2016, 2015). Isotopic analysis is providing more innovative quantitative data on environmental change in South Africa, an important area of future research (Fitchett, 2019).

Dendroclimatic studies have shown that the *Afrocarpus falcatus* (formerly *Podocarpus falcatus*) in the tropics and subtropics has dendroclimatic potential because it can live for hundreds of years (Hall et al., 2008; Krepkowski et al., 2013, 2011; McNaughton and Tyson, 1979; Siyum et al., 2019). Since *Afrocarpus falcatus* is not critically endangered and is widespread in southern Africa (Adie and Lawes, 2011), it is, in terms of its distribution alone, an ideal species for use in dendroclimatology. Museum *Afrocarpus falcatus* specimens are rare and thus important. Hall (1976) measured the ring widths on a cross-section of a museum housed *Afrocarpus falcatus* specimen from the Karkloof, KwaZulu-Natal (the Karkloof specimen), reporting a 596-year rainfall proxy record dating back to 1320 CE. The well-known biological principle of limiting factors is an important concept for dendroclimatology and states that tree growth cannot proceed faster than is allowed by the most limiting factor (Fritts, 1976). The Karkloof specimen grew in a mistbelt-mixed *Podocarpus* forest (Rutherford et al., 2006). If classical tree-ring width theory were applied to develop a growth-climate hypothesis for this growing area, then temperature would be proposed as the growth-limiting factor (Fritts, 1976). It is evident from global application of dendroclimatic studies, that when analysing a fossil tree, the development of a modern tree-ring analogue to compare with instrumentally recorded climate data is the best way to confirm the growth-climate relationship for that species (McCarroll and Loader, 2006). Considering the increasing interest and importance of climate reconstruction in South Africa, further investigation on the Karkloof specimen is urgent.

The aim of this research is to investigate tree-growth climate relationships and develop a modern analogue for *Afrocarpus falcatus* in the Karkloof, KwaZulu-Natal, South Africa. The objectives are:

1. To develop a mean tree-ring-width chronology using classical methods;
2. To develop a mean stable carbon isotope ring-based chronology; and
3. To test the mean ring-width and $\delta^{13}C$ series against instrumental climate records of rainfall, relative humidity, temperature, solar irradiance, evaporation, sun duration, and precipitation minus evaporation.

	Hypothesis	**Alternative**
Hypothesis 1:	*Afrocarpus falcatus* tree rings from the Karkloof are annual - **TRUE**	*Afrocarpus falcatus* tree rings from the Karkloof are not annual - **FALSE**
Hypothesis 2:	*Afrocarpus falcatus* tree-ring widths are driven by climatic environmental forcing - **TRUE**	Climate cannot be reconstructed from *Afrocarpus falcatus* using tree-ring widths - **FALSE**

The structure of this thesis deviates from the traditional structure of a research thesis. As there are two tree-ring environmental proxies being investigated (tree-ring widths and stable carbon isotopes ($\delta^{13}C$)), each proxy has a separate chapter which presents the methods, results, discussion and a conclusion specific to the proxy being analysed.

Chapter two is the literature review, and the theoretical background for the two proxies has been combined into this chapter because there is so much commonality between the two environmental proxy approaches, that a separate chapter for each would have generated substantial overlapping information.

Chapter three will deal specifically with the tree-ring width proxy approach, whilst Chapter four will report on the use of $\delta^{13}C$ as a tree-ring environmental proxy.

In Chapter five a summary of the results from the application of the two tree-ring environmental proxies used to investigate the growth-climate relationships of *Afrocarpus falcatus* at the Karkloof growing site is given. The extent to which these proxies met the thesis objectives and addressed the research question will be assessed. The chapter will conclude with a true or false statement for the hypotheses and discuss implications for palaeoclimate reconstructions using *Afrocarpus falcatus* in the Karkloof, KwaZulu-Natal.

CHAPTER 2: LITERATURE REVIEW

Annual tree rings occur when there is one major growth period and one major dormant season each year (Fritts, 1976). The growth of large, thin-walled earlywood cells in cambium peaks in the early part of the summer season, gradually slowing down until smaller and denser latewood cells are laid down (Schweingruber, 1988). Latewood eventually reaches a dormant cell state, marking the end of the season's growth with a dark tree-ring boundary (Fritts, 1966). Identification of tree-ring boundaries and the ability to pattern match (crossdate) tree-ring properties between trees, gives dendrochronology the capability to date rings to calendar years (Hughes, 2002). Since tree-ring widths vary with environmental conditions, dendroclimatologists use tree-rings as proxy climate indicators to reconstruct climate (Hughes, 2002).

Climate reconstruction from tree-ring width proxies requires an understanding of the operational environment of the sampling site (Cook, 1987). Site characteristics like topography, substrate, elevation, and biotic factors affect the local energy and water balance of the site thereby uniquely altering the tree growth-climate relationship (Fritts, 1976). For the purposes of dendroclimatology, the growth-climate model is simplified so that it can be applied as a hypothesis (Fritts, 1976). The most practical climate variables for use in dendroclimatology are those measured instrumentally such as precipitation and temperature (Schweingruber, 1988) but few trees respond exclusively to a single climate variable (Hughes, 2002).

In testing the growth-model hypothesis for a sampling site, statistical correlation of the primary climate drivers that appear to control tree growth at the site, with the tree-ring width developed chronology is performed in a response function analysis (Bradley, 1999). Tree-ring data are regressed against the monthly climate data to identify which months are more highly correlated with tree growth (Bradley, 1999). Climate reconstruction, or calibration, involves transforming tree-ring widths into estimates of past climate by establishing an appropriate statistical/mathematical transformation to convert the measurements of tree-ring width into measurements of climate (Bradley, 1999). A variety of multivariate regression models can be used to apply weightings and transformations to the predictor variables (ring-widths) to create the transfer function (Bradley, 1999). While it is usually possible to make a distinction between early and latewood tissue, tree growth anomalies can challenge the fundamental requirement for the crossdating of samples (Fritts, 1976).

Mechanical cues in a tree can trigger a growth response to change biomass allocation (Bonnesoeur et al., 2019). The tree reacts structurally to slope by producing compression wood (narrow rings) in gymnosperms and tension wood in angiosperms (Bonnesoeur et al., 2019). Other tree-ring anomalies

include false, discontinuous, partial (wedging) and consequent locally absent and missing rings (Cook, 1985; Cook and Kairiukstis, 1990; Cook and Peters, 1981; Fritts, 1966) and these will henceforth be referred to collectively as ring width eccentricity.

Direct injury can produce scars on a stem which affect ring-width structure. Scars on the stems of trees have been widely used in the northern hemisphere to date and study the frequency of past events like disease, earthquakes, snow-falls, fires, and browsing herbivore populations (Schweingruber, 1988). All these exogenous events can result in ring eccentricity. Disturbance pulses which can be identified in ring-width series are transient trends and can be local, stand-wise or regional (Cook, 1985). Tree competition effects within a forest will influence the structure of a forest community (Seifert et al., 2014). Suppression and release patterns are associated with gap-phase forest dynamics (Adie and Lawes, 2011). These non-climatic growth trends can be identified in individual ring-width series through the comparison of sufficient samples, and then removed (Cook, 1985). Stand-wise disturbances are identified as common patterns but may not be climatic in nature. Such disturbances could come from disease or fire that sweeps through a forest affecting all the trees in varying degrees (Dale et al., 2001).

The general growth pattern of open canopy ring series is a linear decrease in width with age as the tree establishes more wood over an increasing circumference (Cook, 1985). More complex non-linear growth patterns of suppression and release associated with gap-phase dynamics are found in denser closed canopy forest where ‘growing up’ can last for decades (Cook, 1985). Light availability is more varied in a closed, productive forest and the tree records a unique experience until it reaches the canopy, whereupon ring-widths tend to take on a steadier more uniformed response to environmental forcing (Cook, 1985).

All non-climatic trends serve to obscure the tree growth-climate relationship (Cook and Peters, 1981). The aim of dendroclimatology is to isolate the tree’s growth response to climate to enable inferences about environment conditions to be made (Stokes and Smiley, 1968). To isolate the growth-climate response, non-climatic trends must first be identified and removed (Cook, 1985). To identify non-climatic trends, there must be sufficient samples to compare against (Cook and Peters, 1981).

Typically, meteorological records like rainfall and temperature are used to establish the growth-climate relationship of crossdated and averaged modern trees samples. If the ring widths do not correlate well with climate records, then either the ring-width representation is poor (insufficient samples); there is no common climate signal; or the growth-climate relationship is complex, and not well described in a general approach (Cook, 1985; Fritts, 1976).

2.1 RULES FOR CREATING TREE-RING WIDTH CHRONOLOGIES

Dendroclimatology methods have been thoroughly documented (Bradley, 2015; Cook, 1987, 1985; Cook and Kairiukstis, 1990; Cook and Peters, 1981; Fritts, 1976; Hughes, 2002; Osborn and Briffa, 2000; Speer, 2010; Stokes and Smiley, 1968; Wigley et al., 1987). Strong statistical bases for quantitative, calibrated climate reconstruction continue to be evolved, particularly with a view to developing and improving the statistical quality of longer tree-ring chronologies (Bradley, 2015; Hughes, 2002; Jones et al., 2009; Martinelli, 2004; Speer, 2010).

The main methodological sequence for developing tree-ring width chronologies for climate reconstruction is as follows: tree-ring series replication, crossdating, and calibration with available climate records. In this way, the relationship between the tree rings and climate data are quantified and ring widths which predate the instrumental climate record are then used as proxies to estimate past climate variability. (Speer, 2010).

Here the accepted traditional approaches for sampling, dating, standardisation and climate reconstruction will be described. Improvements that have been made to advance the methods will be included, with particular attention to the growth challenges persisting for species growing within closed canopy forests. These species and environments constitute a large portion of the global tree-ring network deficit from the southern hemisphere.

2.1.1 Sampling tree-ring widths

Tree-ring widths can be analysed from museum sources, cross sections of tree trunks, archaeological sources e.g. buildings, and cores extracted from living trees (Hughes, 2002). Cores from living trees are preferred as these can supply a higher replication rate needed for dendroclimatological analysis (Bradley, 2015). An incremental borer with a drill bit styled end is used to extract a cylindrical core from the trunk. The core lengths from the bark to the pith will vary from tree to tree. Cores are orientated in a vertical perspective, mounted to wooden blocks and polished to expose the tree rings (Stokes and Smiley 1968).

2.1.2 Crossdating

Manual crossdating methods were developed to identify similarities between tree-ring width series (Fritts, 1966; Stokes and Smiley, 1968; Fritts, 1976; Grissino-Mayer, 2001; Maxwell et al., 2011; Cook and Kairiukstis, 1990). If, for example, temperature is the limiting growth factor to trees in a forest, then an extremely cold growing season could produce a common narrow ring associated with that colder season. With sufficient replication, the narrow ring resulting from the extremely cold growing season in the given example may be identified in the majority of the tree-ring width series being analysed, acting as a pointer year for assisting with the crossdating of the tree-ring width series (Cook and Kairiukstis, 1990; Schweingruber, 1988). Crossdating using climate related pointer years can be easily achieved using trees from open canopy environments because there are few patterns relating to forest disturbance to conceal the climate signal. Dunwiddie and La Marche (1980), used frost rings common in all of the samples to cross date the *Widdringtonia cedarbergensis* chronology from the Western Cape. Visual comparison of the cores is typically undertaken using methods such as Skeleton Plotting which (Stokes and Smiley, 1968). A skeleton plot involves marking down the relative narrowness of each ring ranging from no mark to a maximum vertical line to represent extreme narrowness (Figure 1).

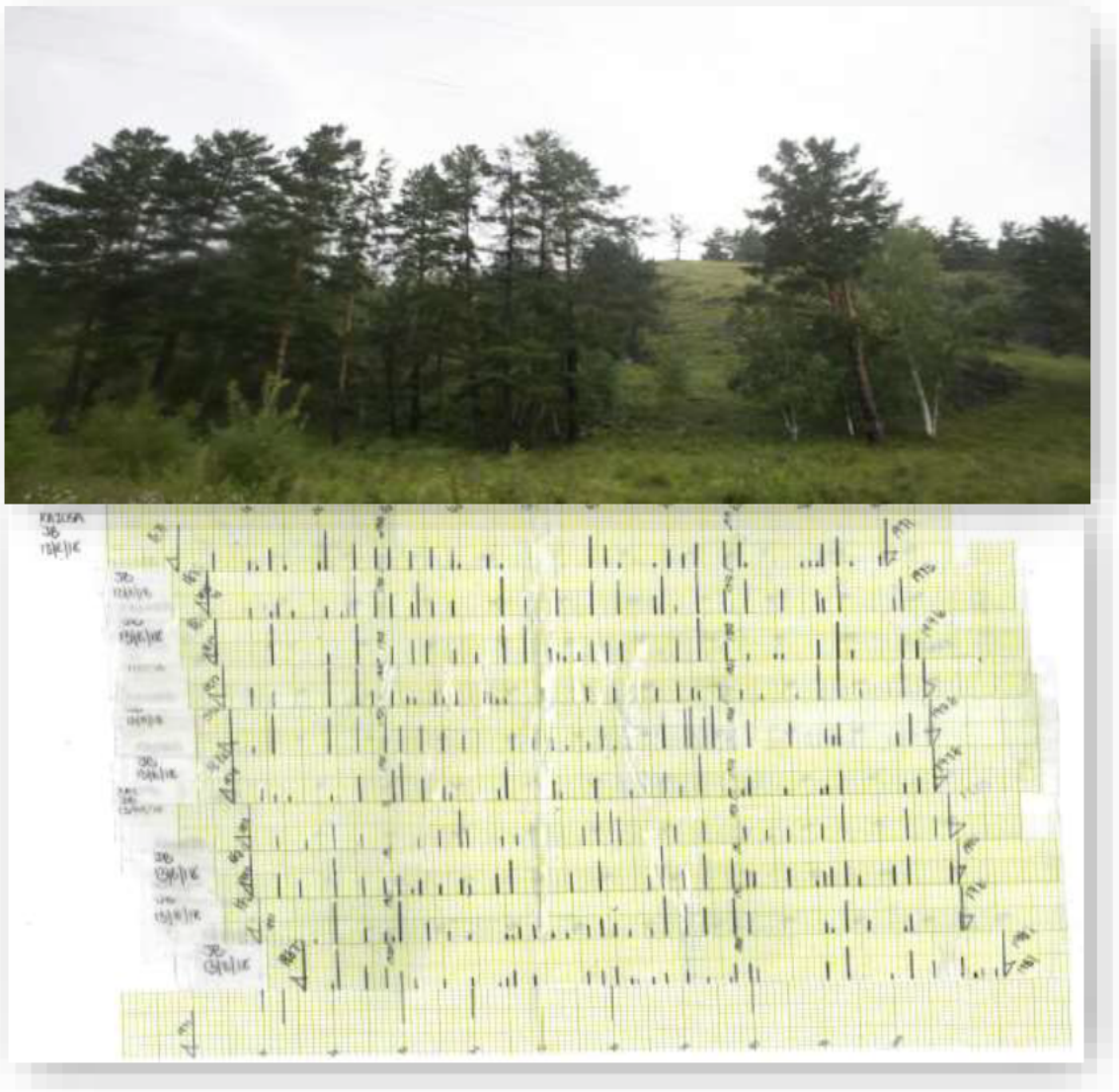

Figure 1: Ten Scots pine (Pinus Sylvestris L.) from an open-canopy forest in the Republic of Khakhassia, Siberia, manually crossdated using the skeleton plot method (International Summer School 2018. Tree Rings, Climate, Natural Resources, and Human Interaction, Cheryomushki, Khakassia, Russia)

Crossdating is the most important principle of dendroclimatology and is among the most precise dating methods of Quaternary research (Cook and Kairiukstis, 1990; Fritts, 1976) (Cook and Kairiukstis, 1990; Fritts, 1976; Grissino-Mayer, 2001; Schweingruber, 1988). Crossdating is essentially a high frequency process because the identification of year-to-year variations is more important in the crossdating process than identifying the low frequency climate trends (Cook and Kairiukstis, 1990). The objective is to date the annual rings by identifying common patterns between series, even if these patterns arise from non-climatic events. Series from shade tolerant trees of

closed canopy forests are more difficult to crossdate due to high stand disturbance and the growth suppression and release patterns relating to forest gap-phase dynamics (Cook,1985).

Since cross-dating is of such fundamental importance to dendroclimatology, several applications have been designed to measure and improve the statistical quality of tree-ring series. The most influential is the ANSI Fortran programme COFECHA (Spanish for “cross-date”) developed by Richard Holmes in 1982 (Grissino-Mayer, 2001). COFECHA was developed to aid dendroclimatologists working with ring series that were difficult to crossdate such as those from upper treeline sites, high latitudes and moist forests (Holmes, 1983). Both dated and undated multiple tree-ring series could be efficiently examined for dating errors or potential correlation between series. For dated series, COFECHA evaluates the quality of manual crossdating, and the ring width measurement using segmented time series correlation techniques to compare the samples and generate warning flags to identify potential errors (Holmes, 1983; Maxwell et al., 2011). These flags prompt the user to go ‘back to the wood’ to inspect the identified outliers and, where necessary, to re-measure the ring widths. This iterative process of verification and re-measurement continues until errors have been satisfactorily resolved. If warning flags persist, the program is probably identifying a localised anomaly. Where manual crossdating methods have failed, COFECHA also uses time series correlation techniques to examine segments within the undated series, suggesting possible overlaps between them.

To accomplish dating tree-ring series, ring-width pattern disparities between trees must first be resolved (Cook and Kairiukstis, 1990). Dating trees from closed canopy environments and trees that have ring anomalies like compression wood will be more difficult, and sometimes impossible. Samples which hold unresolved dates will weaken pattern-matching and where possible, should be set aside (Stokes and Smiley, 1968). A cross-dated collection of samples refers to the general year-to-year agreement, or correlation between the variations of ring widths. The mean inter-series correlation is a measurement of this synchronicity between ring-width series (Briffa and Jones, 1990).

Low correlation values for mean inter series correlation could range between 0.10 - 0.19, intermediate values between 0.20 - 0.29, and high mean inter series correlation series could be represented by values above 0.30 (Holmes, 1983). COFECHA employs a mean inter series correlation value of 0.3281 to represent a 99% confidence level for significance when comparing ring series and segments thereof. The programme outputs are an effective way to document the chronology confidence of data sets (Holmes, 1983). A crossdated series with a high mean inter-series correlation value (rbar) is very desirable, but the rbar value will depend on the species examined, geographic location and regional climate (Holmes, 1983). A mean inter-series correlation value of 0.5 would be considered very high for pine species growing in the south-eastern United States, but only moderately high for Douglas-fir trees growing in the south-western United States (Grissino-Mayer, 2001). This can also be true for

tree-ring series taken from the same region but at different elevations as Fritts (1966) showed by correlating tree rings from a San Francisco mountain gradient. Correlation among ring series within the high elevation dense San Francisco mountain forest interior was lower when compared to series from the same range at the lower elevation semi-arid forest border. The forest interior trees had higher between-tree-ring variation (lower mean inter-series correlation) and were more difficult to crossdate than the series from the lower elevation semi-arid border

Tree-ring width series naturally vary from one another and in statistical terms, 66.6% of normally distributed tree-ring width series are anticipated to vary from the mean by one standard deviation on either side of the mean (Fritts, 1976). Statistical reliability is greatly improved through increasing the sample size. Theoretically, the expected statistical error of 50% based on a sample of three trees reduces to 16% when the sample size is increased to 20 (Fritts, 1976). Tree-ring width series of drought sensitive conifers in the American southwest yielded a high mean inter-series correlation and 20 samples were sufficient to obtain a high statistical confidence level (Jones et al., 2009). Complex closed-canopy environments produce a high number of outliers to the mean, and even with many samples, can still yield a low mean inter-series correlation (Cook and Peters, 1981). To strengthen the common signal of a site, dendrochronologists often need to reject individual samples, or portions of samples which correlate poorly with the mean of the series, and so for these areas a higher replication than 20 trees is likely to be needed (Cook and Kairiukstis, 1990). To remove the high frequency influence of high stand disturbance and competition within tree-ring width series of the closed-canopy deciduous forests of eastern North America and Europe, Cook and Peters (1981) recommend analysing at least 40 trees per stand. For the development of longer-timescale variability (beyond multi-decadal chronologies to millennial timescales), the focus on identifying a low frequency climate signal requires many series, young and old, to be overlapped (Jones et al., 2009). Higher sample replication is needed to address the low sample depth and chronology confidence associated with overlapping segments and older chronologies. Jones et al (2009) suggested that even well-known spatially expansive tree-ring networks of the Northern Hemisphere were not sufficiently replicated to enable long tree-ring chronologies to be represented with adequate confidence.

A statistical quality measure that estimates how representative a mean tree-ring index is of a theoretically infinite population, is the ‘Express Population Signal’ (EPS) (Wigley, 1984). EPS and the arbitrary threshold of > 0.85 is routinely used by dendroclimatologists to establish when the sample depth (number of trees contributing to the indexed ring for any particular year) of a tree-ring index becomes too low to represent the whole population (Buras, 2017). If the sample depth in the tree-ring index reduces with age (older trees being less numerous), then climate is reconstructed back in time to the point at which EPS =< 0.85. Buras (2017) critically assessed whether EPS and the threshold

of 0.85 was an appropriate measure to determine how far back a chronology could be reconstructed to. Buras (2017) shows that the threshold is a common misinterpretation of Wigley et al. (1984), and that EPS does not consistently improve in line with increased sample replication. Buras (2017) concludes that earlier classical transfer functions or the subsample signal strength (SSS) statistic should be preferred over the erroneous application of EPS when judging suitability of tree-ring indices for climate reconstruction. These statistical threshold checks guide the number of additional samples needed to ensure an adequate sample depth for the planned reconstruction.

2.1.3 Standardisation of tree-ring width series

After dating has been resolved for measured ring series, unwanted non-climatic trends can be removed through the statistical process of standardisation (Cook, 1985; Cook and Peters, 1981; Fritts, 1976, 1966). The sequence of tree-ring series standardisation includes trend removal, indexing, and averaging (Cook and Kairiukstis, 1990; Fritts, 1976). The process of standardisation is the most subjective of the statistical data transformations and distinguishing the climate signal from non-climatic trends remains a major challenge.

2.1.4 Detrending and indexing

Statistical methods to remove non-climatic trends in tree-ring width time series have evolved in line with the locations and species being researched. Earlier work comprised trees from conifers in semi-arid open canopy environments of the Northern hemisphere, where soil moisture was determined to be the common limiting climate factor for tree growth (Cook and Peters, 1981). The ring width series thus presented very low ‘noise’ to climate signal ratios and only the simple growth-trend needed to be removed (Cook and Peters, 1981). Deterministic models of simple linear regression were found to adequately remove this growth trend (Cook, 1985; Cook and Peters, 1997). Exponential curves were used to deal with the growth pattern fluctuations caused by gap-phase dynamics of forest interiors (Cook and Kairiukstis, 1990). Research in other regions, like the closed-canopy deciduous forests of eastern North America and Europe, where ring series presented high noise to signal (climate) ratios, led, to the use of a more versatile orthogonal polynomial function replacing the exponential curve, and then the smoothing spline (Cook and Peters, 1981). Unlike orthogonal polynomials, a smoothing spline is a series of piecewise cubic polynomials with a flexible knot at each datum point and is better able to address the disjointed episodic nature of a forest interior (Cook and Peters, 1981). This allows the user to choose a more ‘natural fit’ for the series (Cook and Peters, 1981). The risk with using the spline is that the user can specify a high degree of smoothing and overfit the spline to the series, removing some of the low frequency climate signal (Cook and Peters, 1981). Conversely, a low degree of smoothing will include high frequency non-climate variation in the ultimate mean

chronology. Splines with a 50% frequency response cut-off of around 50-80 years have been found to perform best at removing age-related trends while preserving the climate signal (Cook, 1987, 1985; Cook and Peters, 1981). It is important to note that any filtering process will cause a portion of climatic datum to be lost (Briffa and Jones, 1990; Briffa and Melvin, 2011; Cook et al., 1995; Cook and Peters, 1981) The choice of method to remove the age-related trend can be either deterministic or stochastic depending on the type of species and environment being analysed (Cook, 1985). The growth trend of a species in a closed canopy forest could be a series of suppression and release curves lasting several decades and not able to be removed by simple deterministic methods. A hybrid approach can be used to address this issue using a double trending method, where a deterministic method is initially used (e.g. negative exponential), and then a stochastic method (e.g. spline) follows to address the unwanted remaining high frequency variance (Holmes et al., 1986).

Once an appropriate trend removal method has been chosen, each ring-width series is independently fitted with a curve and the trend is removed, with a ratio method to stabilise the variance (Cook, 1985). Stabilising the variance, or scaling all the series to mean values of 1, importantly addresses the disproportionate ring widths resulting from varying growth rates (Cook and Peters, 1997; Fritts, 1976).

Last, as with other environmental proxies, tree-ring series can be highly autocorrelated to previous years of climate and its influence on tree physiological resource deployment (Cook and Peters, 1981; Fritts, 1976). Depending on the previous year(s) climate and level of environmental stress, trees reserve, prioritise and allocate growth resources to future years. Artificial autocorrelation can also result from standardisation where residual non-climatic growth variations are not removed. This non-random, year-to-year natural and unnatural persistence is removed from the smoothed series by autoregressive modelling for a specified number of years (lag value) (Cook, 1985; Cook and Kairiukstis, 1990)

To optimise low frequency climate preservation in the series while simultaneously removing non-climate trends, the splines should be compared and checked for covariation through time before a mean tree-ring width index is developed (Cook and Peters, 1981). This reasonability check relies on an adequate number of samples being available for comparison (Cook and Peters, 1981). The filtering action used in the standardisation step should be thoroughly documented so that researchers who are combining chronologies from different regions to develop longer-timescale climate reconstructions, can avoid arriving at biased conclusions (Cook and Peters, 1981).

2.1.5 Mean value function (averaging)

Once a growth curve has been fitted to each series and the trend removed, a mean value function is computed from the new tree-ring width indices year-by-year to produce a single chronology for the site (Cook, 1985). This process isolates the common climate signal but will likely retain any stand-wide exogenous disturbances such as disease (Cook, 1985). Averages for each year can be computed using an arithmetic mean value function or a biweight robust mean estimation (Fritts, 1976). Ring width series from closed canopy environments will typically be affected by endogenous disturbances like suppression and release intervals which are unique and random in nature from tree to tree (Cook and Peters, 1981). These disturbances will manifest as outliers in the series. Although the arithmetic mean produces the smallest variance and is the most efficient estimator possible, simple averaging of ring width series which have known outliers will result in a biased mean value function (Cook, 1987). A biweight robust mean which serves to discount outliers by applying a weighting function can be used (Mosteller and Tukey, 1977). The biweight mean is thus more suitable for shade tolerant species and ring width series from closed canopy environments (Cook and Peters, 1981). Loss of information is inevitable in the case of the biweight mean when a weighting function is applied, and wider confidence limits result, but the net reduction in total error variance increases the signal (climate) to noise ratio (SNR) (Cook and Peters, 1981). The SNR is an important statistical measure of strength and improves with sample size (Fritts, 1976). The resulting values are referred to as ring-width indices, with a mean of one.

2.2 APPLICATIONS OF RING WIDTH STUDIES IN SOUTH AFRICA

In South Africa, two long-lived indigenous conifers were initially favoured for classic dendroclimatic research: *Podocarpus and Widdringtonia*. Preliminary investigations confirmed for both species that rings were annual (Curtis et al., 1978; Hall et al., 2008; Lilly MA, 1977; McNaughton and Tyson, 1979).

2.2.1 Hall (1976)

Ring widths along the longest transect of an *Afrocarpus falcatus* cross section specimen from the Karkloof, KwaZulu-Natal, were measured (Hall, 1976) (Figures 2,3). The specimen is housed in the KwaZulu-Natal Museum. No crossdating could be performed but what resulted was, for South Africa, a very long *Afrocarpus falcatus* ring-width series. Hall's hypothesis was that precipitation was the limiting factor driving tree growth in the Karkloof because (a) frost and low temperatures were reportedly uncommon; (b) The Karkloof has cool dry winters and warm summers with high rainfall; and (c) (Gillooly, 1975)) showed that ring widths from Rustenburg showed a potential response to rainfall. Hall proposed that the climate in the Karkloof is the same as Rustenburg.

No instrumental climate records existed for the lifespan of the tree, so Hall used the ring width measurements to test the Tyson and Dyer (1975) proposition of a 16-20-year rainfall oscillation in the summer rainfall area. Hall did not note any structural abnormalities of the trunk or any difficulties in working with the specimen.

Figure 2: The Afrocarpus falcatus cross section from The Natal Museum, Pietermaritzburg

Figure 3: A section of the transect used by Hall, 1976, from the Afrocarpus falcatus specimen housed in the Natal Museum, Pietermaritzburg

2.2.2 Curtis et al. (1978)

To test the findings from Hall (1976), Curtis et al. (1978) improved on Hall's transect method when they undertook complete cross-section analysis on a single *Afrocarpus falcatus* from Magoebaskloof, Limpopo. This method entails tracing the circumference of each ring to address the occurrence of converging and missing rings. Approximately 13 rings were missing (10% of the sample). Other studies referenced by Curtis et al. (1978) reported 6 – 10% of total rings missing. Curtis et al. (1978) concludes that incremental cores cannot be used for dendroclimatic studies involving *Afrocarpus falcatus* because of complicated ring structure and missing rings. Despite this, some segments of the cross section were analysed and the study concluded that future research on the species will be difficult but is justifiable (Curtis et al., 1978).

2.2.3 McNaughton and Tyson (1979)

McNaughton and Tyson (1979) drastically improved replication by undertaking complete cross-sectional analysis on 12 *Afrocarpus falcatus* from Witelsbos, Eastern Cape. The site is warm temperate (humid) with a MAP of 750 mm. The sampling terrain was fairly level (10% incline). The study removed five series from the analysis due to converging rings (42%). The study retained five whole series (42%) and two series were split to remove bad segments (16%). Common patterns between the retained series were identified, and then compared to wet and dry periods as defined by Tyson and Dyer (1975). Temperature was not investigated. The study concluded that sometimes wider ring widths related to wet periods and narrow ring width related to dry periods, but inverse relationships were also evident resulting in no clear qualitative relationship for growth and rainfall (McNaughton and Tyson, 1979).

2.2.4 Thackeray (1996)

The ring widths of a sectioned *Afrocarpus falcatus* from the Ditsong National Museum of Natural History were first measured in 1996, and again in 2000 (Thackeray, 1996; Thackeray and Potze, 2000). Thackeray and Potze (2000) suggest that the disk may be from the same tree in Knysna as that of the specimen housed in the n the Durban Natural Science Museum. The methods used to analyse the museum specimen were the same as those used by Hall (1976) and the resulting ring-width measurement series was compared to rainfall records for southern Africa (Preston-Whyte and Tyson, 1988). Oscillations of 17.4 years were presumed to be rainfall oscillations in the ring-width measured series, and it was noted that these corresponded closely to the frequencies that Hall (1976) had identified in the KwaZulu-Natal Museum Karkloof specimen. It was also noted that rings in the Knysna specimen were generally wider than the Karkloof specimen because Knysna rainfall was higher than in the Karkloof (Thackeray and Potze, 2000).

2.2.5 Dunwiddie and LaMarche (1980)

Dunwiddie and LaMarche (1980) extracted incremental cores from 28 living *Widdringtonia cedarbergensis* in the Cedarberg, Western Cape. An additional 19 cross sections were included to bring the total collection to 47. Lobate growth and ring convergence were noted to be uncommon for the species. It was noted that the traditional method of using common narrow rings to pattern match samples was not successfully applied because they were not common enough. Instead, common wide rings and frost rings were used to crossdate the samples (Figure 4). Only 32 samples were retained (68%). The mean ring-width response to climate was high but the relationship was described as complex, with opposite responses to the same variables (precipitation and temperature) occurring

in different seasons of the year. A record of spring/summer moisture availability was thus tentatively proposed.

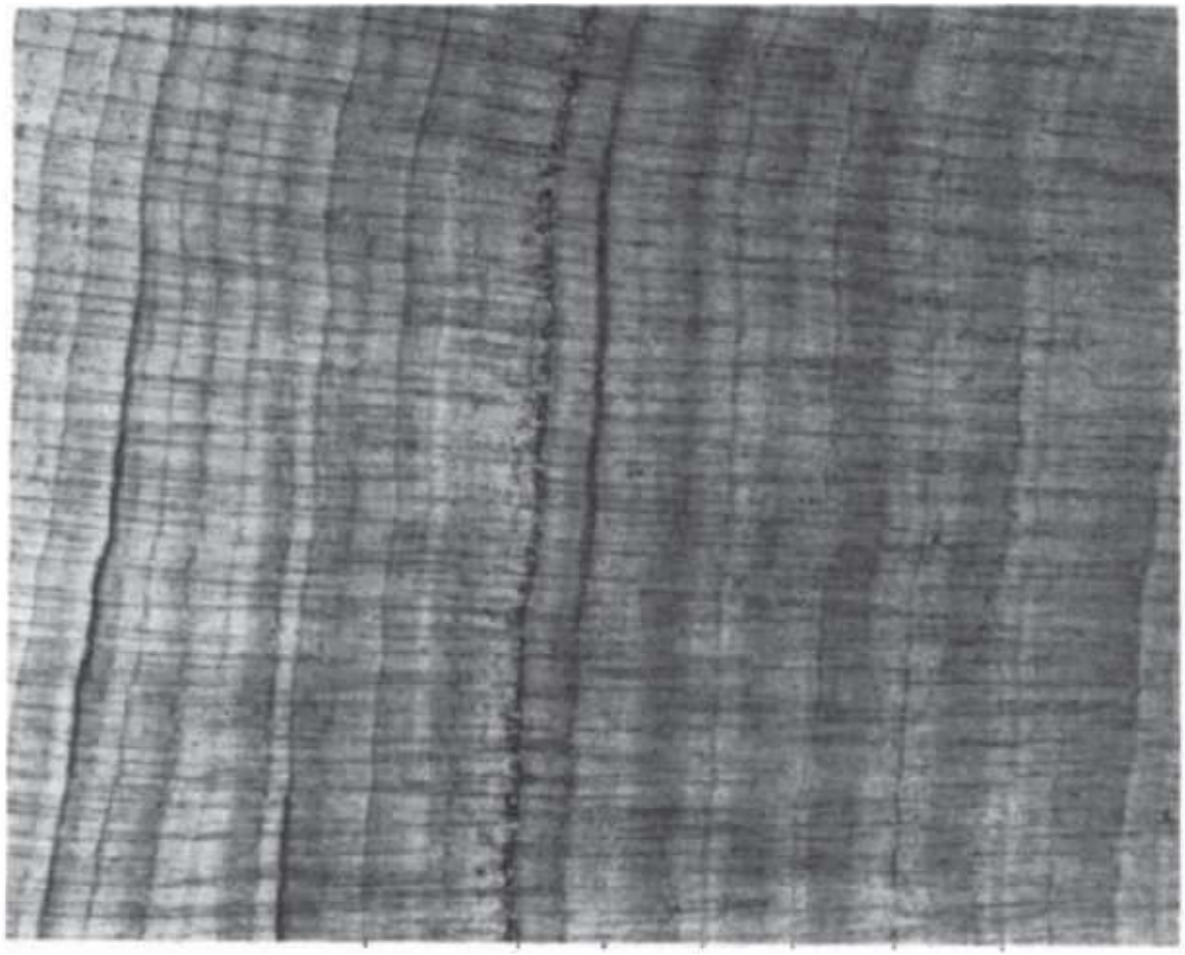

Figure 4: Tree rings of the Widringtonia cedarbergensis (Dunwiddie and LaMarche, 1980 p.796)

2.2.6 February and Stock (1998)

February and Stock (1998) re-evaluated the dendrochronological potential of *Podocarpus* by undertaking complete cross-section analysis of eight *Podocarpus latifolius* and six *Afrocarpus falcatus* from Harkerville, Eastern Cape (non-seasonal rainfall, MAP 750 mm, Ave T 14°C). The study concluded that due to poorly defined, locally absent, converging rings combined with lobate growth, crossdating (Skeleton plotting, COFECHA) within and between trees was not possible. February and Stock (1998a) suggest that to investigate the relationship between trees and rainfall, drier areas should be targeted for sampling, but not using *Podocarpus*, which they concluded, was not suitable for future dendrochronological research.

February and Stock (1998) analysed 14 *Podocarpus* samples, six of which were *Afrocarpus falcatus.* It is thus preferable to combine samples within distinct genera, rather than mixing genera. February and Stock (1998) only had half the sample size as McNaughton and Tyson (1979). By applying the McNaughton and Tyson (1979) retention rate of 58% to the February and Stock (1998) study, theoretically only a maximum of 4 ring-width series would have been retained. This sample size is too low to establish an inter-series correlation for *Afrocarpus falcatus* using ring widths. It may be worthwhile combining the *Afrocarpus falcatus* Harkerville samples with the Witelsbos series as the sites are only within 80 km of each other and experience similar climate.

2.2.7 February and Stock (1999)

February and Stock (1999) accumulated a collection of 47 *Widringtonia. cedarbergensis* samples from Algeria (26) and Krakadouw (21) in the Cedarberg, Western Cape . Classical methods (Stokes and Smiley, COFECHA) were used to crossdate the collection. The mean of cores crossdated was 25%, whilst the mean of cross sections crossdated was 80%. ARSTAN was used to develop a ring width index for each site. The two site chronologies did not correlate with one another (February and Stock, 1999).

Both study sites are located near the study site of Dunwiddie and La Marche (1980). The 'Die Bos' study utilised Wupperthal's rainfall records (nearest town). One of the aims of the February and Stock (1999) study was to test whether more localised rain records could improve the ring width/rainfall correlations. Mean indices were compared to local rainfall records (no temperature records existed). The drier site (Krakadouw MAP 250 mm) correlated significantly with rainfall (0.23) whilst the moister site (Algeria MAP 750 mm) did not. The rainfall correlation for the Krakadouw mean ring-width index was not high enough for use in climate reconstruction.

2.2.8 Vogel et al (2001)

Vogel et al. (2001) re-examined the Hall (1976) *Afrocarpus falcatus* transect and made a significant contribution to furthering the knowledge of the Natal Museum specimen's age. Carbon dating of 26 positions along the transect were assessed. Two scars were identified on the transect which coincide with approximately 162 missing rings in total. The oldest scar represents the potential position of 143 missing years which could be a signature event dated to AD1220, and theoretically might be found on similarly aged specimens from the same study area. Fire or disease could be an explanation for the scars found on the Hall (1976) transect. Approximately 20 rings were also found to be false (Vogel et al., 2001). Although Hall never reported any anatomical abnormalities along the measured transect, Vogel et al. (2001) confirmed the occurrence of wedged rings (Figure 5).

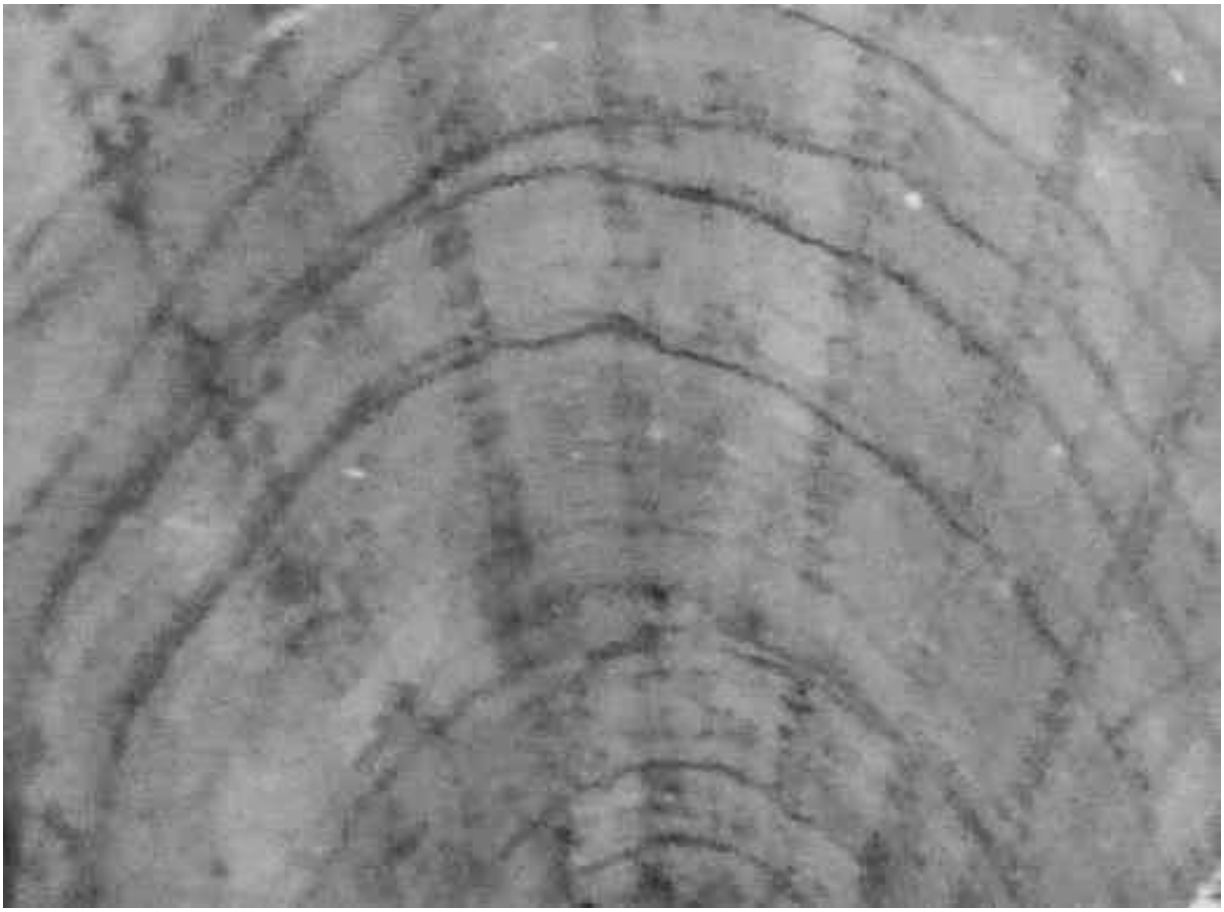

Figure 5: Instances of ring eccentricity on the Natal Museum Afrocarpus falcatus cross-section measured by Hall (1975) showing converging, wedging and compression

2.2.9 Summary of literary review

Ring width eccentricity was identified in both *Widringtonia cederbergensis* and *Podocarpus* (February and Stock, 1998; February and Stock, 1999). Latewood is however more difficult to identify in *Widringtonia.cedarbergensis* than in *Podocarpus*, but due to greater ring uniformity, is an easier species to crossdate (February and Stock, 1999). The largest sample size of all ring-width studies in South Africa was completed by Dunwiddie and LaMarche (1980) for 47 *Widringtonia cedarbergensis* trees in the Cedarberg (Figure 6). The study retained 68% for climate investigation. Both Dunwiddie and LaMarche (1980) and February and Stock (1999) identified a complex tree growth-climate relationship for *Widringtonia cederbergensis* which responded to both temperature, and rainfall. Deep tap roots accessing groundwater may be the reason why the ring-width chronologies do not correlate strongly with rainfall records (February and Stock, 1999).

The *Podocarpus* that were sampled, all came from closed canopy Mistbelt Mixed *Podocarpus* forest sites (Karkloof, Diepwalle, Witelsbos) . All these sites are situated within humid zones (Peel et al., 2007). Dense vegetation competes for sunlight and nutrients while contributing to high humidity levels within the canopy forest. Ring-width patterns of these forests typically have a high noise to climate signal ratio which make crossdating between trees difficult. To identify common ring-width patterns in these types of forests, the sample size must be large enough so that once samples with low correlation with the mean have been removed, there are enough samples remaining to ensure adequate population representation. Despite the crossdating constraints of moist forests, *Afrocarpus falcatus* from Witelsbos in the Eastern Cape had some success in identifying growth-climate relationships but the relationship was described as complex with the chronology identifying with both temperature and rainfall at different times (McNaughton and Tyson, 1979).

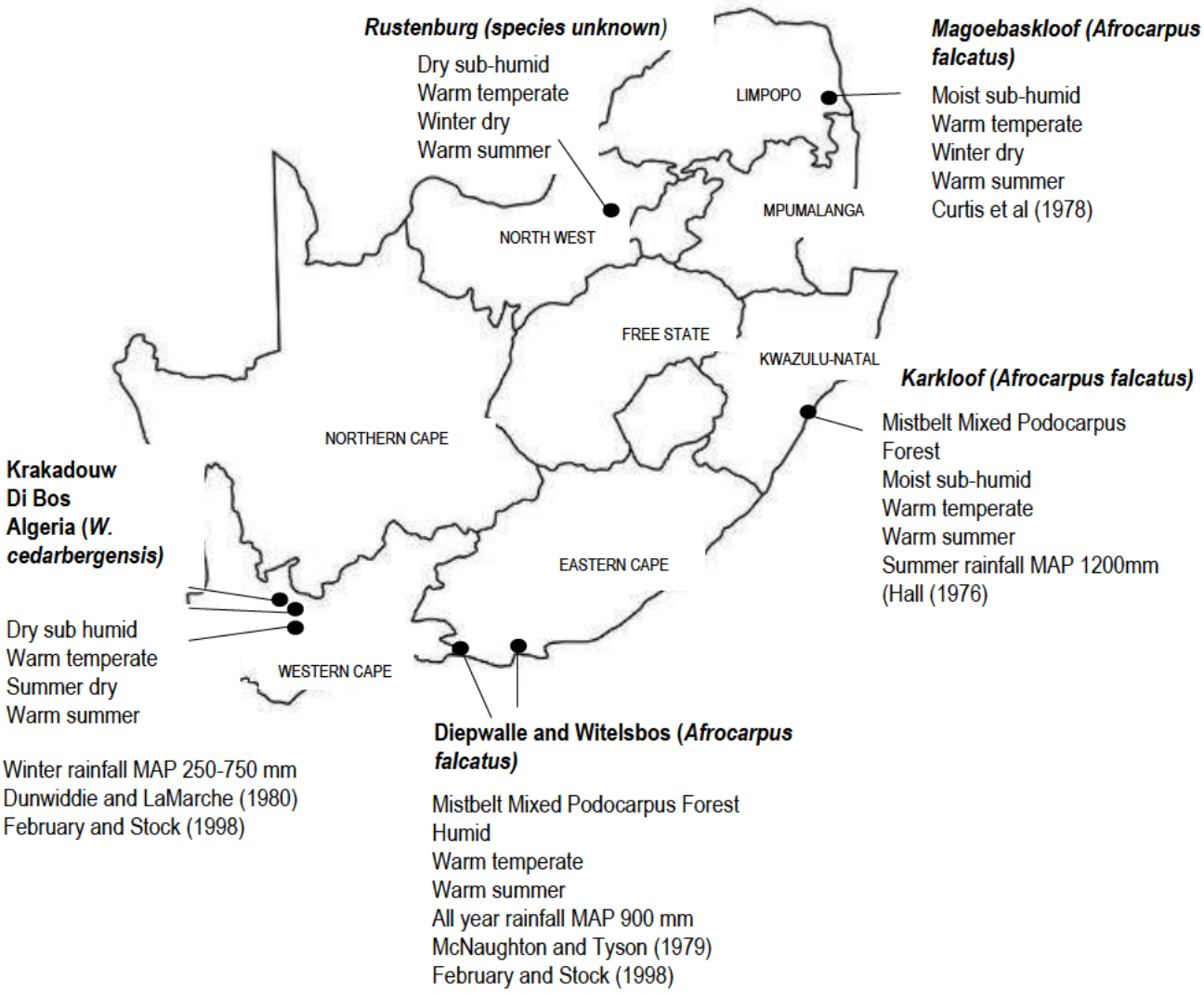

Figure 6: Map showing the location of the ring width investigations completed in South Africa, with climate descriptions based on Köppen-Geiger classifications (Peel et al., 2007)

February and Stock (1998) strongly discouraged further research on *Podocarpus* in South Africa. Incremental coring on *Podocarpus* was believed to be an impossible sampling strategy and has never been done for a ring-with dendroclimatic study in South Africa. In the tropics in 2019, 20 Ethiopian highland *Afrocarpus falcatus* from a remnant dry Afromontane forest were crossdated and the ring-widths were correlated with rainfall (Siyum et al., 2019). Eight years previous to this, ring-width studies on *Afrocarpus falcatus* growing in a moist dry Afromontane Ethiopian forest encountered missing, fake and eccentric rings and had limited crossdating success (Krepkowski et al., 2011). Thus, ring width studies for *Afrocarpus falcatus* in the tropics succeeded by sampling from drier sites.

2.3 ALTERNATIVE APPROACH: STABLE ISOTOPE ANALYSIS

It has been shown that the annual growth of a tree can be studied using ring widths, but there are many confounding factors that make this less tenable in southern Africa than in other regions of the world. As an alternative, the chemical composition of the wood in a tree ring can also proxy environmental conditions from plant physiological processes that influence isotope assimilation. Stable isotopes of carbon, hydrogen and oxygen from tree rings can record temporal variation in source materials because cellulose and lignin are abundant and stable (McCarroll and Loader, 2006).

The analysis of annual growth rings in tree rings using stable isotopes is well established in the northern hemisphere (McCarroll and Loader, 2006; Robertson and Leavitt, 2008). Studies in tropical and subtropical areas are comparatively more recent, and follow the well-established methods that were developed for higher latitudes (Van der Sleen et al., 2017).

Ring width studies have been used to produce high resolution paleoclimate data sets, but their potential is limited by: (a) general ring width eccentricity and reaction wood that obscure climate signal; (b) a tree ring is only one component of many biomass outputs (roots, leaves, fruit) and a tree will allocate resource according to its priorities, thus affecting the extent of wood produced in a given year; (c) ring widths decrease geometrically with age and low-frequency climate signals can inadvertently be removed during statistical detrending in ring-width studies (Cook et al., 1995).

The stable isotopic composition of the wood tissue is not affected by ring-width eccentricity or reaction wood in tree-rings, nor does it need to be statistically detrended when investigating long chronologies.

For this thesis, only carbon isotopes will be discussed further.

2.4 FACTORS AFFECTING CARBON STABLE ISOTOPES IN TREE RINGS

All elements have isotopes which can be stable or unstable (radioactive) (O'Leary, 1988). Isotopes in an element have the same number of protons but different numbers of neutrons (O'Leary, 1988). Carbon occurs naturally in three isotopes: carbon 12, which has 6 neutrons (plus 6 protons equals 12), carbon 13, which has 7 neutrons, and carbon 14, which has 8 neutrons (O'Leary, 1988). Thus, these isotopes have different weights. Isotope fractionation in simple physical and chemical processes is well understood and used to establish biological pathways, with methods developed to measure the carbon flow in plants (O'Leary, 1988). In early stable isotope studies, plant processes were poorly understood and the source of CO_2 variation was the focus but observations made through the 1980s and 1990s demonstrated that plant processes were not constant, had high variation and were dynamic (Ehleringer, 2017). CO_2 is necessary for plants to synthesise glucose in photosynthesis (Ehleringer, 2017). In the presence of CO2 cells can convert this solar energy to organic molecules like glucose (Farquhar et al., 1982). Using chemical methods, carbon can be extracted from a plant sample, and a method called accelerator mass spectrometry (AMS) can be used to separate out the individual carbon isotopes by weight (Ehleringer, 1991). Since the processes involved when plants take CO2 in for photosynthesis discriminate against the heavier ^{13}C, they contain less ^{13}C than the atmosphere (Ehleringer, 2017). Most variations in $\delta^{13}C$ in terrestrial systems are a consequence of plant-related fractionation processes (Ehleringer, 2017).

2.4.1 Carbon isotope theory

Atmospheric CO_2 enters the tree through leaf stomata (Ehleringer, 1991). Atmospheric $^{13}CO_2$ is discriminated against relative to $^{12}CO_2$ because it diffuses slower (a 1.044 isotope effect is derived from the square root of the ratio of the masses) at a rate of 4.4 ‰ (Farquhar et al., 1982). An economic model of supply and demand is useful to understand tree operation. There are trade-offs during photosynthesis when the stomatal pores open to allow CO_2 diffusion inwards to increase the rate of photosynthesis. As stomatal pores open, transpiration also increases. The CO_2 diffuses into the leaf and is taken up by photosynthesis, creating a lower CO_2 concentration inside the leaf. This creates a difference between the CO_2 concentration outside the leaf (c_a) and the CO_2 concentration in the intercellular air spaces (c_i). This difference is driven by the rate of demand for CO_2. The balance between the CO_2 inward diffusion rate and the rate of photosynthesis which decreases CO_2 is referred to as the ratio of intercellular to ambient CO_2 concentration ratio (c_i/c_a). It is the balance point between the inward diffusion and the uptake of CO_2 (Farquhar et al., 1982).

The ci:ca relationship is linear and can be calculated using the widely applied Farquhar et al. (1982) model of carbon isotope discrimination (Δ) in C3 plants:

$$\Delta^{13}C = a + (b-a)(c_i/c_a)$$

where a is the discrimination against $^{13}CO_2$ during stomata diffusion (–4.4%), b is the net discrimination due to carboxylation (-27%), and c_i and c_a are intercellular and ambient CO_2 concentrations.

Atmospheric CO_2 enters the leaf stoma where the carbon fixing enzyme Rubisco catalyses the carboxylation of RuBP which discriminates against ^{13}C with an isotope effect of 1.030 (30 ‰). Other non-photosynthetic carboxylation fix carbon (e.g. respiration) and account for between 8-10% of ^{13}C fractionation. The theoretical expected value of 27 ‰ is then assigned to the total discrimination of ^{12}C in favour of ^{13}C (Farquhar et al., 1982).

When the stomates close, the c_i/c_a ratio goes down (as low as 0.5). When the stomates open the ratio goes up (as high as 0.7) (Ehleringer, 2017). If the fractionation rate of atmospheric CO_2 (-4.4 ‰) and plant processes (-27 ‰) are constant, then the remaining input to the Farquhar et al. (1982) equation is the carbon isotope ratio of the air.

2.4.2 Effects on the variability of tree-ring $\delta^{13}C$ series

Atmospheric $\delta^{13}C$

The carbon isotope ratio of the air has changed since the industrialisation age. Fossil fuel usage, industrialisation, and land use change have released ^{13}C depleted CO_2 and changed the $^{13}C/^{12}C$ ratio in atmospheric CO_2 (Francey et al., 1999). The pre-industrial atmospheric $\delta^{13}C$ was 6.5 and now it is 8.5. Data sets comprising direct measurements of the $\delta^{13}C$ of atmospheric CO_2 and measurements of CO_2 in air trapped in ice bubbles are typically used to correct for the ^{13}C depleted CO_2 gradient (Feng, 1998; McCarroll and Loader, 2004).

Physiological factors

Atmospheric concentrations of CO_2 have been rising through the industrial age (Francey et al., 1999). There is an observed foliar physiological effect on plants, which is independent of the effect on climate (Ainsworth and Rogers, 2007; Feng, 1999; Rezaie et al., 2018; Saurer et al., 2004). The increasing partial pressure of CO_2 modifies the gaseous exchange functions in leaves and increases the photosynthetic discrimination against ^{13}C (Savard and Daux, 2020). Most plant species show

improved intrinsic water-use efficiency (W_i) as an active response to CO_2 fertilisation (Brienen, 2011; Feng, 1999; Rezaie et al., 2018; Saurer et al., 2004). Not all studies have assumed that rates of photosynthesis increase with increased W_i. Brienan (2011) notes a constant ci, reasoning that a reduction in stomatal conductance is responsible for improved W_i, not photosynthetic rate (Brienen, 2011) Rezaie et al. (2018) confirmed a reduction in stomatal conductance when they investigated conifer response in northern Eurasia. Most trees showed an adaptation in gas exchange and reduced transpiration which would have returned a drier air layer (Rezaie et al., 2018).

Canopy effect

Van der Merwe and Medina (1991) describe a canopy effect in a closed canopy tropical forest. Variations of $\delta^{13}C$ were observed to become less depleted with increasing forest height. The reasons for this are still unclear (Van der Merwe and Medina, 1991). Soil respiration, litter decomposition and plant respiration below canopy recycle photosynthesised air and return more depleted ^{13}C values than above canopy atmospheric air (Van der Merwe and Medina, 1991) but in the Amazonian rain forest, their assignment did not account for the relatively steep gradient observed in $\delta^{13}C$ values with increasing height (-4.5 ‰ unaccounted for) (Van der Merwe and Medina, 1991). The use of carbon isotope ratios is more easily applied to an open canopy site where air is mixing. Source air varies within the system and air measurements in dense canopies have shown that (Jackson et al., 1993; Offermann et al., 2011; Van der Merwe and Medina, 1991; West et al., 2000).

Age-related trend / juvenile effect

Tree-ring width declines with age and is statistically removed during detrending (Cook and Kairiukstis, 1990). An age-related trend has also been identified in tree-ring $\delta^{13}C$ series research but the reason for the effect is not well understood (McCarroll and Loader, 2004). Potential reasons for the "juvenile effect" have included the effects of CO_2 derived from soil respiration, degradation of organic matter, hydraulic changes as the trees gain height and reduced light levels lower in the canopy (McCarroll and Loader, 2004).

The Regional Curve Standardisation (RCS) approach can be used to remove age-related trends of $\delta^{13}C$ ring series. In an open canopy forest in Finland a subfossil *Pinus sylvestris* was studied using five modern *Pinus sylvestris* to construct a modern tree-ring $\delta^{13}C$ analogue (Helama et al., 2018). Using RCS, a mean 50 year juvenile period was observed and removed (Helama et al., 2018). A 7500-year long tree-ring $\delta^{13}C$ chronology resulted. In closed canopies, the individual patterns of suppression and release, based on overstory light availability, do not align with one other in terms of the RCS biological growth trend theory (Dietrich and Anand, 2019). A size-deterministic model

approach for tree-ring standardization over the traditional RCS, using the tree size to determine the common age between tree-ring series can be applied to closed-canopy sites.

These models might not be useful for sites disturbed by logging as each series would have a unique growth trend relative to their overlap with the disturbance period which may last for up to a century. A common ring-width method which could be employed to a $\delta^{13}C$ series is a flexible regression curve which slopes in either direction, allowing for typical and atypical growth trends in a disturbed site (light variation and extent of source air mixing would be factors affecting the growth curve). In ring $\delta^{13}C$ studies it is common to remove the estimated juvenile segment (McCarroll and Loader, 2006). This might be the most practical solution if the purpose is only to develop a modern analogue and losing older rings is an acceptable trade-off.

Carry over factor

It has been in shown in Section 1.3.4 that ring-width series can be highly autocorrelated to previous years of climate. Remobilisation of stored resources has also been shown to occur in ring $\delta^{13}C$ studies (Kagawa et al., 2006; Krepkowski et al., 2013; Monserud and Marshall, 2001). Experiments using pulse-labelling of $\delta^{13}C$ have shown that trees can allocate assimilates of photosynthesis from a previous year to the earlywood of the next year (Kagawa et al., 2006; Krepkowski et al., 2013). Latewood was found to contain mainly the current year photoassimilate (Kagawa et al., 2006).

Krepkowski et al. (2013) undertook a labelling experiment in tropical trees in an Ethiopian forest *(Croton macrostachyus and Afrocarpus falcatus).* They recorded a three-year carry over effect for *Afrocarpus falcatus* in earlywood (latewood contained current year photoassimilate) and half a year of autocorrelation in *Croton macrostachyus* (Krepkowski et al., 2013). These studies show that autocorrelation is species specific and should be taken account of when deciding whether to sample early or latewood.

Variability between sites and trees

Stomatal conductance is influenced by water availability to the tree and its ability to access the water with its root system (McCarroll and Loader, 2004). Water availability at a site can also differ between trees as well, for example, and older tree may have a more extensive root system that has tapped into a more reliable water source than a younger tree at the same site. The values of the carbon isotope ratios of wood tissue are influenced by the level of radiation received, thus a core taken from the side of a tree that receives more radiation will have different f $\delta^{13}C$ values (McCarroll and Loader, 2004). However, limited knowledge exists to explain the large variability of $\delta^{13}C$ values between trees

from the same site (McCarroll and Loader, 2004). As in ring widths, standardisation of ring $\delta^{13}C$ series enhances the relative coherence between trees by distinguishing the common inter-annual variability. McCarroll and Loader (2004) explain that when developing modern analogues with an aim to identify climate response to meteorological data, standardisation of the data can be beneficial. Standardisation would not be appropriate when the aim is to retain low-frequency climate variations (McCarroll and Loader, 2004). Standardisation methods such as the RCS approach has been used for the removal of long trends that are common within the forest stand (Savard and Daux, 2020).

2.5 RULES FOR CREATING STABLE ISOTOPE CHRONOLOGIES

As with ring-widths, tree-ring isotopes can be analysed from museum sources and modern cores which have been extracted from living trees. To create stable isotope chronologies, dendrochronology methods described in Section 1.3 are applied. Crossdating of the ring widths is still a critical step. Absolute dating of the tree rings is essential and dendrochronological crossdating skills can be used in isotope analysis. Since AMS radiocarbon dating is more accessible and affordable than it used to be, tree-rings can also be dated this way.

2.5.1 Sampling and dating tree-ring width series

Drier sites are controlled by stomatal conductance and are more sensitive to edaphic precipitation and relative humidity. Moist sites are controlled by photosynthetic rate and correlate to irradiance and temperature (McCarroll and Loader, 2004). A dry or moist site can be chosen according to the climate of interest. Where the aim of the study is to develop a modern analogue for a museum specimen, then sampling must be undertaken in the museum specimen's growing site (McCarroll and Loader, 2004).

Topography and position of the forest will have an effect on solar radiation and coring on different sides of the stem of a tree will return varying $\delta^{13}C$ values based on light availability (Ehleringer, 2017; McCarroll and Loader, 2006). Coring positions must be recorded to predict the dominant controls effecting the plant processes for an individual core. Cross sections and cores can be sampled for $\delta^{13}C$ analysis. Standard dendrochronology incremental coring methods are employed but when it is intended to analyse wood for stable isotopes, a second mount is glued to the core, and once dried, can be split into two halves with a fine saw.

Crossdating of the series on the basis of the rings remains a critical step. Common signatures such as frost rings can be used to physically pattern-match the wood. Visual comparison of the cores can

be undertaken using methods such as Skeleton Plotting (Stokes and Smiley, 1968). For more difficult species and sites, tree-ring width methods can be used. Crossdating on the basis of the resulting $\delta^{13}C$ series is another option. $\delta^{18}O$ series in England have been dated using COFECHA to assist with crossdating accuracy (Loader et al., 2019). Radiocarbon dating is another option to establish the ages of tree-rings. The identification of the latewood for the stable isotope analysis must be achieved before samples can be prepared.

2.5.2 Sample preparation

Wood from rings can be removed under magnification using a scalpel. For absolute annual resolution the latewood is sampled because there is little to no persistence from previous years (McCarroll and Loader, 2004). The identification of ring-widths and distinguishing between early and latewood is challenging in southern hemisphere trees (Dunwiddie and LaMarche, 1980; February and Stock, 1998; McNaughton and Tyson, 1979). Once identified, the latewood slithers are removed using tweezers and placed into pre-labelled micro-centrifuge tubes.

Different components of the wood can be analysed of which cellulose is the most popular because of its relative immobility and the $\delta^{13}C$'s similarity to the whole plant (Macfarlane et al., 1999). A variety of techniques for cellulose extraction from wood can be used (Leavitt, 2010; Leavitt and Danzer, 1993; Loader et al., 1997).

Purification of the cellulose is undertaken by (a) oxidation of the lignin in an acidified sodium chlorite solution; and (b) removal of hemicelluloses in sodium hydroxide followed by thorough washing and drying (McCarroll and Loader, 2006) The lignin oxidation process time will vary depending on the species.

The resulting carbon stable isotope alpha-cellulose samples are weighed before being converted to gas through combustion, either off-line using chemical procedures prior to mass spectrometry, or on-line as an integrated system before being admitted to the Stable Isotope Ratio Mass Spectrometer (IRMS) (McCarroll and Loader, 2004). A sample of gas enters the IRMS where it is ionised and accelerated down a flight tube and deflected according to its' mass. The resulting measurements of tree-ring $\delta^{13}C$ values are expressed in parts per thousand (‰) (McCarroll and Loader, 2004).

2.5.3 Data corrections

The tree-ring $\delta^{13}C$ series must be corrected for the effects described in Section 1.6 before application of the Farquhar et al. (1982) equation to calculate the $\delta^{13}C$ fractionation for each tree-ring $\delta^{13}C$ value.

Canopy effect

For closed canopy environments, the canopy effect must be dealt with before a correction for atmospheric CO_2 can be applied. Sampled trees will be of different ages within the canopy, and so the correction for the canopy effect is unique to each $\delta^{13}C$ ring series. Trees that have reached the canopy can be assigned an atmospheric CO_2 value of 8.5 ‰ at the youngest end of the series. In undisturbed sites, the RCS might be a useful way to help distinguish a common age for reaching canopy level for a specific species. Otherwise, truncation of the relevant portion of the relevant portion of the series can be done (McCarroll and Loader, 2004).

Correction for Atmospheric $\delta^{13}C$ trend (Seuss effect)

The dataset comprising direct measurements of the $\delta^{13}C$ of atmospheric CO_2 and measurements of CO_2 in air trapped in ice bubbles (Belmecheri & Lavergne 2020) are typically used to remove the deviation for the C^{13} depleted CO_2 gradient (McCarroll and Loader, 2004).

Physiological factor

Consideration of the potential for a response to the elevated levels of carbon since industrialisation in the $\delta^{13}C$ series by investigating W_i is should be undertaken. Most plant species show improved W_i as an active response to CO_2 fertilisation. Tree respiration decreases but photosynthetic rate does not always increase and trees response genetically (Brienen, 2011; Feng, 1999; Rezaie et al., 2018; Saurer et al., 2004) .

2.5.4 Mean value function (averaging)

A mean value function is computed from the corrected $\delta^{13}C$ series year by year to produce a single chronology for the site. Averages for each year can be computed using an arithmetic mean value function or a biweight robust mean estimation. Ring width series from closed canopy environments generate outliers in the series so simple averaging of $\delta^{13}C$ ring series will result in a biased mean value function (Cook, 1987). The Mosteller and Tukey (1977) model applies a weighting function to generate a biweight robust mean. This can be used to deal with outliers, but loss of information is inevitable (Cook, 1985). If the aim is to create a modern climate analogue for a species and site, then the loss of information will not be as critical as for the aim to develop a long chronology. The Farquhar et al. (1982) equation is then applied to calculate the $\delta^{13}C$ fractionation for each measured $\delta^{13}C$ value.

2.5.5 Climate reconstruction

Direct or indirect climate factors that operate on the photosynthetic or respiratory function of a tree modify the fractionation factor and change the $\delta^{13}C$ value in the wood. The extent of $\delta^{13}C$ variation to these factors varies with species and sites. Studies have shown that stomatal conductance is the dominant control in dry sites, and $\delta^{13}C$ is likely to correlate with relative humidity and antecedent precipitation. Moist sites are controlled by photosynthetic rate and $\delta^{13}C$ is likely to correlate with irradiance and temperature (McCarroll and Loader, 2004). It is important to note that $\delta^{13}C$ cannot be used directly as a palaeothermometer or a measure of water availability because fractionation is only a measure of the balance between stomatal conductance and photosynthetic rate (McCarroll and Loader, 2004). As discussed in detail for ring-width driven climate reconstruction in Section 1.3.7, strong significant correlations between tree-ring $\delta^{13}C$ chronology and meteorological climate data must precede climate reconstructions. Applied methods will generally be the same as those employed for tree-ring width chronologies. Multiple linear regression methods are the most widespread statistical approach to fit the response function between the chronology and the climate data (McCarroll and Loader, 2006). Cross-validation techniques assess the calibration model to validate its skill, and if robust, the transfer function serves to reconstruct the climate for the period where no instrumental records exist.

2.5.6 Temporal instability

Climate reconstruction from tree-ring proxies hold an underlying assumption that stationarity exists between the series and the climate variable, and where this assumption is not valid, temporal instability in chronologies leads to inaccurate climate reconstruction. Preventable causes of climate-proxy divergence have already been discussed in Section 1.3.8 (sampling and data treatment). Observations of more recent isotopic-climate divergence have been linked to anthropogenic climate change, but climatic regime change may be the reason for isotopic divergences observed over longer timescales (Savard and Daux, 2020). Climate change has been shown to cause divergences between isotope series and climate records with increased temperature causing the advance of spring in some regions, triggering physiological changes in trees (Savard and Daux, 2020). Large-scale atmospheric circulation change was cited as a potential reason for the decoupling of irradiance and temperature which caused the divergence between temperature records and a tree-ring $\delta^{13}C$ chronology in northwestern Norway (Savard and Daux, 2020). Tree-ring $\delta^{13}C$ values of *Abies alba* in Germany correlated to relative humidity and temperature until moisture and temperature relations changed at the site (Savard and Daux, 2020). Recurring droughts in western China led to changed response in tree-ring $\delta^{13}C$ values of *Abies georgei* as the dominant control of photosynthetic rate moved over to

stomatal conductance (Liu et al., 2014 cited in Savard and Daux, 2020). Multi-proxy and multi-site investigations are suggested by Savard and Daux (2020) to be useful strategies for helping to identify and eliminate the isotopic divergence issue. In the future, divergence is likely to be resolved using complex inverse process-based modelling which simulates the multiple physiological constraints of natural conditions developed through the combined efforts of vegetation biologists, ecophysiologists, modellers, dendrochronologists, isotopists, statisticians and paleoclimatologists (Savard and Daux, 2020).

2.6 APPLICATIONS OF STABLE ISOTOPES TO TREES IN SOUTH AFRICA

2.6.1 February and Stock (1999)

February and Stock (1999) extracted cellulose for $\delta^{13}C$ analysis from six samples of *Widringtonia cedarbergensis* from the Cedarberg which had been crossdated by Dunwiddie and LaMarche (1980) in a ring width study. Juvenile years were truncated leaving only 76 rings from each core. Each ring was extracted and pooled so that each year was represented by six samples from the site. Dunwiddie and LaMarche (1980) in their ring-width study did not show a significant correlation with rainfall. The $\delta^{13}C$ chronology returned the same result (February and Stock, 1999).

2.6.2 Norström et al. (2005)

Norström et al. (2005) analysed variations in tree-ring $\delta^{13}C$ and wood anatomy (vessel diameter, vessel density and growth rate) from 2 *Breonadia salicina* cross-sections from Tzaneen, Limpopo. *Breonadia salicina* are angiosperms of riparian habitat. The trees grew in a summer rainfall region (BSk by the Köppen-Geiger system (cold semi-arid)) with an MAP of 500 mm and an average annual temperature of 17.3°C. Radiocarbon dating was used to develop an age model and revealed that the 600-year-old trees did not produce annual rings. Resulting growth trends for the two samples were similar but variable throughout the records and correlated better in the earlier and more highly resolved portion of the record (Norström et al., 2005). Norström et al (2005) interpreted the $\delta^{13}C$ and anatomical variability as a response to moisture stress using other collaborative evidence of past climatic events.

2.6.3 Norström et al. (2008)

Norström et al. (2008) used the 2 *Breonadia salicina* cross-sections described in Section 1.8.5 from Tzaneen to analyse for $\delta^{18}O$. At the higher resolution portion of the record, the previously developed $\delta^{13}C$ and this $\delta^{18}O$ series positively correlated (Norström et al., 2008). The changes in $\delta^{18}O$ are explained as changes in relative humidity, but the correlations are too weak to be used for climate

reconstruction (Norström et al., 2008). Both the $\delta^{13}C$ and $\delta^{18}O$ records would benefit from a study which develops a modern climate analogue for the *Breonadia salicina* old samples (Norström et al., 2005).

2.6.4 Hall et al. (2008)

Hall et al. (2008) developed a modern analogue for $\delta^{13}C$ of *Podocarpus* archaeological charcoal extracted from Sibudu Cave in KwaDukuza, KwaZulu-Natal. Modern *Podocarpus* from Seaton Park, Durban North, KwaZulu-Natal and the Baviaans Kloof, Eastern Cape were sampled. Hall et al. (2008) used a modern analogue to establish that combustion temperature during charcoal formation is a factor influencing isotope composition and used this to interpret the $\delta^{13}C$ archaeological series. Hall et al. (2008) show that modern analogues are a critical step to understand species physiology, and to construct a baseline response for a specific site. Hall et al. (2008) does not establish a consistent significant relationship between the four modern *Podocarpus* $\delta^{13}C$ series and climate data in Durban North. The archaeological specimen is then interpreted through the ages and plausible suggestions of *Podocarpus* adaptation are shared for this remnant portion of coastal forest.

These results confirm that *Podocarpus* has dendroclimatic potential and can be studied using stable isotopes. The relationship between climate and *Podocarpus* is not well understood yet but this study demonstrated some coherence in the $\delta^{13}C$ series.

2.6.5 Hall et al. (2009)

Hall et al. (2009) sampled 2 whole wood samples of *Mimusops caffra* specimens that grew on the coastline of northern Kwa-Zulu-Natal and provided a potential measure of past rainfall. High-precision radiocarbon dating was used to date the $\delta^{13}C$ series and it confirmed annual rings. The use of wavelets as an alternative means to interpreting traditional time series suggested that long term climate forcing was chaotic, and would be difficult to model (Hall et al., 2009).

2.6.6 Woodborne et al. (2015)

Woodborne et al. (2015) obtained two very old *Adansonia digitata L.* specimens from northern Limpopo. Younger samples were collected from the same area. Tree-ring $\delta^{13}C$ time series were developed for all samples and radiocarbon analyses was undertaken (Woodborne et al., 2015). Woodborne et al. (2015) confirmed annual rings for this study. There was good coherence between trees such that the juvenile periods were able to be retained. The resulting near-annual 1000-year $\delta^{13}C$ ring chronology is compared to other ring series and rainfall records (Dunwiddie and LaMarche,

1980; Neukom et al., 2014; Therrell et al., 2006). The $\delta^{13}C$ chronology shows rainfall decadal and centennial oscillations, and a rainfall regime shift caused by a northward displacement of the subtropical westerlies (Woodborne et al., 2015)

2.6.7 Woodborne et al. (2016)

Woodborne et al. (2016) analysed five *Adansonia digitata L*. specimens from the Mapungubwe region, in northern Limpopo. The Mapungubwe chronology showed that *Adansonia digitata L*. rings were not annual, necessitating a revision to the Pafuri record. The Mapungubwe and revised Pafuri tree-ring $\delta^{13}C$ records were shown to correlate significantly with each other and local rainfall (Woodborne et al., 2016).

2.6.8 Summary of literary review

Tree-ring width studies for *Widringtonia cedarbergensis* in the Western Cape had failed to yield a strong correlation with climate and February and Stock (1999) tried to improve on this using tree-ring $\delta^{13}C$ analysis. The depleted $\delta^{13}C$ trend of atmosphere was identified in the chronology but climate correlation was not successful. There has been no further dendroclimatic research published for this species in the Cedarberg.

Stable isotope analysis ($\delta^{13}C$ and $\delta^{18}O$) on old specimens of *Breonadia salicina* from northern Limpopo yielded a 600-year tentative moisture availability and humidity record which concluded that future research would benefit from a modern tree analogue (Norström et al., 2008, 2005).

A modern *Podocarpus latifolius* $\delta^{13}C$ analogue was developed by Hall et al (2008) for northern KwaZulu-Natal which reportedly showed some coherence with the archaeological *Podocarpus* charcoal. Coherence in the $\delta^{13}C$ series confirmed that *Podocarpus* has dendroclimatic potential and can be studied using stable isotopes.

The variability in *a* $\delta^{13}C$ chronology from *Mimusops caffra* specimens that grew on the coastline of northern Kwa-Zulu-Natal provides a potential measure of past rainfall but Hall et al. (2009) demonstrated using wavelets that long term climate forcing was probably chaotic and that deterministic climate models would be difficult to develop.

Adansonia digitata L. tree-ring $\delta^{13}C$ time series from modern and old tree specimens from northern Limpopo, on the border of South Africa and Zimbabwe have shown strong coherence. Rainfall

decadal and centennial oscillations were identified in the $\delta^{13}C$ chronology as well as a rainfall regime shift caused by a northward displacement of the subtropical westerlies (Woodborne et al., 2015)

Stable isotope analysis has been more successful in dendroclimatic research than ring-width studies in South Africa. Where the stable isotope research described above has used modern analogues to study very old tree specimens, a deeper species understanding has been developed for a particular site and this has resulted in better interpretations of climate. The limited number of dendroclimatic studies highlight the need for more research (Figure 7). The last ring-width study undertaken was in 1998 (February and Stock, 1998). Currently the majority of dendroclimatic research in South Africa is based on the use of stable isotope analyses of growth rings.

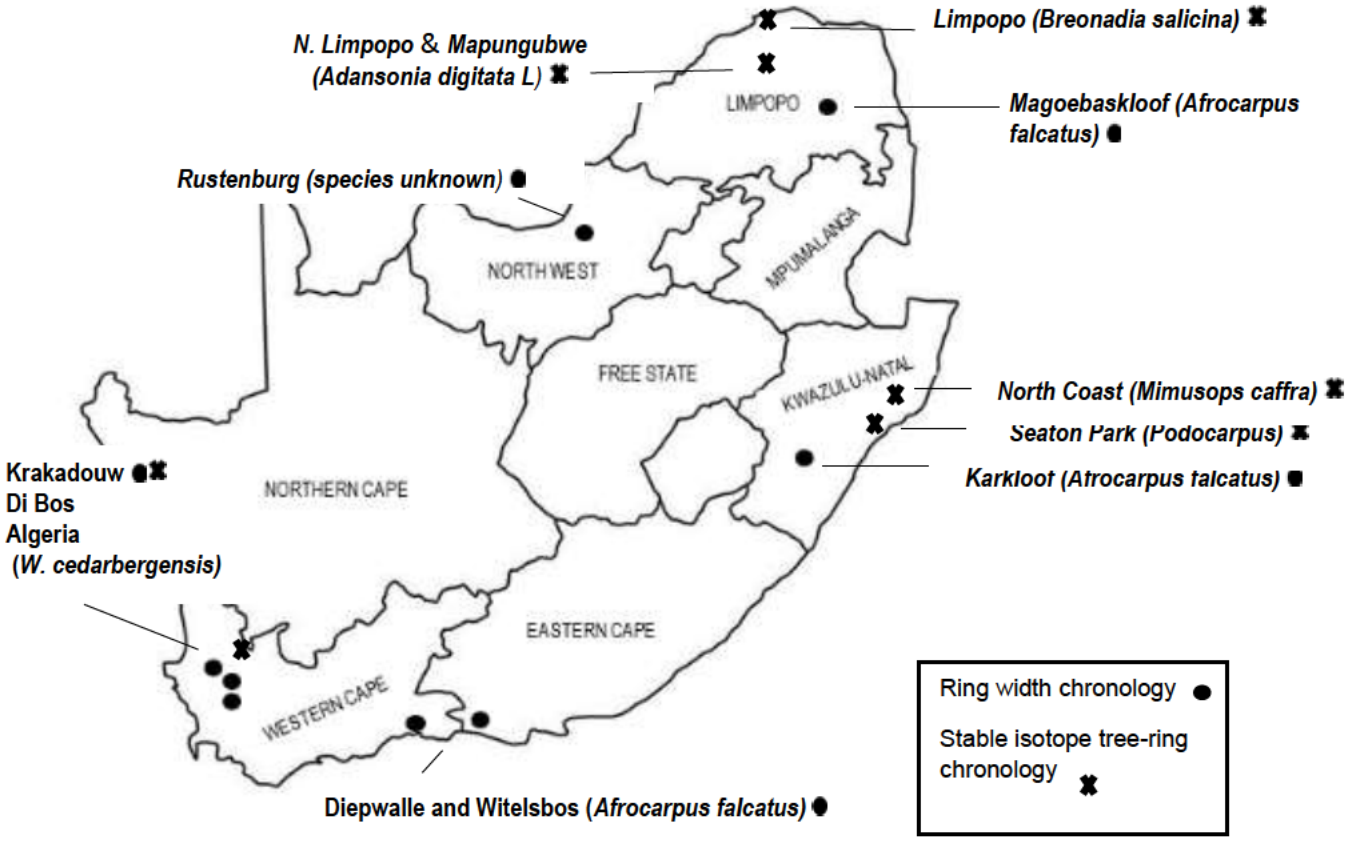

Figure 7: Locations of dendroclimatic tree-ring studies completed in South Africa.

2.7 *AFROCARPUS FALCATUS* MUSEUM SPECIMENS IN SOUTH AFRICA

There are two *Afrocarpus falcatus* museum cross-sections housed in South-African Museums. Both have been the subject of ring width studies (Hall, 1976; Thackeray, 1996; Thackeray and Potze, 2000; Vogel et al., 2001). In this thesis, the museum specimen studied by Hall (1976) will be referred to henceforth as the Karkloof specimen, and the Thackeray (1996) studied museum specimen will be referred to as the Knysna specimen. The Karkloof specimen is housed in the KwaZulu-Natal Museum, and the Knysna specimen is housed in the Ditsong National Museum of Natural History.

These studies assume that (a) the rings of *Afrocarpus falcatus* are annual; and (b) the ring-widths are formed exclusively as a response to rainfall. These studies had no supporting evidence on which to base these assumptions. Later, studies showed that *Afrocarpus falcatus* do produce annual rings but for those tree-ring series analysed, missing and false rings were commonplace (Curtis et al., 1978; February and Stock 1998; McNaughton and Tyson 1978). Vogel et al (2001) provides radiocarbon dating evidence of missing and fake rings for the Karkloof specimen. It is reasonably certain that the ring-width measurement series for the Karkloof and Knysna specimens are not annually resolved. The characteristics of the growing sites of the Karkloof and Knysna forest provide some explanation for the dating uncertainties. Both specimens grew in closed canopy Mistbelt Mixed Podocarpus Forests (Figures 8, 9). Section 1.2 explained how tree ring formation from this type of site is dominated by non-climatic factors which influence tree-ring structure and ring-width. This is a serious problem for ring-width studies on a single sample because, as explained in Section 1.3.2, the statistical error is anticipated to be well over 50%. Under these circumstances, proxy-based interpretation will be tentative, no matter which climate factor is used. A separate but potentially compounding issue is the choice of rainfall for use in both proxy-based interpretations. Even using traditional ring-width theory available at the time these studies were undertaken, the limiting factor for these sites would not automatically be identified as moisture. Similarly, stable carbon isotope theory has shown that the physiological control in moist sites is photosynthetic rate, which relates more to irradiance and temperature, and less to relative humidity and antecedent rainfall. Moist sites in mild climates have less limiting growth-controlling processes and as already explained, are more influenced by non-climatic factors (Fritts, 1976). The results of the study undertaken for *Afrocarpus falcatus* near Knysna in 1978 by McNaughton and Tyson identified these challenges.

Figure 8: Mistbelt Mixed Podocarpus Forest Diepwalle Forest, Knysna (Source: walking festival.co.za)

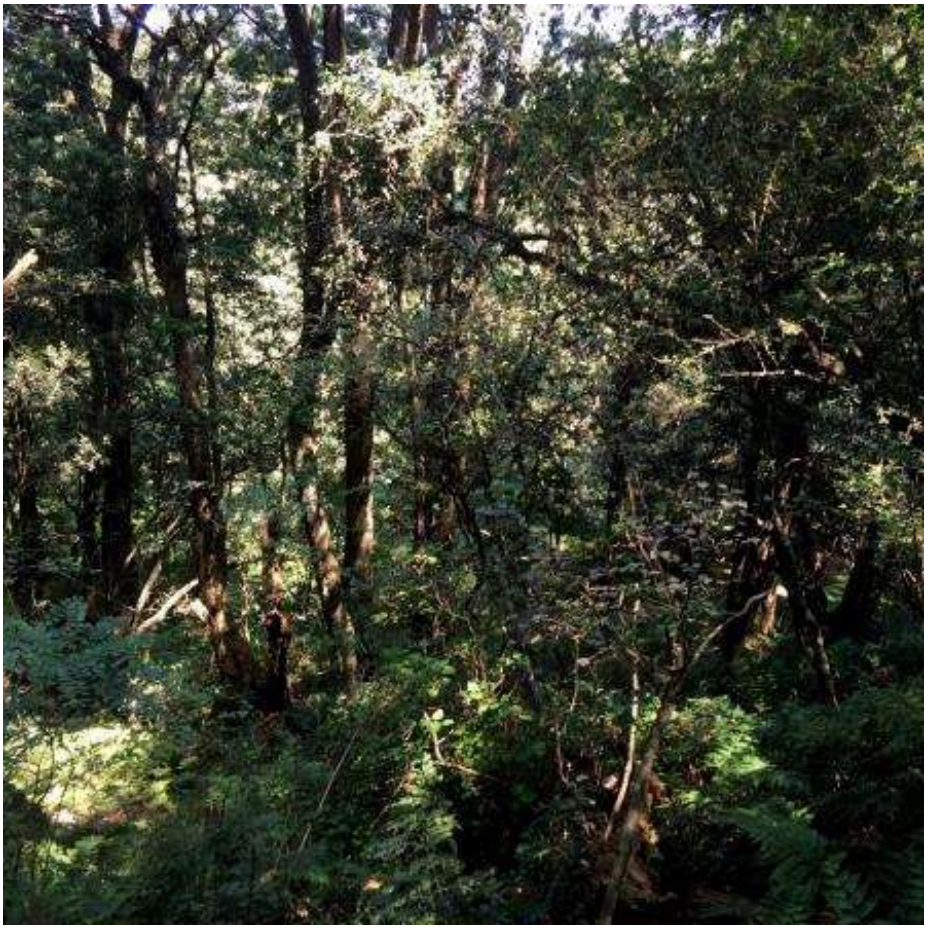

Figure 9: Mistbelt Mixed Podocarpus Forest in 'The Forest', Karkloof, KwaZulu-Natal

Thackeray (1996) and Thackeray and Potze (2000) together have been cited 17 times in scientific journals and books. Hall (1976) and Vogel et al., (2001) have earned a total of 148 citations, half of which fall into the last decade. The Karkloof rainfall proxy record is the more persistent and pervasive of the two and its influence will be reviewed in the next section.

2.8 THE KARKLOOF RECORD

According to the Google Scholar search engine, the Hall (1976) rainfall proxy record for KwaZulu-Natal has been cited 115 times in scientific journals and books. The Vogel et al. (2001) review of the Karkloof tree-ring series has been cited 33 times. Of the total 148 citations for the rainfall-proxy, 42% were cited in the last decade, and 66% were cited in the last 20 years (Figure 10). In the last decade, the Hall (1976) study was cited 25% more than Vogel et al (2001).

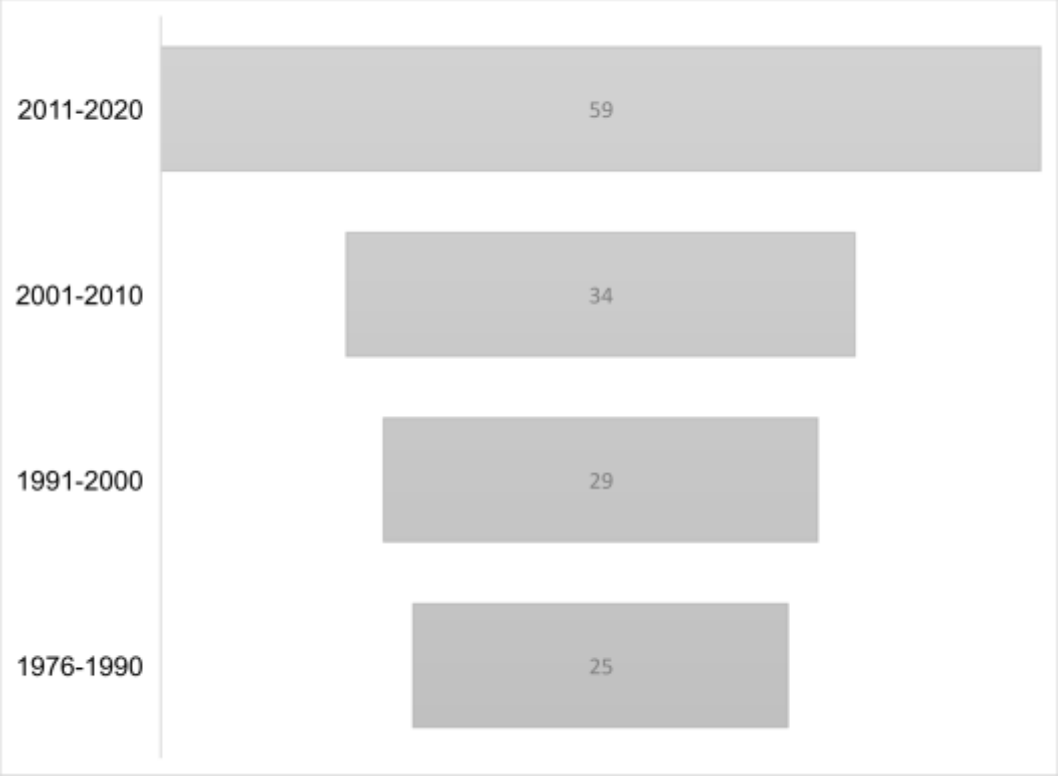

Figure 10: Published articles that have cited Hall (1976) and Vogel et al. (2001) arranged by the decade cited

Of all the scientific research areas, the field of south African archaeology has cited Hall (1976) the most (Figure 11). This is unsurprising given that the aim of the study was to provide evidence for the environmental conditions influencing late prehistoric and early historic human adaptations in KwaZulu-Natal and Zululand. Hall (1976) himself states that the study is a 'first attempt' and that additional

samples would still be required in the development of a representative ring-width series. At the time of the publication, the concept of a global tree network was being driven by dendroclimatologists from the Tree-Ring laboratory in Arizona. In 1980, South Africa was represented at the Second International Workshop on Global Dendroclimatology and the science in South Africa looked set to grow. As very long-lived tree specimens in South Africa are rare, and the results from Hall (1976) looked promising, efforts were directed to the assessment of modern *Afrocarpus falcatus*. Working with the species was reportedly too difficult and after 1998 ring-width studies were surpassed by stable isotope analysis. The initial intention to create a modern analogue from tree-ring widths for *Afrocarpus falcatus* was never achieved and thus the rainfall proxy record presented by Hall (1976) was never validated. Archaeologists frequently reference a dry or wet period from the Karkloof ring-width measurement series to corroborate a proposition. Hall (1976) has had such an insidious influence probably because there is such a dire need for information on past climate in South Africa.

Although dendroclimatic studies make up the second highest field referencing the Hall (1976) study, a closer look reveals that most citations relate to stable isotope studies that are merely listing Hall (1976) as part of tree-ring work already completed in South Africa. These citations are therefore the least concerning.

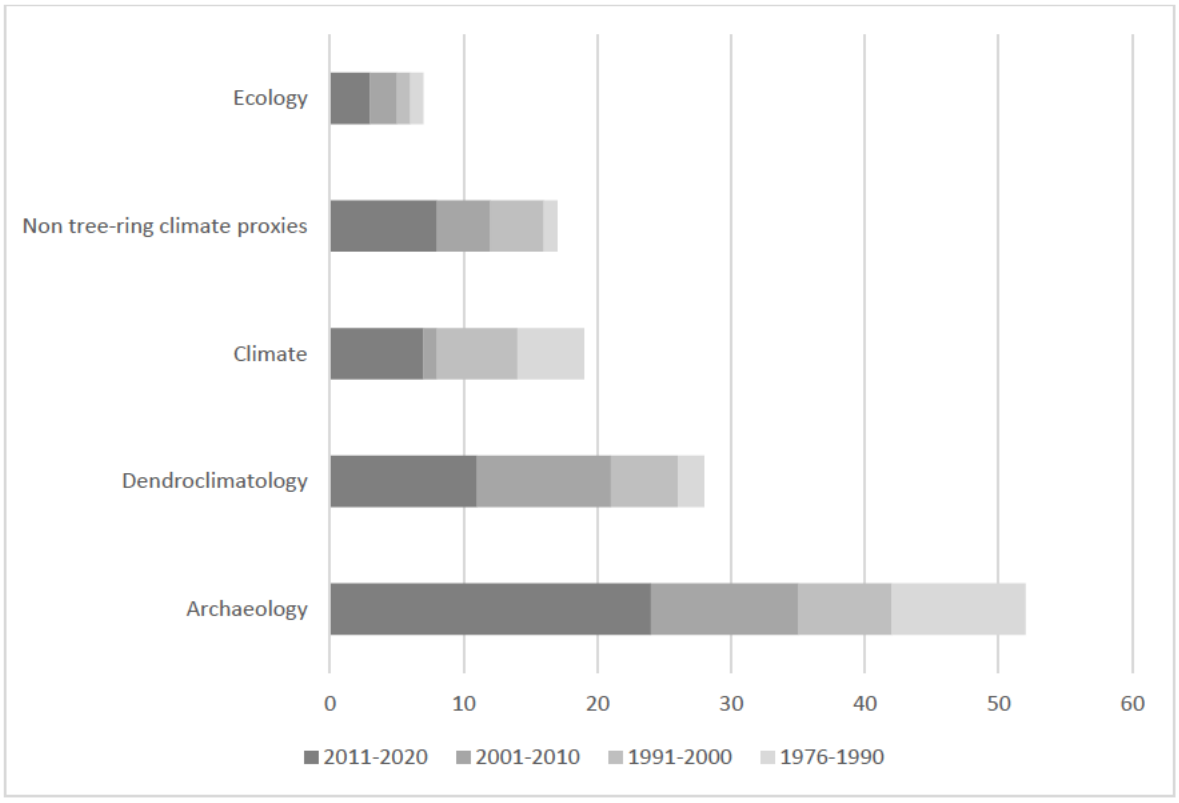

Figure 11: Published articles that have cited Hall (1976) and Vogel et al. (2001) listed by scientific field and decade of study

Of most concern would be instances where the Karkloof ring-width measurement series have influenced the development of other environmental proxy records. One such instance is the development of a 3000-year high-resolution stalagmite based record of palaeoclimate for north-eastern South Africa (Holmgren et al., 1999). The Karkloof ring-width measurements were used to identify annual growth layers in the stalagmite, and to assign dates to the record. Unlike the Karkloof specimen, it was noted that the stalagmite record did not align with summer rainfall oscillations of Tyson and Dyer (1975). Further validation of the Karkloof ring-width series and its relationship with climate, through the development of a modern analogue, would also serve to test the Holmgren et al. (1998) stalagmite-based record.

CHAPTER 3: TREE-RING WIDTHS

3.1 INTRODUCTION

The structure of this Chapter deviates from the traditional structure of a research thesis. As there are two tree-ring environmental proxies being investigated (tree-ring widths and stable carbon isotopes ($\delta^{13}C$)), each proxy has a separate chapter which presents the methods, results, discussion and a conclusion specific to the proxy being analysed. This chapter deals specifically with the tree-ring width proxy approach. The next chapter (Chapter four) will report on the use of $\delta^{13}C$ as a tree-ring environmental proxy.

The aim of this thesis was to develop a modern analogue for *Afrocarpus falcatus* from the growing site of the Karkloof and to investigate tree growth-climate relationships. The objectives were:

1 To develop a mean tree-ring width-based chronology using classic methods (Chapter three);

2 To develop a mean stable carbon isotope ring-based chronology (Chapter four); and

3 To test the mean ring-width (Chapter three) and $\delta 1^{3}C$ series (Chapter four) against instrumental climate records of annual, summer, and winter rainfall, relative humidity, temperature, solar irradiance, evaporation, precipitation minus evaporation (p-e) and sun duration.

This Chapter three thus addresses objective one and two.

In the literature review, it was established that a closed canopy environment causes a high noise-to-signal ratio and affects coherence between ring-width samples. Compression and ring-width eccentricity serve to obscure common signal between the series. This chapter will describe the methods used and results obtained for tree-ring width analysis of *Afrocarpus falcatus* from the Karkloof growing site. The discussion will review the extent to which the analysis was able to address the factors affecting tree-ring width time series that were applicable to this site.

3.2 STUDY AREA

The study area is a forest situated east of the Karkloof range within the KwaZulu-Natal Midlands. The area straddles south-east facing slopes on two adjacent properties (UCL Timbers ('The Forest') and Mbona Private Nature Reserve) (Figure 12). The forest is classified as mist-belt mixed *Podocarpus* forest (Rutherford et al., 2006). The extent of the study area is 2-kilometres and lies between 1200 and 1500 masl on an average 23% incline (1:4.1). The steepness of the study area has resulted in the trees tilting their stems to counteract gravity. The forest is a mixed angiosperm-*Podocarpus*

composition typical of this elevation, with *Podocarpus latifolius* the dominant species (Adie and Lawes, 2011).

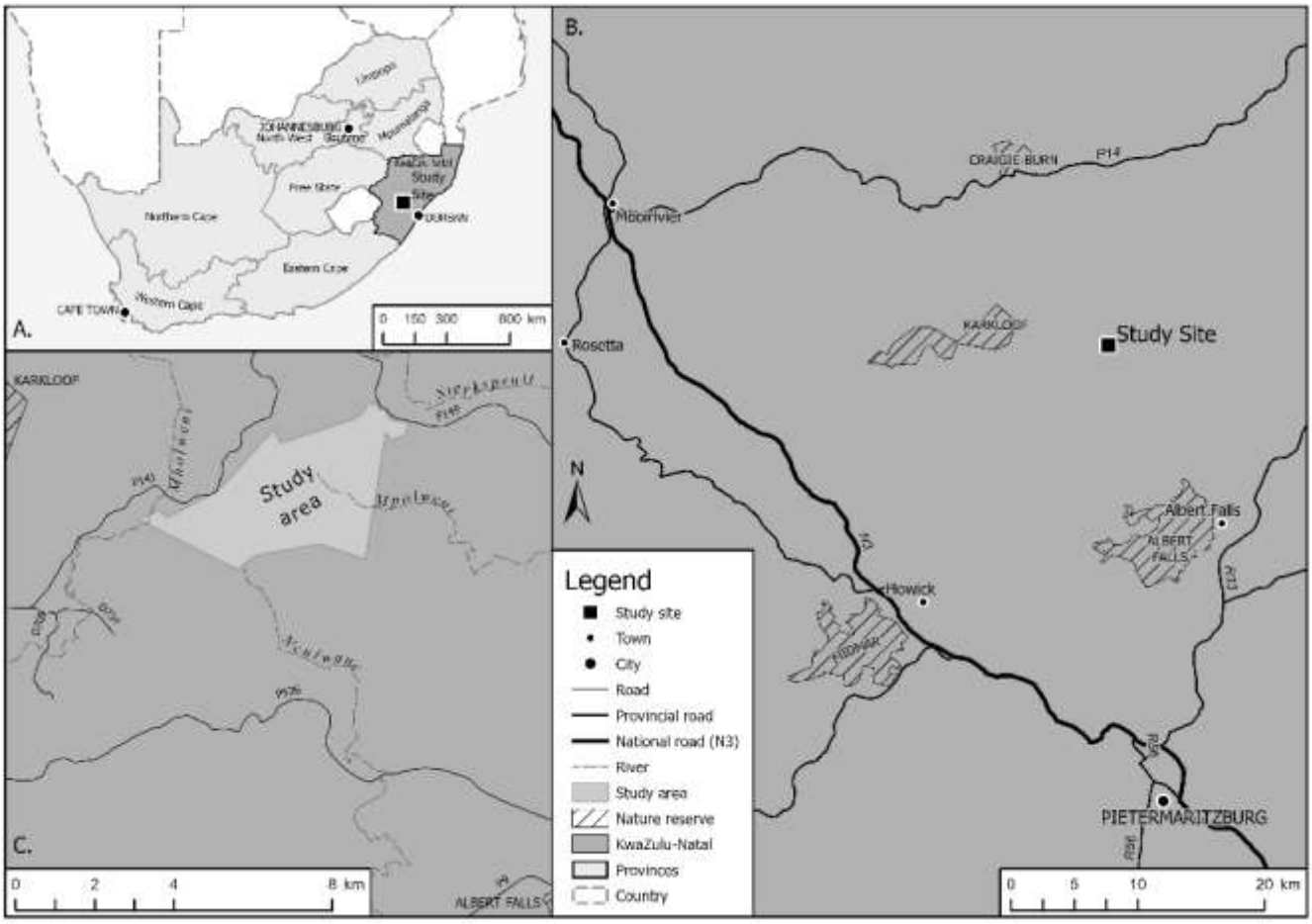

Figure 12: Location of tree-ring study area and climate station.

The climate is warm temperate and most of the annual precipitation falls in the summer months with the coldest months of the year falling in June and July (80%) (Figure 13, Table 1) (Tyson and Dyer, 1975).

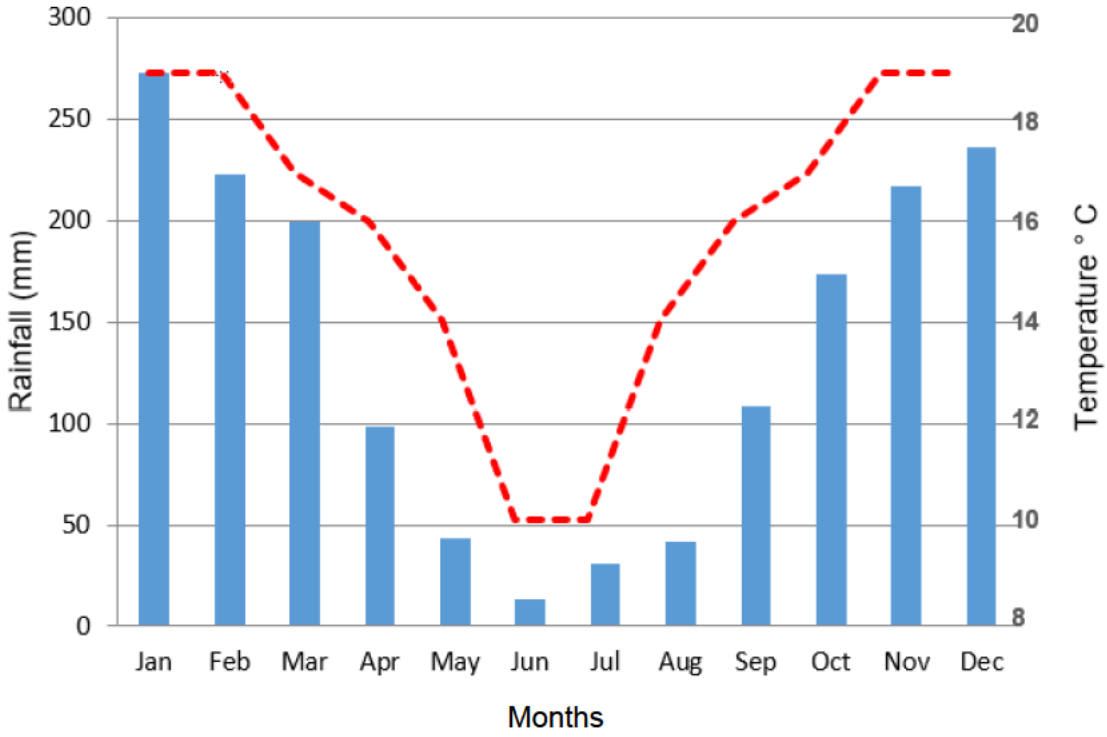

Figure 13: Study area Climograph (derived from OBSHIS4682 Climate data set, UKZN) showing average rainfall on the left y-axis in blue columns, and average temperature on the right y-axis by the red dashed line.

Table 1: Attributes of the study area (Climate data set OBSHIS4682 1950-1999)

Characteristic	Study area attribute
Metres above sea level (range)	1200 - 1500
Average slope (%)	20
Climate (Köppen-Geiger)	Warm, temperate, warm summer
Aridity (De Martonne)	Moist sub-humid
MAP (OBSHIS4682 1950-1999)	1271 mm
MAP range (OBSHIS4682 1950-1999)	606-1642 mm
Mean annual potential evaporation	1600-180mm
Summer rainfall season	October – March
Annual mean maximum temperature	22°C
Annual mean minimum temperature	10°C
Annual mean temperature	16°C
Summer mean maximum temperature	24°C
Summer mean temperature	18°C
Summer mean relative humidity	47%

The head of the Mpolweni River and its tributaries are situated within the study area. The mixed layered forest vegetation community with a closed canopy has a cooling effect on temperatures within the forest (Rutherford et al., 2006). The south-east facing slopes receive less direct sunlight than the northern grassed slopes and are much cooler, with some portions observed to receive more hours of shade than sunlight in a day (Figure 14).

Figure 14: Mistbelt Mixed Podocarpus Forest Karkloof, KwaZulu-Natal

3.3 CLIMATE RECORDS

Schulze and Horan (2007; 2010) sub-delineated Quaternary Catchments into Quinary Catchments, resulting in hydrologically interlinked and cascading Quinaries covering South Africa. A comprehensive 50 year database (1950 - 2000) of quality controlled (and infilled where necessary)

climate data (QDB) was compiled by Lynch (2004) and then expanded to the Southern African Quinary Catchments Database (QnCDB) by Schulze and Horan (2007; 2010). The Karkloof study area falls within the U20D quaternary catchment. The nearest rainstation to the study area is 0269532A which has 60 years of climate data (Figure 15). The 60 years of climate data from this station was used to develop a datasaet entitled OBSHIS4682. The tree-ring variability developed from this study area was compared to this OBSHIS4682 climate data set. It is acknowledged that the instrumental record for this period may not be representative of the climate of the past, and that tree growth responses to climate may also have been different to modern day response. The OBSHIS4682 climate records are contained within Appendix B.

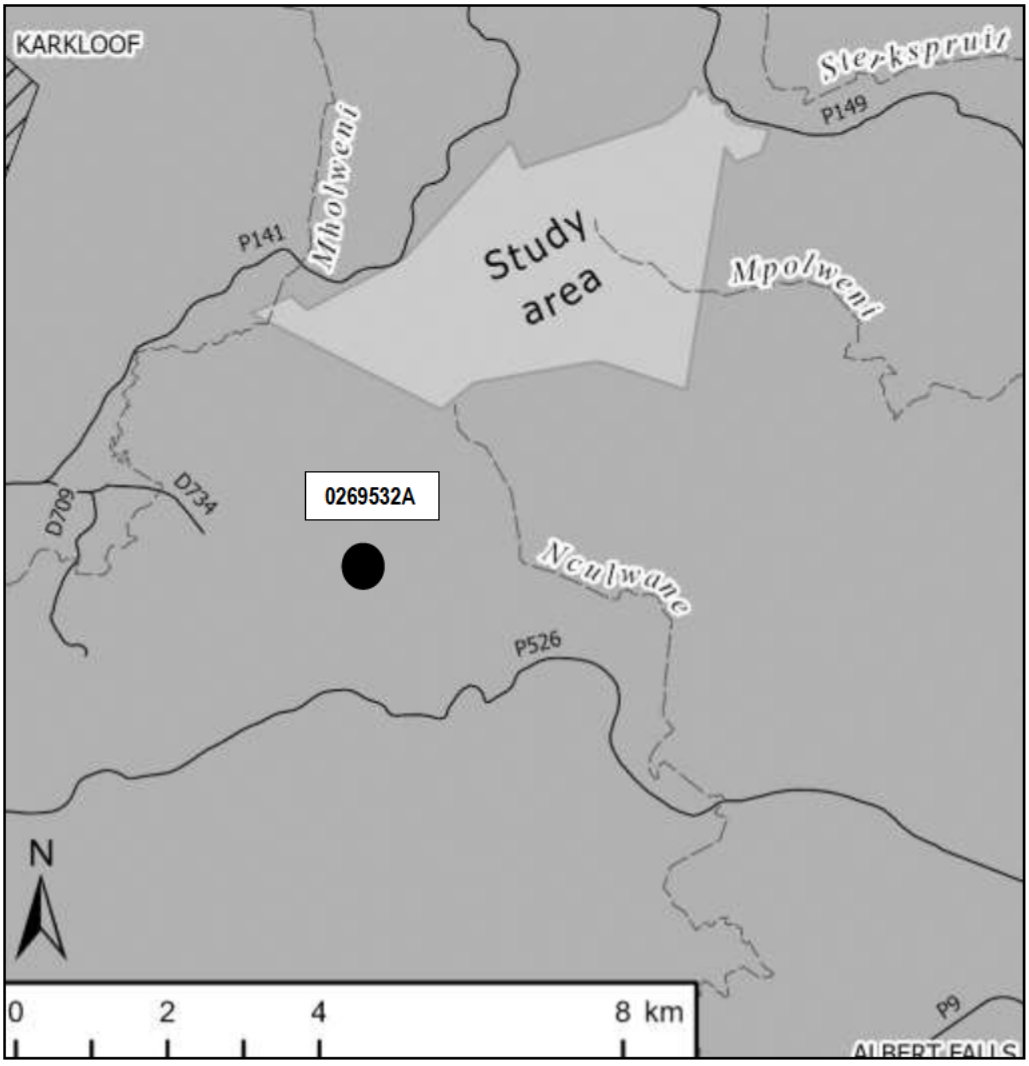

Figure 15: Map showing the location of rainstation 0269532A in relation to the study area

3.4 METHODS

3.4.1 Boring and sample preparation

A Haglöf incremental borer with a 12mm diameter drill bit styled end was used to extract a cylindrical core from the stem of 20 *Afrocarpus falcatus* trees. Cores were extracted at breast height in the centre of each trunk. Multiple cores were taken from 9 of the 20 trees to assess within tree ring-width variability. Where two cores from a tree were taken, one was taken at 45° to the slope, and the other was taken at 90° to the slope (Appendix A: Field sampling records).

Cores were mounted in wooden blocks with a vertical orientation to reveal the ring structure. A second mount was glued to the upper half of the core, and then the core was split in half with a fine saw. Once dry, the core was split in half with a fine saw and polished with progressively finer sanding grit between 125 µm and 600 µm to remove striations created by the previous sanding grit size (Orvis and Grissino-Mayer, 2002).

3.4.2 Crossdating, measurement and inter-series correlation

Prior to measurement, the standard dendrochronological crossdating method of skeleton plotting was undertaken (Stokes and Smiley, 1968). The width of 27 cores from 20 trees were measured to the nearest 0.01 mm using TSAPLINTAB (Rinntech, 2011). All raw tree-ring width measurement records are contained within Appendix C. Crossdating and measurement accuracy was investigated using COFECHA. No calendar dates were assigned to the ring-width measurement series, and the undated collection was run through COFECHA to establish internal dating. All possible matches identified by COFECHA were investigated, and where appropriate, series were adjusted (offset) to better positions relative to the collection using criteria developed for the analysis (Table 2). A flexibility of three ring positions was set to account for potential discrepancies relating to missing and/or false rings.

The realigned collection was re-run in COFECHA to measure the inter-series correlation. Prior to correlation analysis, COFECHA applied a general smoothing to enhance common signal for the crossdating quality check. Unwanted trends were removed using a smoothing spline with a 50% frequency response at a wavelength of 32 years. Segment lengths tested for correlation were set at 50-year segments with 25-year lags for successive segments. Pre-whitening to remove low-frequency variance in the ring-width series before comparison using autoregressive modelling was selected. Each series was transformed via spline fitting, autoregressive modelling, and log transformations. The transformed series were tested against a master chronology using correlation analyses (COFECHA automatically removes the series being tested from the master chronology). COFECHA then assesses the performance of each series in relation to the mean. A and B flags draw attention to

portions of the series that perform badly (A flags identify ring widths that are unique to the stand and B flags list better offsets for individual series in relation to the mean). Where possible, the flagged portions with low correlation to the mean were cut out and the resulting split portions were retained. Where suggested dating offsets resulted in realistic improvements within the developed acceptance criteria (Table 2), adjustments were made to the end-date positions for better alignment with the mean. Series which significantly lowered the mean inter-series correlation were discarded. The revised collection was then re-run in COFECHA to obtain the final mean inter-series correlation.

Table 2: Acceptance criteria applied to ring width series

	Type	Offset ring movement / year	Length	CorrC to rest of collection	T Test
1	whole series	=<3 years	=>50 rings	r=>0.3258	T Test=>2
2	Split segment	None	=>50 rings	r=>0.3258	T Test =>2
3	Split segment	None	=>30-49 rings	r=>0.5	T Test =>2

3.4.3 Detrending and averaging

To standardise the ring-width series and develop the mean chronology, the dendrochronology Program ARSTAN was used (Holmes et al., 1986). ARSTAN detrends and indexes (standardises) ring-width series before removing endogenous trends which it calculates for each series through estimation of the mean value function (Holmes et al., 1986)

Growth trend

Investigation of growth trends for each series was undertaken using a running mean window of ten years, a growth percentage change of 10%, and a standard error threshold of 2. Potential suppression and release events for each series were identified in ARSTAN. A stand disturbance analysis was run in ARSTAN and potential endogenous stand disturbances were identified. These were all considered when user interactive detrending within ARSTAN was undertaken to remove unwanted growth trends within each series. Four detrending options were investigated to determine the best growth curve fit for each series: (a) a least squares regression line was independently fit with a curve and the identified trend was removed. Linear regression (any slope) was chosen because the series are relatively short and have an unusual growth pattern that a negative exponential curve cannot accommodate (Cook, 1985); (b) a cubic smoothing spline with a 50% frequency response at a wavelength of 32 years was applied to each series with a ratio method to stabilise the variance, scaling all the series to mean index values of 1; (c) a linear or cubic smoothing spline was individually applied according to best fit;

and (d) double-detrending was undertaken by first detrending with a linear regression (any slope) followed by the cubic smoothing spline. For all options, a ratio method was applied to stabilise the variance, scaling all the series to mean index values of 1. The resulting indices were compared, and the best performing detrending option was chosen.

Persistence

Non-robust autoregressive modelling was used to prewhiten time series so that non-random, year to year natural and unnatural persistence was removed from the smoothed series. First, multivariate autoregressive modelling was performed (pooled autoregression) followed by univariate autoregressive modelling to fit an autoregressive process of the selected order to each series (autoregressive coefficients are calculated for each series) and lastly, multivariate modelling was re-applied to check for residual lag effects.

Chronology computation was done by means of a biweight robust mean estimation. The resulting mean ring-width chronology was then compared to climate records (rainfall, relative humidity, radiation, temperature).

3.5 RESULTS

3.5.1 Within tree variability

Variability within trees was investigated for 9 trees. Visual observation confirmed that there were missing rings between radii from within the same trees. Correlation within-trees ranged from between -0.16 and 0.30 with a mean correlation of 0.018. It was noted that through small adjustments of between three and five ring offsets between radii that the correlation range could be improved to between 0.16 and 0.72 with a mean correlation of 0.37 (Table 3).

Table 3: Within tree variability

No.	Sample	Ring 1	CorrC with annual ring assumption	Experimental offset to test relationship	Revised CorrC
1	PF1	2013	0.20	+5	0.35
	PF1BJB	2017		0	
2	PF3SW	2013	0.30	+2	0.73
	PF3BJB	2017		0	
3	PF5B	2014	-0.15	0	0.40
	PF5C	2017		0	
4	PF12A	2013	-0.12	+3	0.28
	PF12C	2017		0	
5	PF14	2014	-0.10	+2	0.16
	PF14	2014		0	
6	PF15	2014	0.01	+6	0.54
	PF15	2014		0	
7	PF17AB	2014	0.04	-6	0.24
	PF17CD	2014		0	
8	PF19AB	2014	-0.16	-2	0.28
	PF19CD	2014		0	
9	PF20AB	2014	0.15	+4	0.42
	PF20CD	2014		0	
	Average		**0.018**		**0.37**

3.5.2 Crossdating and between tree variability

Crossdating between trees was not achieved through skeleton plotting (Stokes and Smiley, 1968). Ring-width measurements assumed dating relative to the last growing season of the incremental core dates. The Mean Sample Segment Length (MSSL) for the 20 ring-width measurement series was 104 years. Mean inter-series sensitivity was 0.522. The mean inter-series correlation for the collection, was -0.042 (Table 4).

Table 4: Statistics for the 20 tree-ring width series (COFECHA)

								Unfiltered original ring width measurements				Filtered detrended series measurements			
Sequence	Series	Assigned year	Length	No. Segments tested	No. flags (possible dating problems)	Correlation with master chronology	Mean msmt average of all ring measurements	Max msmt maximum ring measurement	Standard deviation	Autocorrelation	Mean sensitivity	Max value largest index value in the detrended series	Standard deviation	Autocorrelation	Autoregression modelling order (AR)
1	PF1	2013	66	1	1	.030	1.69	3.24	.756	-0,92	.508	2.95	,87	-,072	1
2	PF3SW	2013	101	4	4	.206	1.69	4.33	.871	.302	.477	2.63	.451	-.066	1
3	PF4	2014	119	5	5	.077	.128	4.02	.639	.467	.410	2.63	.432	-.003	1
4	PF5	2014	84	3	3	.068	.164	5.06	1.051	.364	.521	2.78	.613	.027	1
5	PF6	2014	71	3	3	-.159	.155	4.73	.899	.187	.518	2.98	.678	-.011	1
6	PF7	2014	99	4	4	-.094	.126	6.46	.868	.148	.552	3.34	.674	.001	1
7	PF8	2014	41	1	1	-.282	.143	1.92	.387	.159	.377	2.59	.526	-.010	1
8	PF9	2014	78	1	1	-.050	.86	4.15	.707	.366	.607	2.92	.490	.010	2
9	PF10	2014	75	3	3	.087	1.90	5.05	.990	.433	.401	2.80	.510	.015	3
10	PF11	2014	94	4	4	-.181	1.79	4.11	.816	.198	.474	2.81	.538	-.059	1
11	PF12	2014	132	5	5	-.091	1.36	5.19	1.044	.320	.543	3.04	.464	.042	1
12	PF13	2014	69	3	3	.029	1.88	5.90	1.343	.454	.620	3.14	.550	-.107	2
13	PF14	2014	145	6	6	-.060	1.34	4.67	.978	.100	.849	2.64	.476	-.006	2
14	PF15	2014	73	3	3	-.245	1.25	3.21	.674	.190	.585	2.82	.501	-.031	3
15	PF16	2014	92	4	4	.139	1.83	3.55	.750	.352	.385	2.61	.447	-.032	1
16	PF17	2014	97	4	4	.053	2.14	4.56	.827	.155	.405	2.84	.488	.005	2
17	PF18	2014	81	3	3	-.082	1.52	3.68	.884	.507	.582	2.61	.576	-.026	1
18	PF19	2014	142	6	6	-.040	.86	4.15	.707	.366	.607	2.92	.490	.010	2
19	PF20	2014	109	4	4	-.183	2.19	8.38	1.388	.452	.543	2.61	.438	.007	1
20	PF21	2014	138	5	5	-.100	.99	2.15	.519	.271	.525	2.81	.518	.021	3
	Mean		**104**		**78**	**-.042**	**1.63**	**18.7**	**.974**	**.296**	**.522**	**3.34**	**-.517**	**-.014**	

COFECHA suggested internal dating between undated measured series yielded 190 possible matches. Using the thesis-developed ring-width series acceptance criteria (Table 2) and the flags generated by COFECHA, each ring width measurement series, and the wood, was analysed. No ring-width measurements were amended during the analysis. The results of the analysis found that there was no significant correlation with the mean for 15 samples within the offset allowance of three ring movements. These series were set aside. Bad segments were removed from three samples to improve correlation and a further two whole samples were retained unaltered. Offsets for two of the series were applied. For the five retained ring-width measurement series, the MSSL was 107 years. The mean sensitivity was 0.513 and the mean inter-series correlation was 0.43 (Table 5).

13 *Table 5: Dates and between tree statistical relationships for the retained Afrocarpus falcatus samples*

No.	Floating series	length	Assigned Ring period date	Offset and date change	Retained rings	removed	Inter-series CorrC	T Test	Overlap (rings)
1	PF3	101	1913-2013	-	All	0	0.60	7.4	100
2	PF7	99	1916-2014	-	51 1964-2014	48	0.33	2.4	50
3	PF11	93	1920-2014	3 offsets 1918-2011	51 1939-1989	42	0.33	2.4	50
4	PF20	107	1906-2014	2 offsets 1904-2012	33 1950-1982	74	0.58	3.9	32
5	PF21	138	1877-2014	-	All	0	0.33	4.0	137
	Total	537			373	164			
	Mean	107			75	33	0.43	4.0	74

14

3.5.3 Detrending and averaging

Investigation and removal of growth trends

Results for the detrended series ((a) linear regression (any slope); (b) cubic smoothing spline; and (c) a mix of a and b and; (d) double-detrending using first linear regression and then a cubic smoothing spline) were compared and the best performing option was (a) linear regression (any slope) (Table 6).

Table 6: Growth trend investigation and results for 3 detrending options for the mean ring-width series

	Detrending option	Inter-series correclation	EPS
a	Linear regression (any slope)	0.43	0.737
b	cubic smooting spline (50% frequency, 32 years)	0.35	0.676
c	Mix of a and b	0.35	0.676
d	Double-detrend (linear regression (any slope) then cubic smooting spline (50% frequency, 32 years))	0.35	0.676

Standardisation

Linear growth curves were removed for all five ring-width measurement series (Figures 16-20)

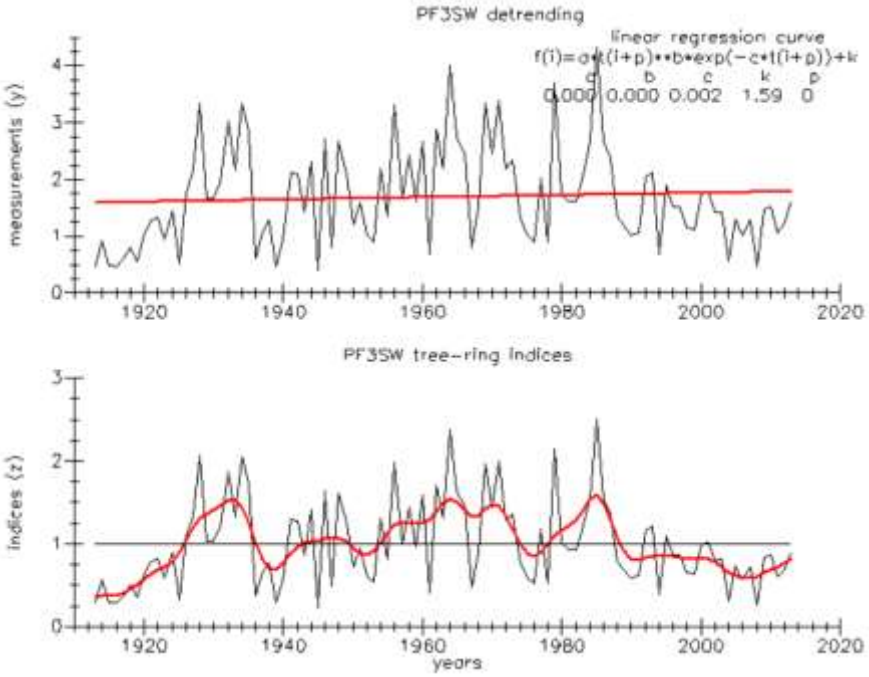

Figure 16: Sample PF3 ring-width measurement series before (top) and after detrending with linear regression (bottom) Ring-width measurement index (black) and detrended ring-width residual index (red) (ARSTAN).

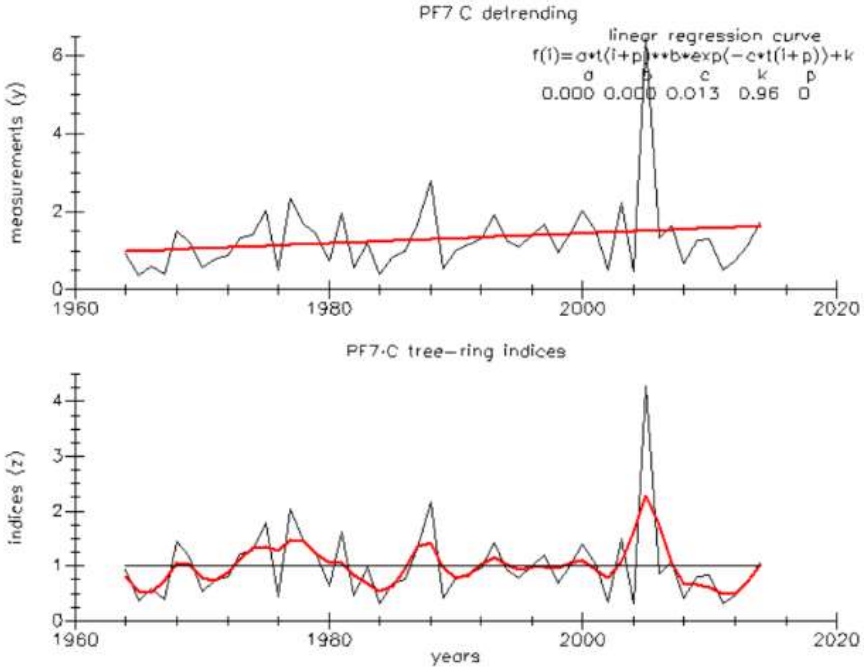

Figure 17: Sample PF7 ring-width measurement series before (top) and after detrending with linear regression (bottom) Ring-width measurement index (black) and detrended ring-width residual index (red) (ARSTAN).

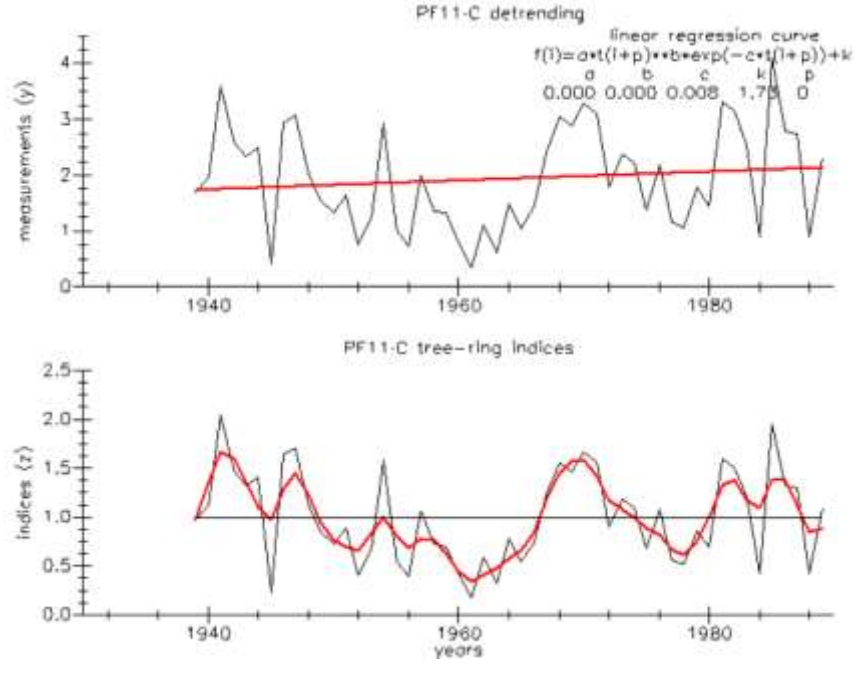

Figure 18: Sample PF11 ring-width measurement series before (top) and after detrending with linear regression (bottom) Ring-width measurement index (black) and detrended ring-width residual index (red) (ARSTAN).

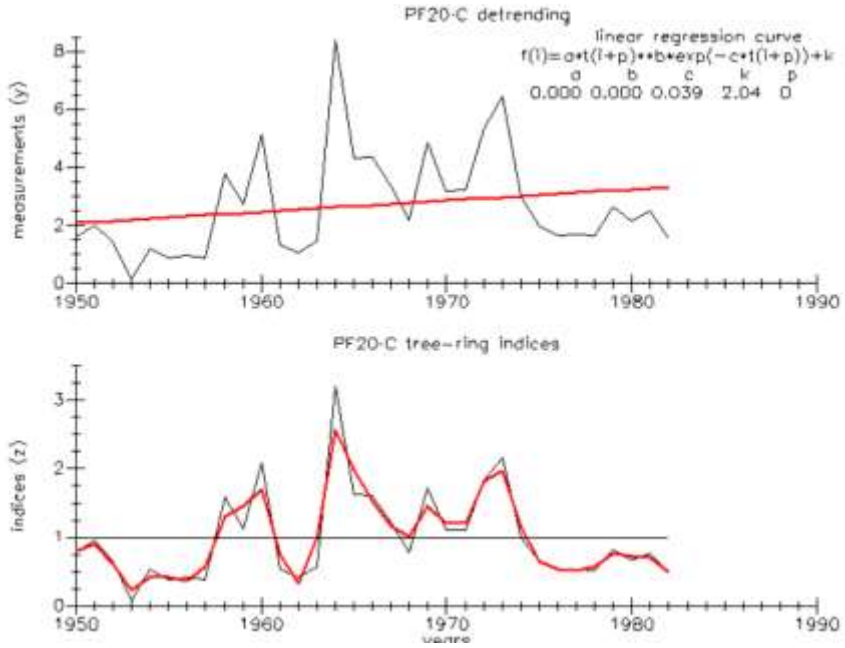

Figure 19: Sample PF20 ring-width measurement series before (top) and after detrending with linear regression (bottom) Ring-width measurement index (black) and detrended ring-width residual index (red) (ARSTAN).

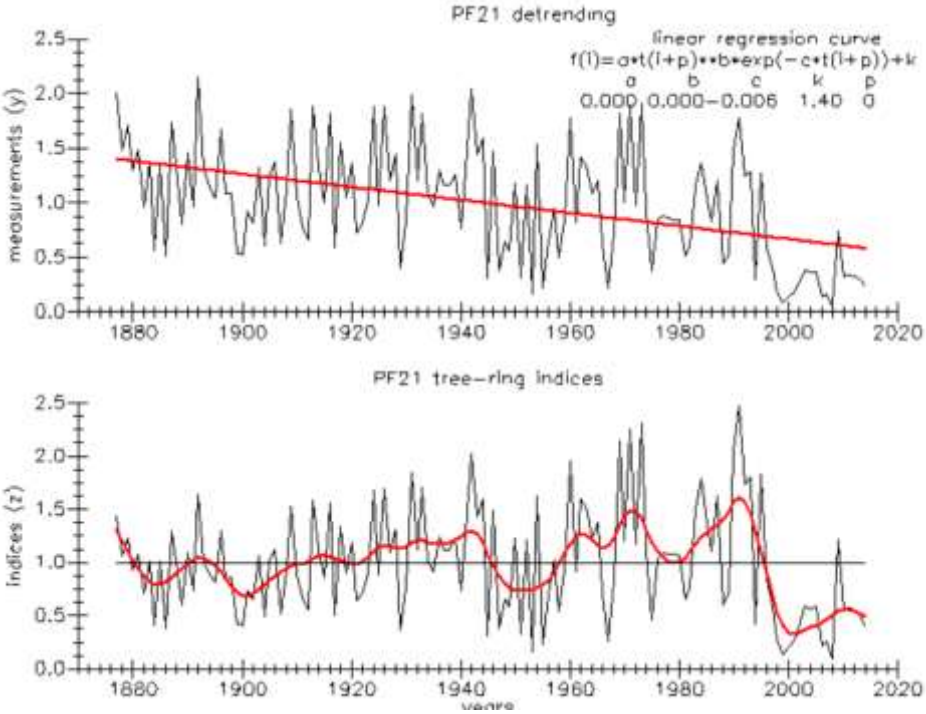

Figure 20: Sample PF21 ring-width measurement series before (top) and after detrending with linear regression (bottom) Ring-width measurement index (black) and detrended ring-width residual index (red) (ARSTAN).

Autoregression

After detrending and indexing each individual tree-ring series, non-robust autoregressive modelling prewhitened the time series to remove detected persistence. Multivariate autoregressive modelling was performed (pooled autoregression) followed by univariate autoregressive modelling to fit an autoregressive process of a selected order to each series and lastly multivariate modelling is re-applied to check for residual lag effects. The same order autoregressive process was selected by multivariate autoregressive modelling to fit to each series using its own coefficients. ARSTAN estimates of autoregression for the raw ring-width measurement series was order 2 (0.104) and for the residual indices, order 1 (0.018).

Averaging

The resulting biweight mean for the ring-width measurements and residual series are shown in Figure 21.

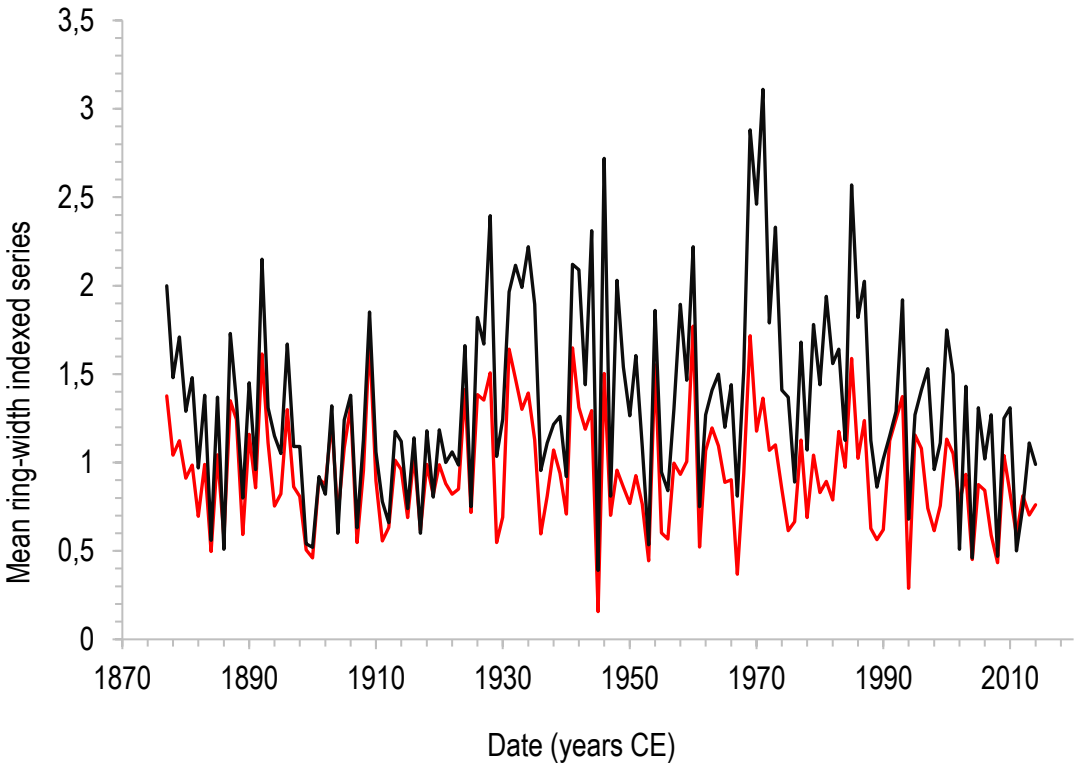

Figure 21: Mean ring-width measurement index (black) and mean detrended ring-width residual index (red)

Statistics for the mean ring-width measurement series are shown in Table 7 and 8.

Table 7: Statistics for the mean ring-width measurement series

First year	last year	total years	mean index	stdrd dev	skew coeff	kurtosis coeff	mean sens	serial corr
1877	2014	138	1.336	0.539	0.716	3.495	0.435	0.163

Table 8: Statistics for the individual ring-width measurement series

series	ident	first	last	year	mean	stdev	skew	kurt	sens	ac(1)
1	PF3	1913	2013	101	1.685	0.871	0.809	3.281	0.482	0.302
2	PF7_C	1964	2014	51	1.298	0.928	4.045	21.98	0.615	-0.117
3	PF11_C	1939	1989	51	1.936	0.920	0.290	2.359	0.493	0.305
4	PF20_C	1950	1982	33	2.702	1.810	1.574	5.117	0.492	0.377
5	PF21	1877	2014	138	0.990	0.519	0.163	2.253	0.529	0.267

Statistics for the mean and individual ring-width detrended residual series are shown in Table 9 and 10.

Table 9: Statistics for the mean ring-width residual series

first year	last year	total years	mean index	stdrd dev	skew coeff	kurtosis coeff	mean sens	serial corr
1877	2014	138	0.952	0.327	0.336	3.028	0.416	-0.128

Table 10: Statistics for the individual ring-width residual series

series	ident	frst	last	year	mean	stdev	skew	kurt	sens	ac(1)
1	PF3	1913	2013	101	1.002	0.454	0.557	3.203	0.537	-0.022
2	PF7_C	1964	2014	51	1.000	0.623	2.757	12.971	0.571	0.004
3	PF11_C	1939	1989	51	1.000	0.446	0.302	3.078	0.526	-0.001
4	PF20_C	1950	1982	33	1.000	0.606	1.883	6.175	0.571	-0.001
5	PF21	1877	2014	138	1.000	0.471	0.662	3.421	0.551	0.001

Comparitive statistics for the mean ring-width measurements and the detrended series are shown in Table 11.

Table 11: Statistics for the mean ring-width measurements and residual series

	Ring-with measurement series	Ring-width residual series
Mean R-bar	0.43	0.42
Mean EPS	0.740	0.737
Mean value	1.366	0.952
Standard deviation	0.539	0.327
Mean sensitivity	0.435	0.416
Signal to noise ratio	3.9	3.9

3.5.4 Climate-growth relationships

Climate-growth relationships

The mean ring-width measurement and residual indices were compared to climate records between 1950 and 1999 from climate data set OBSHIS4682. Correlation coefficients for annual rainfall, relative humidity, temperature, and solar irradiance were calculated. For the analysis, the series end date is assigned to 2014, which is the anticipated year for the youngest ring of the series (Table 12).

Table 12: Correlation coefficients for the mean ring-width series and OBSHIS4682 annual climate records between 1950-1999

OBSHIS4682 annual climate records between 1950-1999	Mean ring-with measurement series		Mean ring-width residual series	
	CorrC	T Test	CorrC	T Test
Annual total Rainfall	-0.09	-0.6	-0.06	-0.4
Annual average relative humidity	-0.29	-2.1	-0.28	-2.0
Annual average temperature	0.27	1.9	0.36	2.7
Annual average maximum temperature	0.14	1.0	0.20	1.4
Annual average minimum temperature	0.33	2.4	0.43	3.2
Annual average solar irradiance	-0.09	-0.6	-0.09	-0.6

The highest correlation was with average annual minimum temperature (Figure 22).

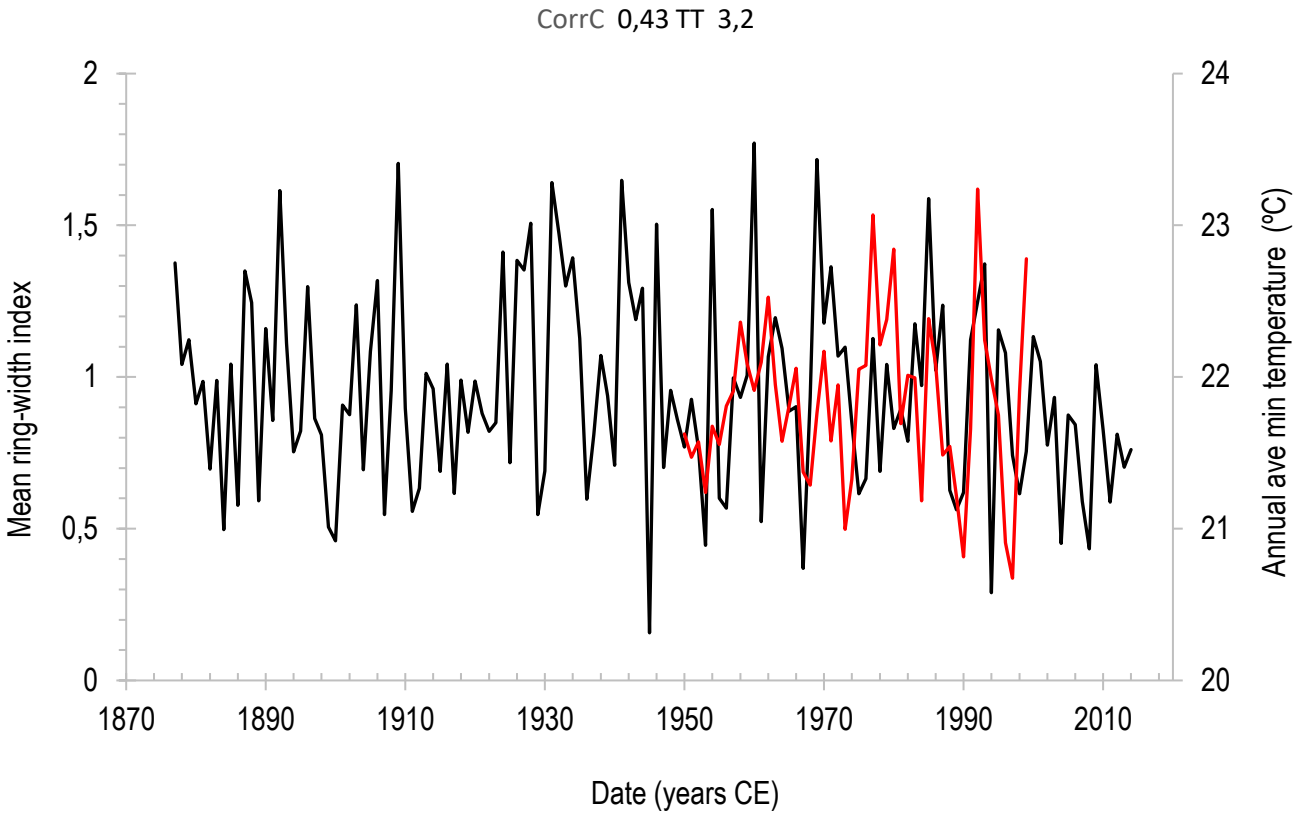

Figure 22 : Mean ring-width series shown on left y-axis, and average annual minimum temperatures between 1950-1999 shown on right y-axis

The mean ring-width measurement and residual series were compared to summer climate records between October and March (1950-1998) from data set OBSHIS4682 (Table 13).

Table 13: Correlation coefficients for the mean ring-width series and OBSHIS4682 (October – end March) between 1950-1999 climate data

OBSHIS4682 Oct-Mar climate records between 1950-1998	Mean ring-with measurement series		Mean ring-width residual series	
	CorrC	T Test	CorrC	T Test
Summer total Rainfall	0.24	1.7	0.20	1.4
Summer average relative humidity	-0.13	-0.9	-0.15	-1.0
Summer average temperature	0.02	0.1	0.12	0.8
Summer average maximum temperature	-0.08	-0.6	-0.02	-0.1
Summer average minimum temperature	0.17	1.2	0.30	2.2
Summer average solar irradiance	-0.22	-1.5	-0.20	-1.4

The highest correlations were with average summer minimum temperature and total summer rainfall (Figures 23, 24).

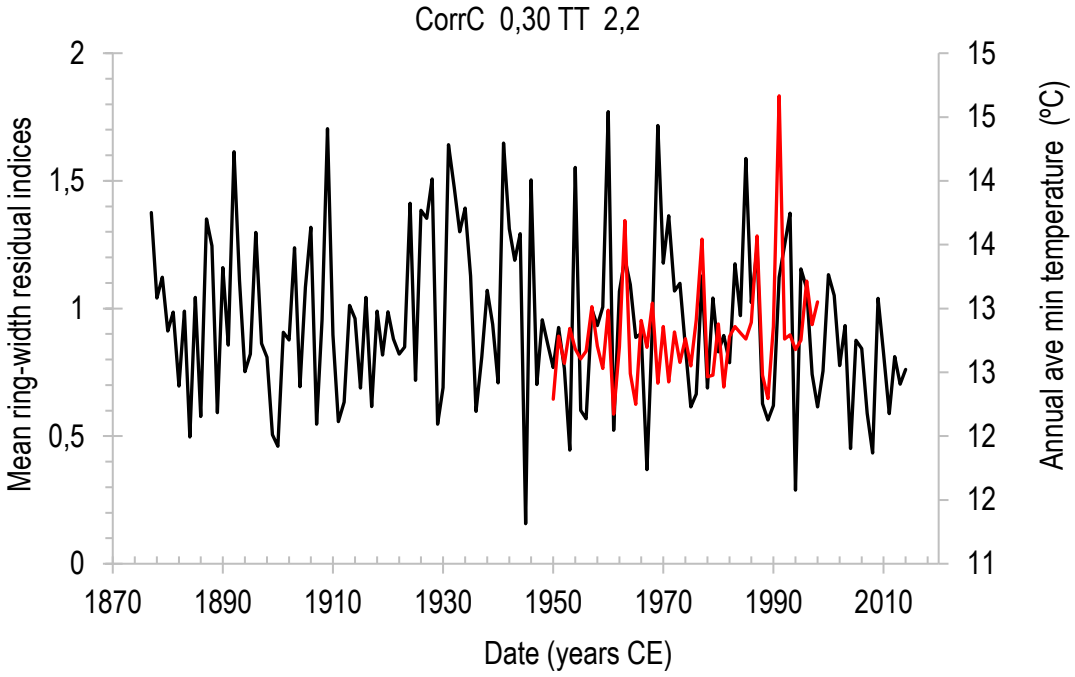

Figure 23: Mean ring-width series shown on left y-axis, and average summer minimum temperatures (October to March) between 1950-1999 shown on right y-axis

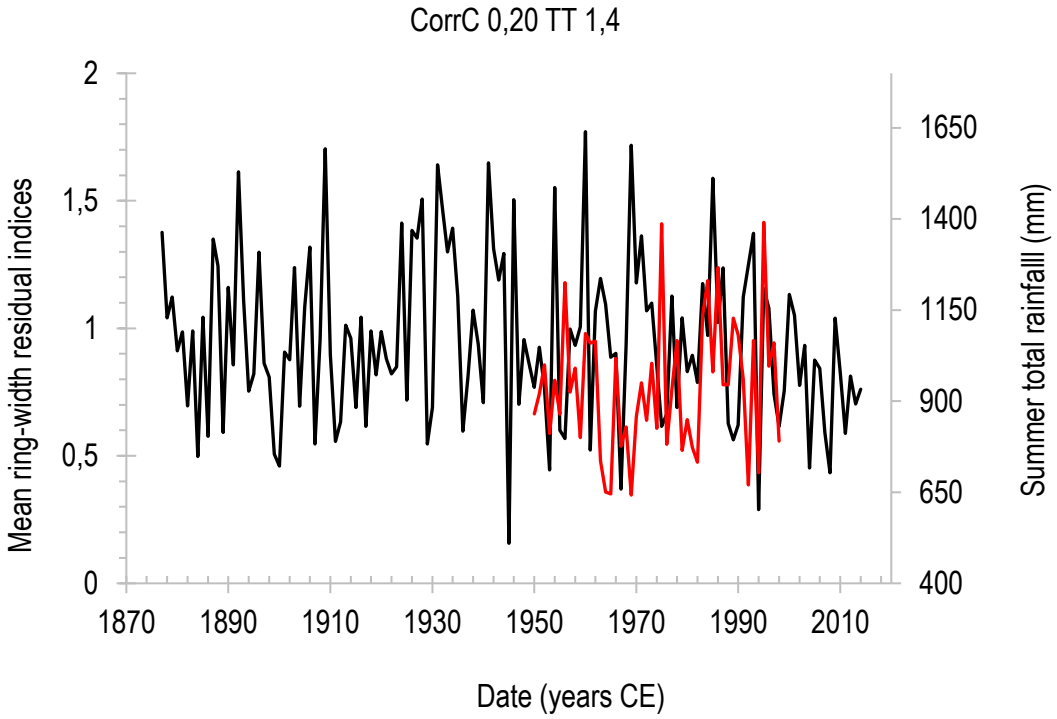

Figure 24: Mean ring-width series shown on left y-axis, and total summer rainfall (October to March) between 1950-1999 shown on right y-axis

The mean ring-width measurement and residual indices were compared to winter climate records between April and September (1950-1998) from data set OBSHIS4682 (Table 14).

Table 14: Correlation coefficients for the mean ring-width index and OBSHIS4682 (April –September) between 1950-1998 climate data

OBSHIS4682 Oct-Mar climate records between 1950-1998	Mean ring-with measurement series		Mean ring-width residual series	
	CorrC	T Test	CorrC	T Test
Winter total Rainfall	0.08	0.6	0.00	0.4
Winter average relative humidity	-0.17	-1.2	0.15	1.0
Winter average temperature	0.11	0.7	0.10	0.7
Winter average maximum temperature	0.02	0.2	0.01	0.0
Winter average minimum temperature	0.16	1.1	0.17	1.2
Winter average solar irradiance	-0.11	-0.8	-0.12	-0.8
Winter P-E	0.10	0.7	0.02	0.1

3.6 DISCUSSION

3.6.1 Compression and ring-width eccentricity

In response to forest incline, reaction wood in conifers is established as compression wood on the upslope side to maintain vertical orientation of the stem (Fritts, 1976). The study area has an average incline of 23%. This coupled with the low occurrence of *Afrocarpus falcatus* neccessitated sampling on the upslope for many of the samples, thereby encountering compression wood. Narrow rings and general tree-ring eccentricity were visually confirmed on most of the cores. These observations were consistent with those of other *Afrocarpus falcatus* ring-width studies (Curtis et al., 1978; February and Stock, 1998; McNaughton and Tyson, 1979; Vogel et al., 2001). For this reason, 15 cores were not included in the mean tree-ring width series; portions of three cores were split to remove bad segments; and only two whole samples were retained from the original collection. This confirmed the need for a larger sample size for ring-width analysis (>40 trees). The sampling strategy for the species and site should consider the sample size in conjunction with the feasibility of downslope sampling from tilted trees. Identifying trees that can be cored downslope might reduce the need for a larger sample size.

3.6.2 Missing and false rings

Missing rings for *Afrocarpus falcatus* were identified in other studies (Curtis et al., 1978; McNaughton et al., 1979; February and Stock, 1998; Vogel et al., 2001). Within-tree variability was investigated and missing rings between multiple radii from the same tree were visually confirmed. Within-tree correlations could only be attained by applying offsets between the series. As an example, the 2014 and 2018 sampled cores from PF3 (four years apart) were matched at two years apart (Figure 25). There are thus most likely two missing rings at the recent end of the 2018 sample. More missing rings within the series are probable and the exact cause is not known. If compression wood is evident, then missing rings are likely to concentrate around wedges.

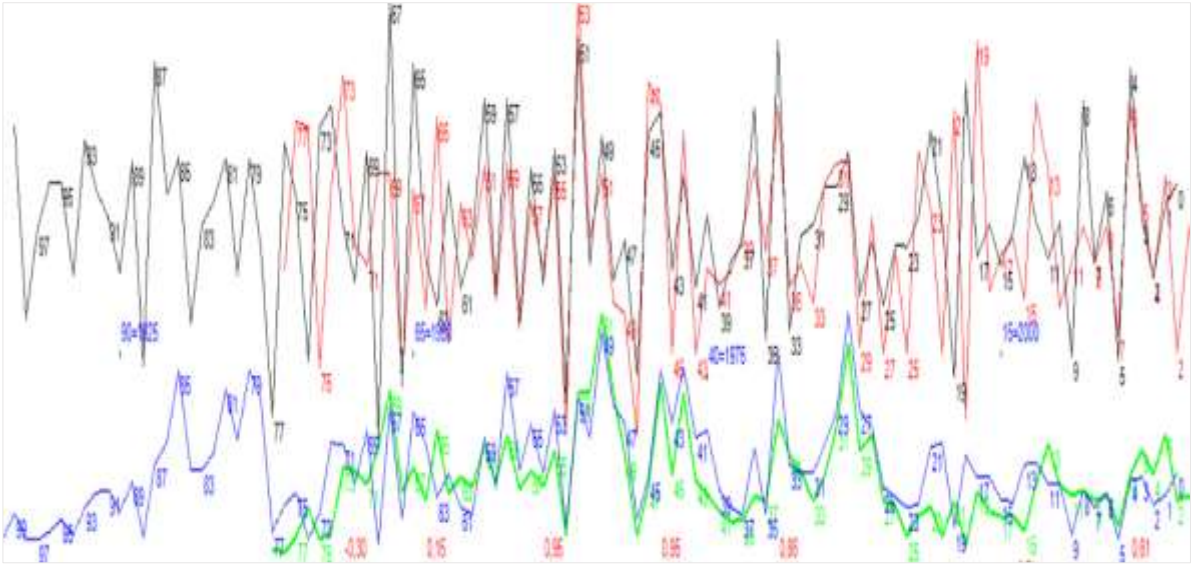

pith bark

Figure 25: Time series of two cores from sample PF3. The bottom row shows the ring-width measurements of the 2018 core (green) and the 2014 core (blue). The top row shows the normalised ring-width indices of the 2018 core (red) and the 2014 core (black). The offset position should be four years but is two, confirming two missing rings.

3.6.3 Between-tree variability

Between-tree correlation was also improved by offsets that were applied to two ring-width series. For this thesis measurement checks were undertaken by a second person, and once all measurement discrepancies had been resolved, the author chose not to alter any ring widths in the subsequent analysis. False rings were not specifically identified in the collection, but are known to occur in this species (Vogel et al., 2001).

3.6.4 Growth trends

Potential release events for each series were identified by ARSTAN through a comparison of mean growth to actual growth over time. An example is given in Figure 26 for PF21, the longest time series. Identified release dates were considered during the interactive detrending of each series but could also be a useful tool for improving dating between the series if there are common stand release dates (Table 15).

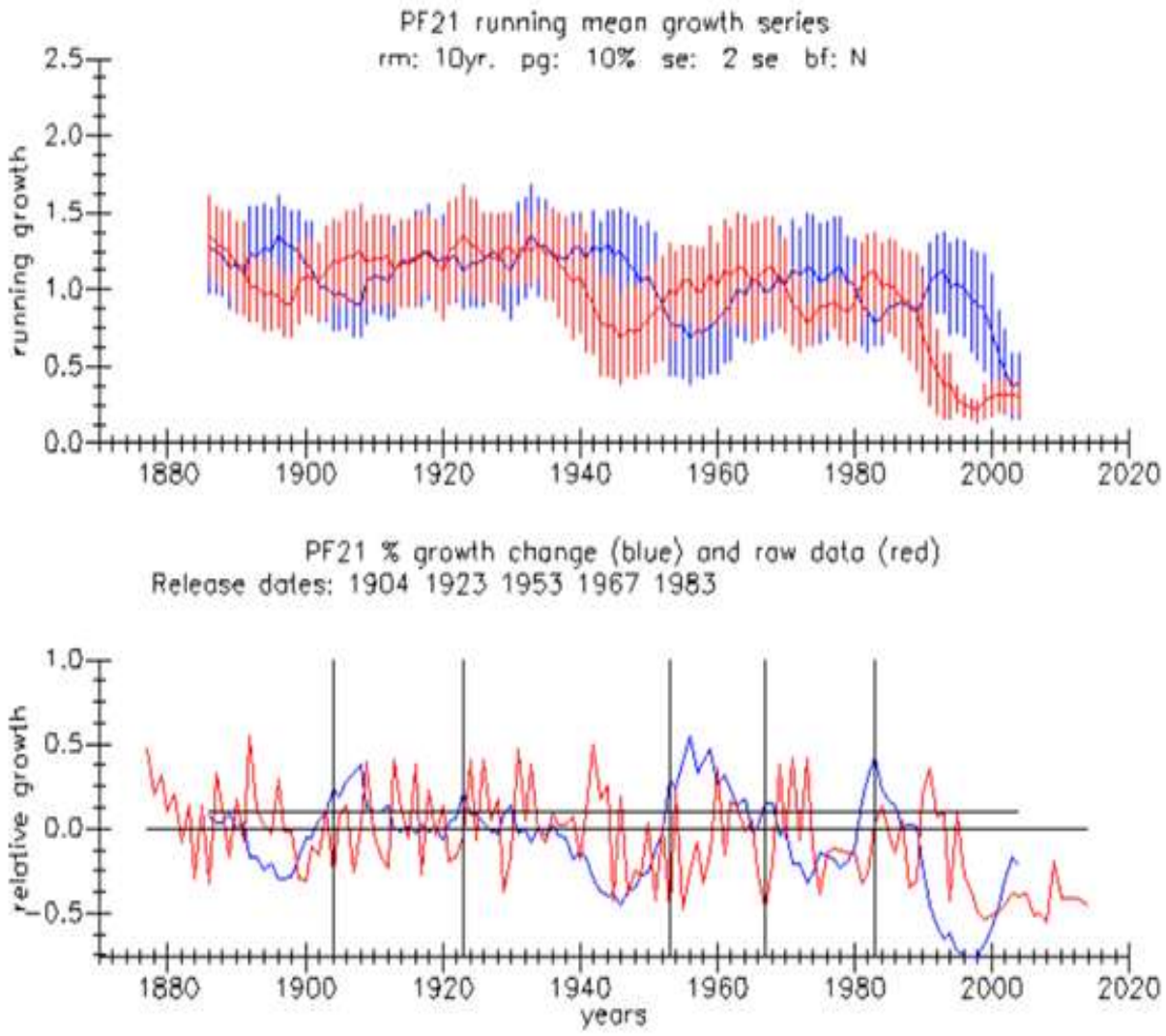

Figure 26: Five potential growth release events for sample PF21

Table 15: ARSTAN identified potential release dates for the five ring-width series

No.	Sample	Potential release dates						
1	PF3		1925	1945			1976	
2	PF7							1985
3	PF11					1965		
4	PF20					1963		
5	PF21	1904	1923		1953	1967		1983

Four detrending options were run and compared. A range of linear growth trends with positive and negative slopes were observed for the five ring-width measurement series (Figure 27). It was noted

that the oldest sample (PF21) demonstrated an atypical trend relative to the rest of the series (a decreasing width with age). This would be the norm in a northern hemisphere open-canopy forest, and a negative exponential curve would normally be fitted to remove this growth trend. PF21 is located on an incline of 25%, and the reason for the progressive decrease in ring width could be due to compression events as the tree stabilised itself during its life to maintain vertical alignment (Figure 28). If PF21 was examined without the benefit of comparative samples, the narrow rings could mistakenly be attributed to climate. A negative exponential curve would still be the best fit to remove this non-climatic growth curve. Thereafter, normalisation of the ring-widths allows the proportional differences of the compressed rings to be investigated for climate signals.

All other growth trends observed in these data have growth trends that are initially supressed as would be expected in a closed-canopy environment. The application of linear regression addressed the deterministic portion of the curves well. The use of the cubic smoothing spline, both on its own and as a second detrending tool, reduced the correlation between series. Various degrees of spline stiffness were tested, but it did not have a more positive impact on the rbar. Here the spline might be reducing a common stand signal while still retaining the trend in mean (Cook, 1985).

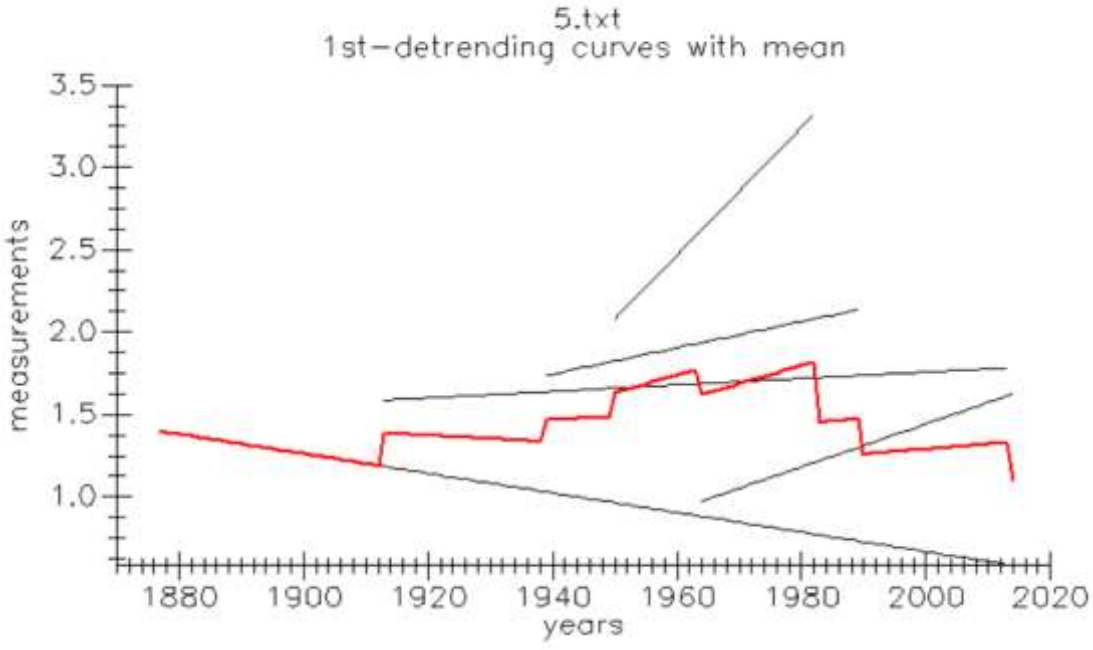

Figure 27: Range of growth trends identified for the individual ring-width measurement series, and the mean growth trend (red) (ARSTAN). Only the 3 longest curves represent whole tree segments from bark to pith.

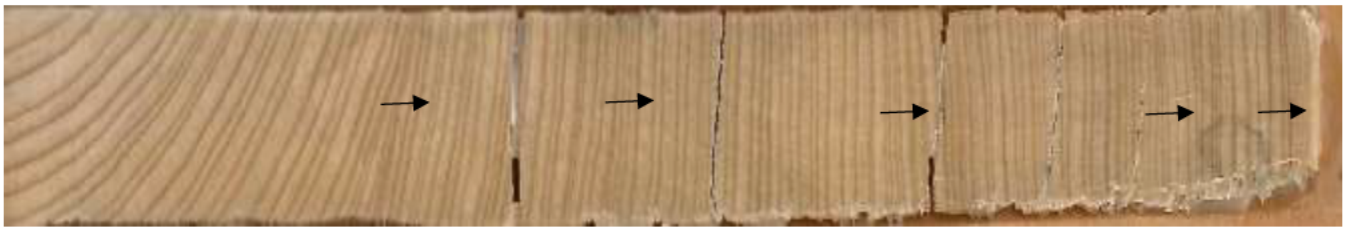

pith *bark*

Figure 28: Sample PF21 with progressively compressed rings from pith to bark with some release events occurring during growth. The compressed ring-widths shown with black arrows could be due to the trees reaction to the steep slope to maintain its vertical orientation.

Growth pulses with > 3.5 standard deviation to the mean were identified as endogenous outliers by ARSTAN (Figure 29). These measurements were checked and retained. The confirmation of outliers, typical of a closed-canopy type forest, justified the use of the bi-weight mean as the best averaging option (Cook and Peters, 1981).

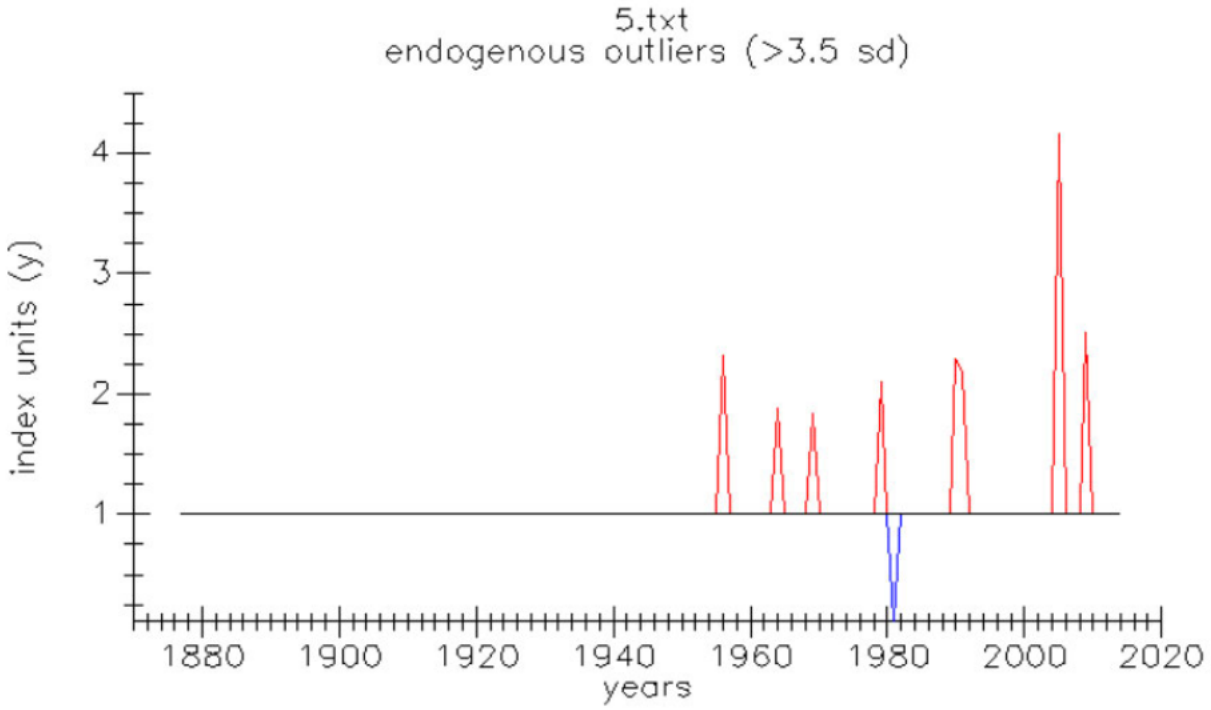

Figure 29: Endogenous outliers identified for growth pulses with >3.5 standard deviation to the mean

3.6.5 Uncertainties and potential sources of error

This ring-width analysis has confirmed that tree-ring formation is dominated by non-climatic factors which influence tree-ring structure and width (compression wood and ring-width eccentricity). This

problem can be addressed through the removal of cores and segments that correlate poorly with the mean. An adequate number of good samples must be retained to represent the population. In this thesis, there were an inadequate number of samples remaining after unsuitable samples were removed (EPS 0.74).

The analysis also confirmed that there are missing rings within the series. False rings were not specifically identified in the collection, but are known to occur in this species (Curtis et al., 1978). To further improve this inter-series correlation (0.43), it is necessary to first resolve discrepancies by adding and removing rings during series comparison, where it is justified. The series have a high mean sensitivity and so this will require time to work iteratively between the wood and the measured series.

One of the limitations of this study is that the dating have not been annually resolved and that the sample depth in portions of the chronology is too low to fully express the population. To improve this, additional young trees should be introduced to improve the weaker sections of the chronology, and they would not need to go beyond the instrumental period for the assessment of signal. Radiocarbon dating could also be used to verify the ring dating.

The climate-growth relationship analysis has used a mean ring-width series that does not meet international tree-ring width best practise. The following section should be read with these uncertainties in mind.

3.6.6 Growth-climate relationships

As discussed in the paragraph above, for the sake of exploring the climate-growth relationship, the year 2014 was assigned to the youngest ring of the series, and the chronology was assumed to be annually resolved. The mean ring-width series was compared to climate records between 1950 and 1999, for both annual and summer months between October and March.

In Chapter 1.9 the characteristics of the Karkloof forest were described and it was stated that high soil moisture availability at this site would theoretically result in a temperature related limiting factor. The result of this climate-growth analysis showed that temperature influences *Afrocarpus falcatus* growth at this site all year round, particularly annual minimum temperatures, which show a strong positive correlation with the mean series (CorrC 0.43; TT 3.2). There was no relationship observed between the ring-width series and total annual rainfall or annual solar irradiance and a negative correlation with the annual average relative humidity was observed. For the growing season between October and March, a positive correlation was returned for both summer minimum temperature (CorrC 0.30; TT 2.2) and summer rainfall (CorrC 0.20; TT 1.4).

3.6.7 Methods

This Chapter used classical methods to analyse the tree-ring widths. Research in closed-canopy forests situated in both the southern and northern hemisphere showed that tree growth consisted of a high noise to signal ratio and a series of suppression and release curves lasting several decades (Cook and Peters, 1981) typically removed through the use of a statistical smoothing spline (Cook and Peters, 1981).South Africa has a range of biomes and thus the choice of methods to use would be dependant on whether the trees come from drier open-canopy forests or whether they come from moist close-canopy forests. Classical methods developed in the northern hemisphere can thus still be applied to research in South Africa.

3.7 CONCLUSION

This chapter described how a ring-width based series was developed for the Karkloof growing site to achieve the first objective of this thesis. The mean series comprised five samples with an inter-series correlation of 0.43 and an EPS of 0.740. Additional crossdated samples are required to build up this tentative chronology to a higher level of species representation for *Afrocarpus falcatus* at the Karkloof site. The main challenge to increasing the sample depth of the mean series is missing and potentially false rings.

In meeting the first and third objective, the mean-ring width series was tested against instrumental climate records of annual, summer, and winter rainfall, relative humidity, temperature, solar irradiance, evaporation, precipitation minus evaporation (p-e) and sun duration.

Once bad segments had been removed, the canopy effects were shown to be the main factors affecting ring-width time series at this site.

Ring-width series showed a strong growth response to temperature and not rainfall. The study area is not deprived by moisture, which is negatively correlated with the ring-width series. Temperature was thus shown to be the limiting growth factor. This is consistent with the growth-climate hypothesis described in the literature review.

The hypotheses developed for this chapter was:

	Hypothesis	Alternative
Hypothesis 1:	*Afrocarpus falcatus* tree rings from the Karkloof, KwaZulu-Natal, South Africa are annual - **TRUE**	*Afrocarpus falcatus* tree rings from the Karkloof, KwaZulu-Natal, South Africa are not annual - **FALSE**

For these reasons, the null hypothesis is rejected. The alternative is thus shown to be true which means that the Hall (1976) Karkloof rainfall proxy record should be challenged.

CHAPTER 4: STABLE CARBON ISOTOPES

4.1 INTRODUCTION

The structure of this Chapter deviates from the traditional structure of a research thesis. As there are two tree-ring environmental proxies being investigated (tree-ring widths and stable carbon isotopes ($\delta^{13}C$)), each proxy has a separate chapter which presents the methods, results, discussion and a conclusion specific to the proxy being analysed. Chapter three dealt specifically with the tree-ring width proxy approach, whilst this Chapter four reports on the use of $\delta^{13}C$ as a tree-ring environmental proxy. In Chapter five, the results of the two tree-ring proxies are compared and the extent to which the original research questions are revisited.

To recapitulate, the aim of this thesis was to develop a modern analogue for *Afrocarpus falcatus* from the growing site of the Karkloof, KwaZulu-Natal, South Africa and to investigate tree growth-climate relationships. The objectives were:

1. To develop a mean tree-ring-width based chronology using classic methods (Chapter three);
2. To develop a mean stable carbon isotope tree-ring-based chronology (Chapter four); and
3. To test the mean ring-width (Chapter three) and $\delta 1^{3}C$ series (Chapter four) against instrumental climate records of annual, summer, and winter rainfall, relative humidity, temperature, solar irradiance, evaporation, precipitation minus evaporation (p-e) and sun duration

This Chapter four thus addresses objective 2 and 3.

In the tree-ring width analysis, a closed canopy environment causes a high noise-to-signal ratio and affected coherence between the ring-width samples. The primary factor affecting ring $\delta^{13}C$ series from closed canopy environments are developmental effects (McDowell et al., 2011). Research on tree-ring $\delta^{13}C$ time series variation between trees in closed canopy forest sites have demonstrated that there is a negative $\delta^{13}C$ gradient that occurs with increasing tree height ($\delta^{13}C$ values increase from the understorey to the canopy level) but the reasons for these effects, the extent to which they influence tree-ring $\delta^{13}C$ values, and how to correct for ring $\delta^{13}C$ time series is still unclear (Jackson et al., 1993; McDowell et al., 2011; Offermann et al., 2011; van der Merwe and Medina, 1991).

This chapter will describe the methods used and results obtained for tree-ring $\delta^{13}C$ analysis of *Afrocarpus falcatus* from the Karkloof growing site. The discussion will review the extent to which the analysis was able to address the factors affecting tree-ring $\delta^{13}C$ time series that are applicable to this site.

4.2 METHODS

4.2.1 Sample preparation and measurement

A Haglöf incremental borer with a 12mm diameter drill-bit-styled end was used to extract cylindrical cores from the stems of 20 *Afrocarpus falcatus* trees growing at the Karkloof site. The cores were mounted in wooden blocks with a vertical orientation to reveal the ring structure with a second mount glued to the upper half of the core. Once dry, the core was split in half with a fine saw (Figure 30) and polished with progressively finer sanding grit between 125 µm and 600 µm to remove striations created by the previous sanding grit size (Orvis and Grissino-Mayer, 2002).

Figure 30: Splitting single cores from the Karkloof growing site into two halves to extract wood for stable isotope analysis while retaining the other half as a witness.

Of the 20 cores sampled, five of the oldest trees (maximum number of visible rings) from the collection were selected for ring $\delta^{13}C$ analysis (PF3SW (2013), PF8 (2014), PF12 (2014), PF14 (2014), PF21(2014)). One short series (PF1JB (2013) with 66 rings) was also selected based on clearly identifiable rings with low ring eccentricity. To test within-tree variability and to investigate whether rings were annual, PF3 was resampled again in 2017. To differentiate between two cores from the same tree, the 2013 sample was labelled PF3SW, and the 2017 core PF3BJB.

For all the samples, one side of each split mount was retained for ring-width analysis and the other side was sampled for $\delta^{13}C$ analysis. Latewood was sampled for absolute annual resolution (McCarroll and Loader, 2004). The wood from each ring was removed using a scalpel under a head mounted magnifier and placed into pre-labelled micro-centrifuge tubes using tweezers (Figure 31).

Figure 31: Extraction of wood in preparation for stable carbon isotope analysis

Pre-treatment processing of the samples followed the methods used in Woodborne et al (2015). The delignification and extraction of α-cellulose from the wholewood applied already well-established techniques using an acidified sodium chlorite solution and Soxhlet distillation (Loader et al., 1997) (Figure 32, 33).

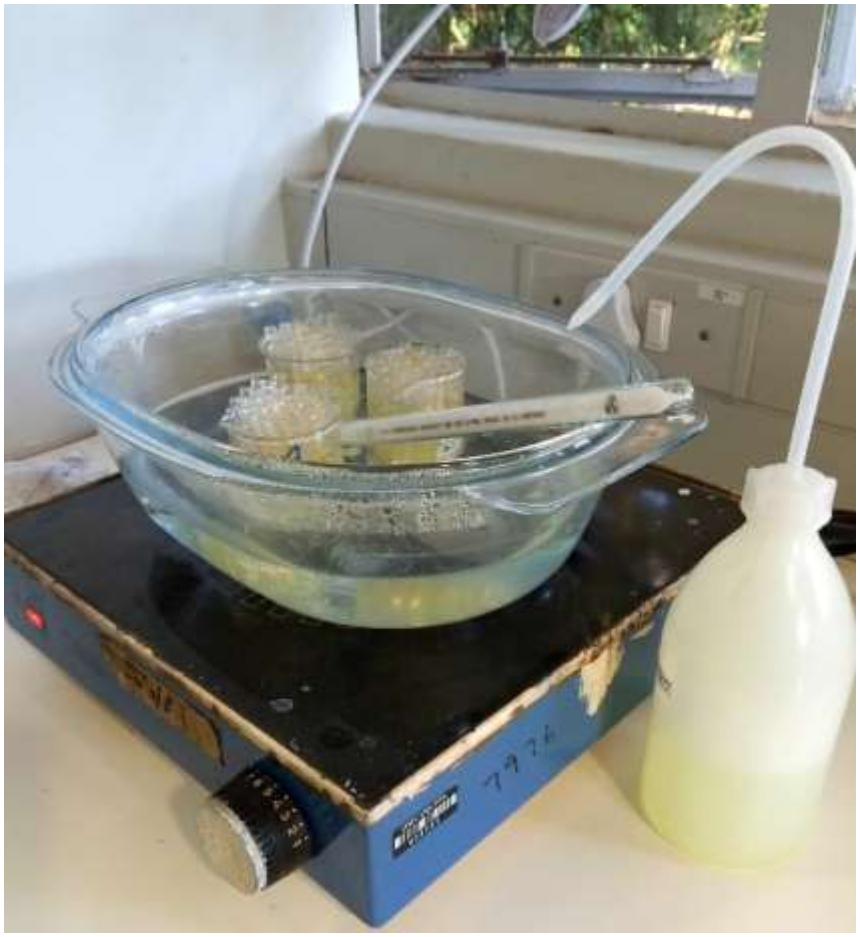

Figure 32: Oxidation and purification of the wholewood samples

Figure 33: Soxhlet distillation at the Mammal Institute, University of Pretoria

Carbon isotope ratio measurement

The carbon isotope ratios were analysed at the Mammal Research Institute, University of Pretoria (Figure 34), using a Delta V isotope mass spectrometer coupled with a Flash EA 1112 series elemental analyser by a Conflo IV. An in-house wood standard (Hall et al., 2009, 2008) and blank were run at the start and end of each analysis, and after every 12 unknown samples. Precision of standards was <0.2‰ (Woodborne et al., 2015).

Figure 34: AMS at the Mammal Institute, University of Pretoria

According to Coplen (2011) stable carbon isotope measurements are expressed as a ratio of ^{13}C to ^{12}C in delta (δ) notation relative to the Vienna Pee Dee Belemnite (VPDB) (parts per thousand (per mil, ‰)):

$$\delta^{13}C \text{ ‰} = ((R_{sample} / R_{standard}) - 1)\ 1000$$

where R is the ratio of ^{13}C to ^{12}C atoms of the sample or standard (Coplen, 2011)

Records of the raw stable isotope measurements are contained within Appendix D.

4.2.2 Tree developmental effects

As mentioned in the introduction, tree developmental effects are one of the main factors affecting ring $\delta^{13}C$ series (McDowell et al., 2011). To investigate developmental effects, the ring $\delta^{13}C$ series were aligned by biological age and the growth trends for each series were examined. Biological age and calendar date arranged graphs were compared to establish if a common year could be identified and used as a cut-off to remove older rings affected by developmental trends (McCarroll and Loader, 2004).

4.2.3 Crossdating and ring $\delta^{13}C$ variability

The ages of the samples were based on the results from the ring-width study (Chapter 3). To restate, only five of the 20 trees could be crossdated using ring-widths. Of those five trees, only two (PF3, PF21) had been sampled for ring $\delta^{13}C$ analysis. Ring $\delta^{13}C$ series variability between radii from the same tree and between trees was checked. The series were run in COFECHA to optimise internal dating positions between series. Where appropriate, series were adjusted (offset) to better positions relative to the collection using the same criteria developed for the tree-ring width analysis (Table 16).

Table 16: Acceptance criteria applied to ring-width and ring $\delta^{13}C$ measurement series.

	Type	Offset ring movement/year	Length	CorrC to rest of collection	EPS
1	Whole series	=<3 years	=>50 rings	r=>0.3258	EPS 0.4
2	Split segment	None	=>50 rings	r=>0.3258	EPS 0.5
3	Split segment	None	=>30-49 rings	r=>0.5	EPS 0.6

4.2.4 Data corrections and averaging

Atmospheric $\delta^{13}C$ trend and the physiological factor

The crossdated samples were corrected for rising atmospheric CO^2 concentrations using the 'Recommended Dataset' from Belmecheri and Lavergne (2020). The 'Recommended Dataset' comprises atmospheric CO_2 from Kohler et al. (2017) over the period 0-2016 CE, and atmospheric $\delta^{13}C$ from Graven et al. (2017) over the period 1850-2015 CE.

The change of plant intrinsic water-use efficiency as a response to increasing atmospheric CO_2 concentration was investigated in this analysis using the incites gained from examining the effect of developmental trends. The results informed a decision not to apply a W_i correction factor to the $\delta^{13}C$ values, and the reasons will be explained in the discussion.

Averaging

Chronology computation was done by averaging. The resulting mean ring series was then compared to climate records.

4.2.5 Climate-growth relationships

The climate dataset OBSHIS4682 (Chapter 3.2) is used in this climate-growth relationship analysis. The mean ring $\delta^{13}C$ measurement and detrended series were compared to OBSHIS4682 climate records from between 1950 and 1999. Correlation coefficients for annual, summer, and winter rainfall, relative humidity, temperature, solar irradiance, evaporation, p-e and sun duration were calculated.

4.3 RESULTS

4.3.1 Tree developmental effects

Aligning the six ring $\delta^{13}C$ measurement series by calendar date showed a general convergence of $\delta^{13}C$ values between the series at around 1950 (Figure 35). Before this date, the majority of ring $\delta^{13}C$ series present more negative/less positive values, with the most negative $\delta^{13}C$ values for each series on average, aligned with canopy understory growing years.

Alignment of the six ring $\delta^{13}C$ measurement series by biological date showed that the linear trend of increasing $\delta^{13}C$ values was evident in four series (PF3, PF8, PF14, PF21) (Figure 36) and that it did not cease once the series reached the canopy and at the time of sampling, were ongoing. Two of the six series presented more negative values with age (PF1, PF12) (Figure 37).

The decision to truncate the series at 1950, once crossdated, was made on the basis that (a) developmental trends are evident, and although they have been observed to continue post convergence at canopy level, trends such as the juvenile effect which is stronger in the oldest portions of the ring $\delta^{13}C$ series will be removed by the proposed truncation; and (b) the aim and objectives of this thesis can be met with a truncated mean series at 1950 because the climate data set OBHIS4687 only spans the period 1950-1999.

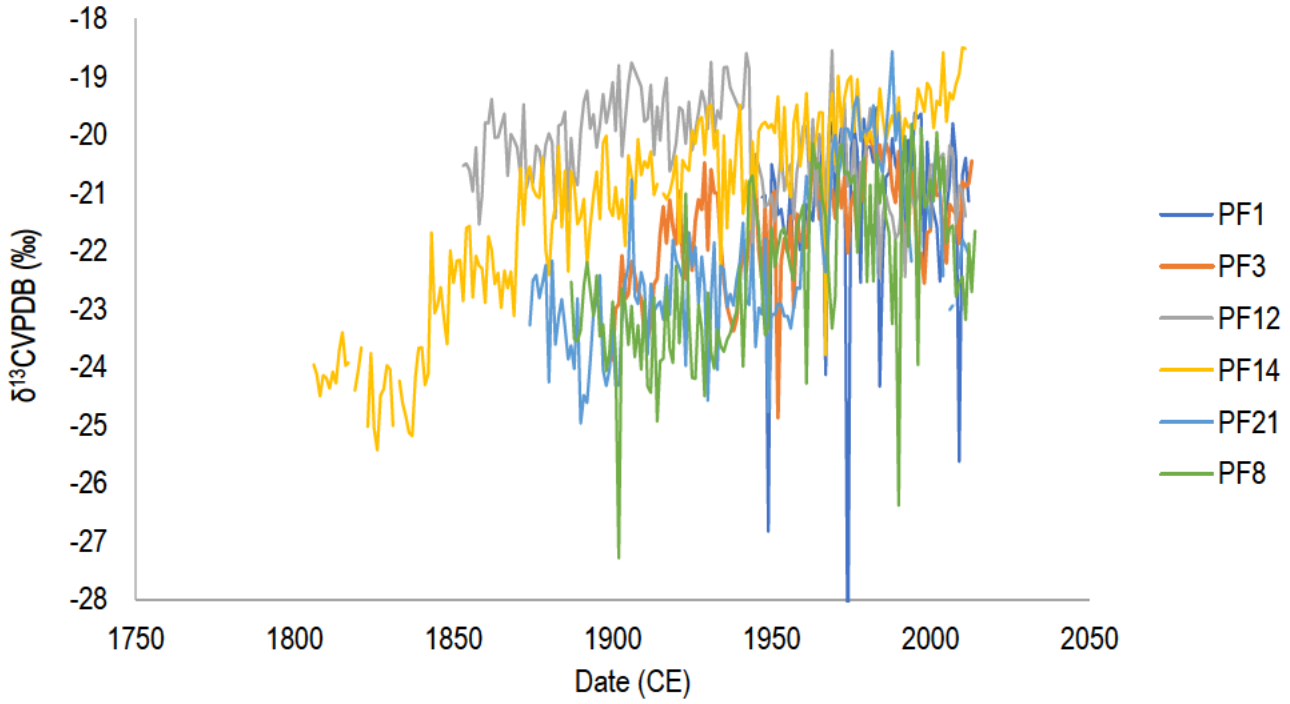

443

444 *Figure 35: The six tree-ring $\delta^{13}C$ series arranged by calendar year showing that the majority of series*
445 *present more negative/less positive values in the understorey growing years.*

446

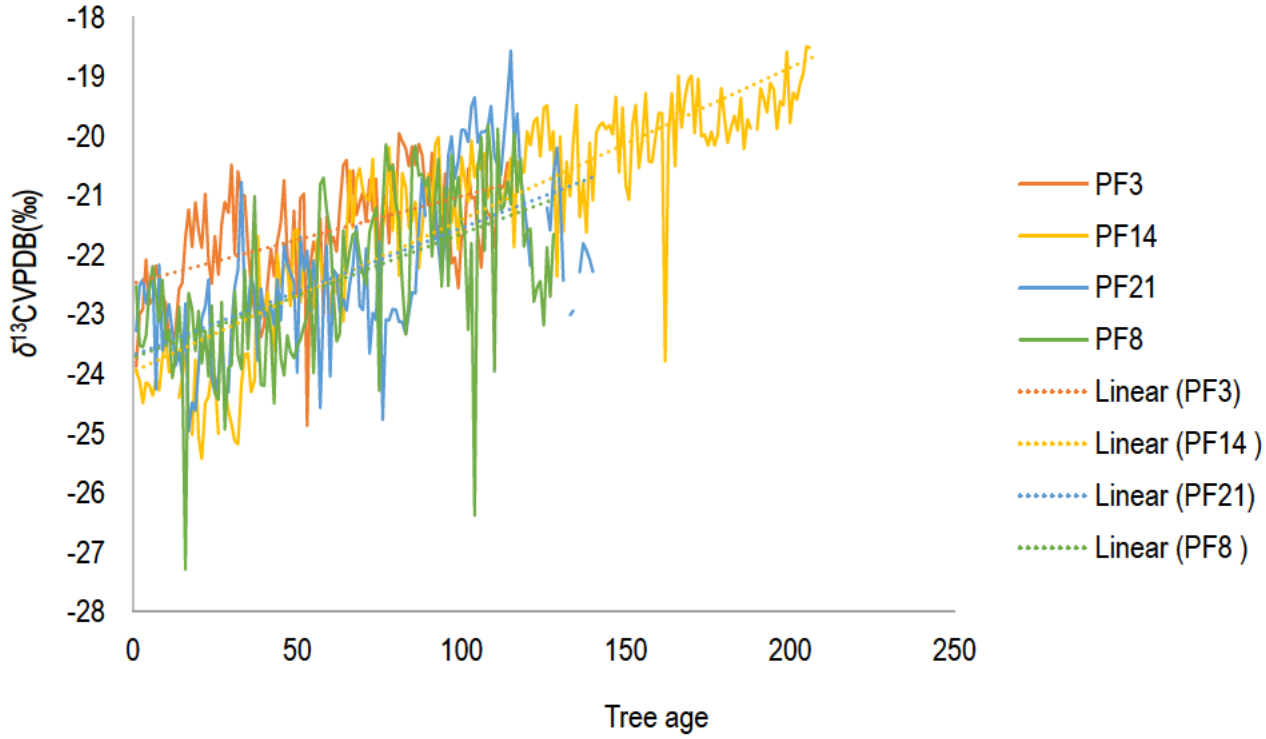

447

448 *Figure 36: The four ring $\delta^{13}C$ series arranged by biological age showing less negative $\delta^{13}C$ values*
449 *with age*

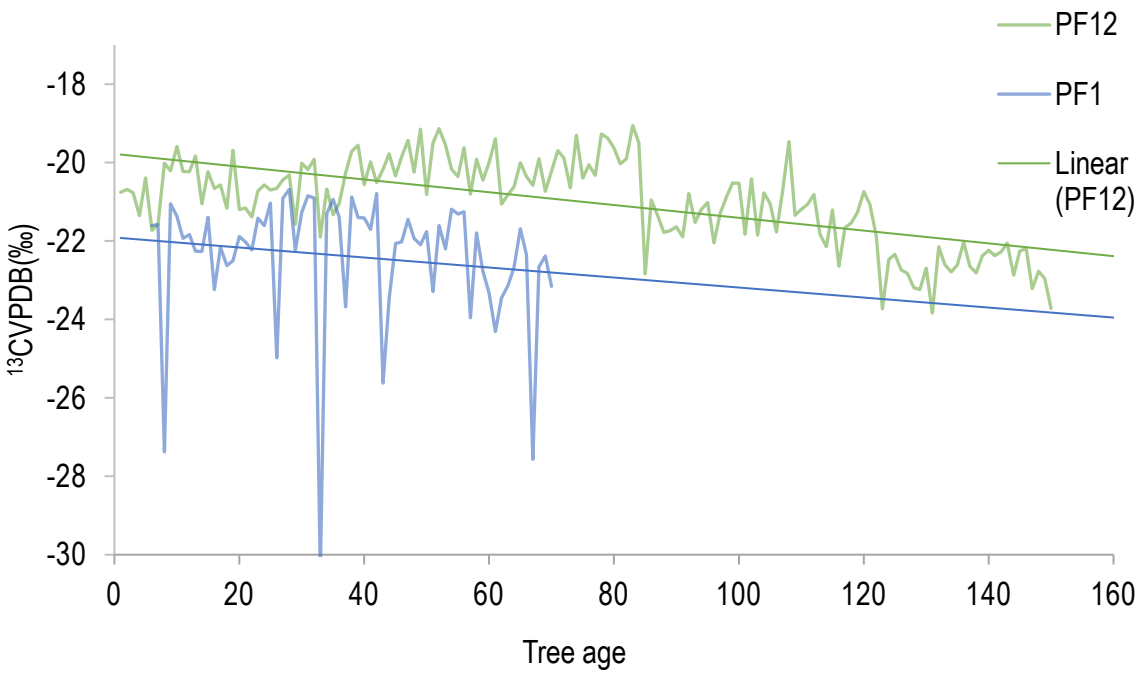

Figure 37: The two ring $\delta^{13}C$ series arranged by biological age showing more negative $\delta^{13}C$ values with age (PF1 and PF12)

4.3.2 Crossdating and ring $\delta^{13}C$ variability

Within tree variability and annual ring determination

Ring $\delta^{13}C$ variability within trees, and annual ring formation were investigated by comparing two ring $\delta^{13}C$ time series developed from two cores taken in different years from a single tree. The first core (PF3SW) was dated 2013, and the second core (PF3BJB) 2017. There were four years difference between the two cored dates (2017-2013), and thus it was anticipated that there would be an additional four rings at the bark end of PF3BJB. However, within-tree correlation was established at two rings instead of four. This confirmed that two rings were missing on the recent end of the 2017 core (PF3BJB) (Table 17).

Table 17: Within tree variability for ring $\delta^{13}C$ series

No.	Sample	Ring 1	CorrC with annual ring assumption	Offset (rings / years)	Revised CorrC
2	PF3SW	2013	-0.03	2	0.32
	PF3BJB	2017		0	

Crossdating

The ring $\delta^{13}C$ series from the six trees were aligned according to the previous growing season year of their cored date and between tree variability was tested in COFECHA (Table 18). The Mean Sample Segment Length (MSSL) for the six ring $\delta^{13}C$ series was 132 years. Mean inter-series sensitivity was 0.136 The mean inter-series correlation for the collection was -0.07.

475 *Table 18: Statistics for ring $\delta^{13}C$ measurement series (COFECHA)*

476

								Unfiltered original ring width measurements				Filtered detrended series measurements			
Sequence	Series	Assigned year	Length	No. Segments tested	No. flags (possible dating problems)	**Correlation with master chronology**	Mean msmt average of all ring	Max msmt maximum ring measurement	Standard deviation	Autocorrelation	Mean sensitivity	Max value largest index value in the	Standard deviation	Autocorrelation	Autoregression modelling order (AR)
1	PF1	2013	66	3	3	-.002	2.21	3.05	.324	-.83	.123	2.38	.270	-.009	3
2	PF3	2013	114	4	4	-.026	2.25	2.54	.083	.494	.028	2.98	.555	.016	2
7	PF8	2014	128	5	4	.144	2.29	2.78	.311	-.023	.103	2.36	.253	-.032	1
11	PF12	2014	150	5	6	.083	1.99	2.39	.494	.275	.194	2.38	.285	.001	2
13	PF14	2014	203	6	6	.081	2.12	2.55	.391	-.016	.143	2.25	.171	.009	1
20	PF21	2014	133	5	5	-.043	2.20	2.53	.482	-.050	.201	2.47	.351	-.003	1
	Mean				**29**	**.049**	**2.16**	**3.05**	**.359**	**.100**	**.136**	**2.98**	**.307**	**-.003**	

477

The crossdating analysis first applied COFECHA generated suggestions for improved dating positions between the series. Two samples had already been crossdated in the ring-width analysis (PF3, PF21) and so these dates were retained. The best possible series alignment showed coherence of signal within five of the six series. Only two series met the threshold (PF1 and PF12) when the acceptance criteria were applied (Table 4.1). The two series had a resulting mean inter-series correlation of 0.35 and an EPS of 0.524 (Table 19, Figure 38).

Table 19: Dating and statistical relationship between truncated and atmospheric corrected ring $\delta^{13}C$ series for samples PF1 and PF12.

No.	series	length	Assigned date range	Offset	Retained rings	Mean sensitivity	Std dev	Inter-series CorrC	EPS
1	PF1	66	1950-2015	-2	65	0.066	0.169	0.35	0.524
2	PF12	65	1950-2014	-	65	0.031	0.069		

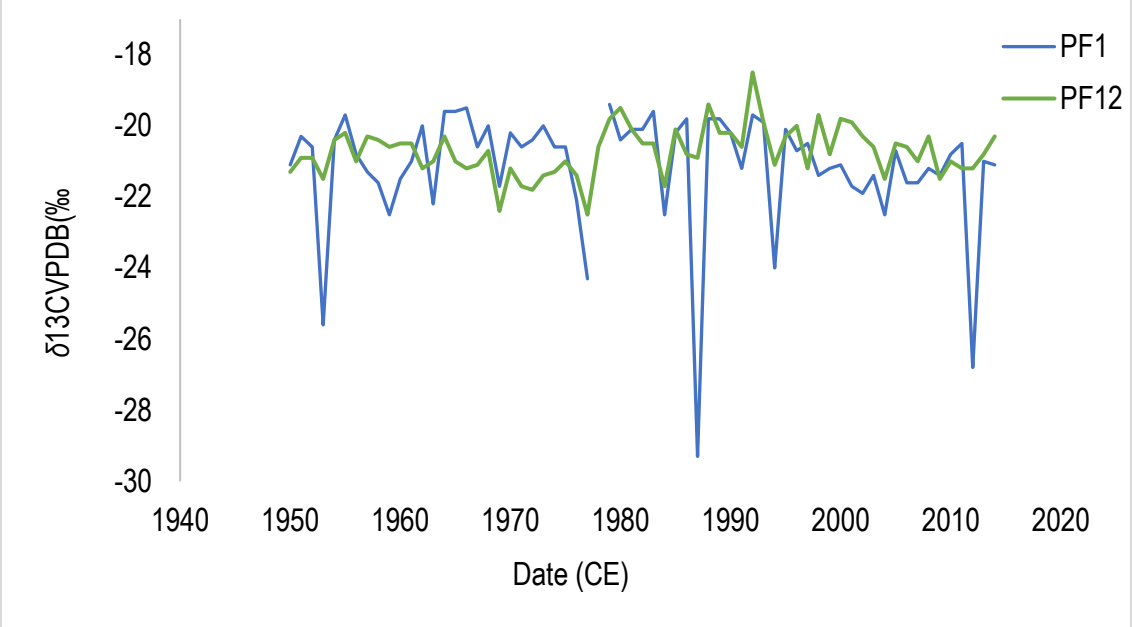

Figure 38: Crossdated PF1 (blue) and PF12 (green) ring $\delta^{13}C$ measurement series (CorrC 0.27, EPS 0.35)

4.3.3 Data corrections and averaging

Correction for atmospheric CO_2 trend

The ring $\delta^{13}C$ values have a declining trend from the post industrialised period onwards and so the crossdated ring $\delta^{13}C$ series were corrected for atmospheric $\delta^{13}C$ trend using (Belmecheri and Lavergne, 2020). Thereafter a correction for the expected change in intrinsic water use (W_i) was applied to each ring $\delta^{13}C$ series (Figures 39, 40).

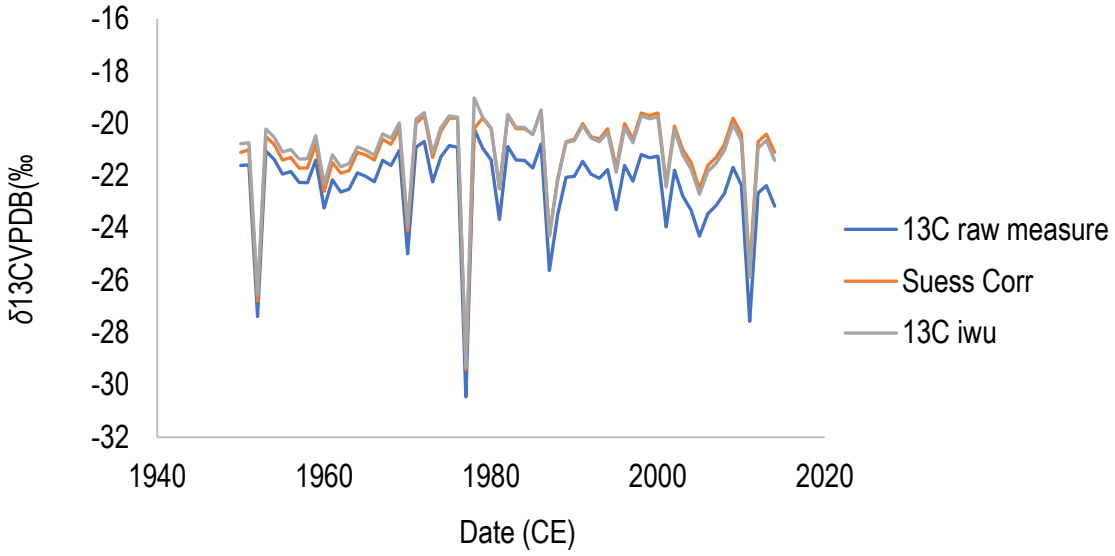

Figure 39: PF1 ring $\delta^{13}C$ series measurements (blue) and the effect of the atmospheric correction (orange)

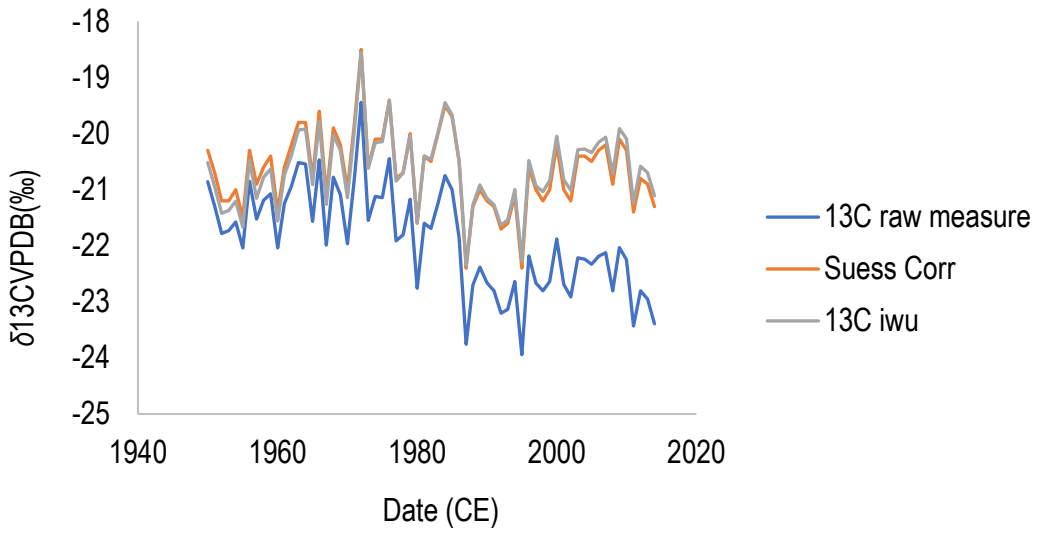

Figure 40: PF12 ring $\delta^{13}C$ series measurements (blue) atmospheric corrected ring $\delta^{13}C$ series (orange) and W_i corrected ring $\delta^{13}C$ series (grey).

Averaging

Averaging was done on the crossdated (PF1 and PF12) atmospheric corrected ring $\delta^{13}C$ series and not the ring $\delta^{13}C$ series corrected for W_i . The reasons for setting the W_i corrected ring $\delta^{13}C$ series aside will be explained within the discussion. Statistics for the individual and mean measurement series are shown in Tables 20-22. The mean measurement series had a correlation of 0.27 and the atmospheric corrected measurement series had a correlation of 0.35 (Figure 41).

Table 20: Statistics for PF1 and PF12 ring $\delta^{13}C$ detrended series

series	ident	first	last	year	mean	stdev	skew	kurt	sens	ac(1)
1	PF1	1950	2014	65	1	0.70	2.993	12.531	0.133	-0.112
2	PF12	1950	2014	65	1	0.069	-0.185	4.281	0.064	0.29

Table 21: Statistics for the mean ring $\delta^{13}C$ detrended series

First year	last year	total years	mean index	stdrd dev	skew coeff	kurtosis coeff	mean sens	serial corr
1950	2014	65	1.000	0.102	2.094	8.187	0.094	-0.098

Table 22: Statistics for the mean ring $\delta^{13}C$ series

	measurement series	Atm corrected series
CorrC	0.27	0.35
EPS	0.426	0.524

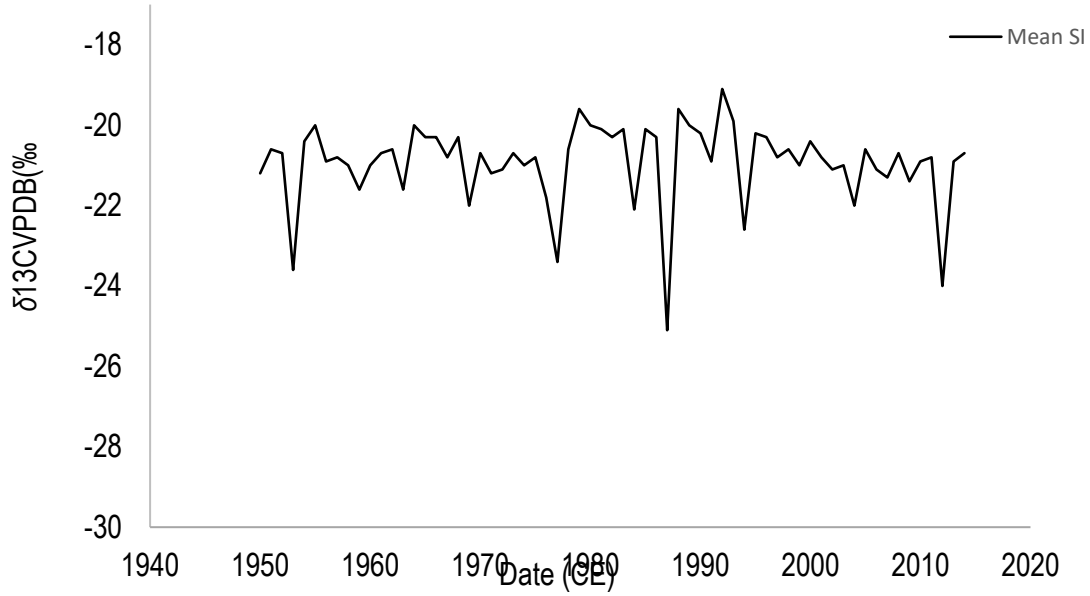

Figure 41: Mean ring $\delta^{13}C$ series (n = 2, r = 0.35, TTest 2.6)

4.3.4 Climate-growth relationships

Annual climate-growth relationships

The mean ring $\delta^{13}C$ series were compared to annual climate records between 1950 and 1999 from climate data set OBSHIS4682. Correlation coefficients for annual rainfall, relative humidity, temperature, solar irradiance, evaporation, p-e and sun duration were calculated (Table 23).

Table 23: Correlation coefficients for the mean ring $\delta^{13}C$ series and OBSHIS4682 annual climate records between 1950-1999

OBSHIS4682 annual climate records between 1950-1999	Mean atm corrected ring $\delta^{13}C$ series	T-Test
Total rainfall	-0.27	-1.5
Ave relative humidity	-0.02	-0.1
Average temperature	0.04	0.3
Ave maximum temperature	0.05	0.3
Ave minimum temperature	0.01	0.0
Ave solar irradiance	0.07	0.4
Evaporation	0.08	0.6
Precipitation – evaporation (p-e)	-0.26	-1.5
Sun duration	-0.02	-0.1

The covariance between the mean ring $\delta^{13}C$ series and annual rainfall was -0.27 (Figure 42).

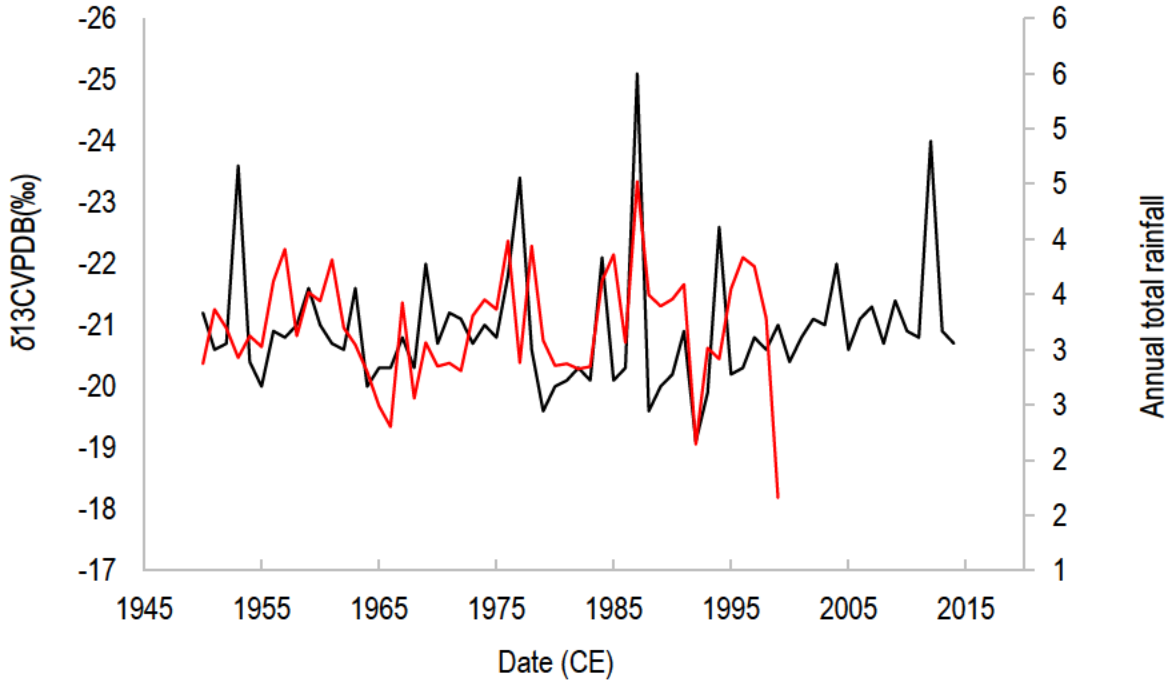

Figure 42: Mean ring $\delta^{13}C$ series (black) shown on the left y-axis and annual average rainfall (red) shown on the right y-axis (CorrC -0.27).

The covariance between the mean ring $\delta^{13}C$ series and annual p-e was -0.26 (Figure 43).

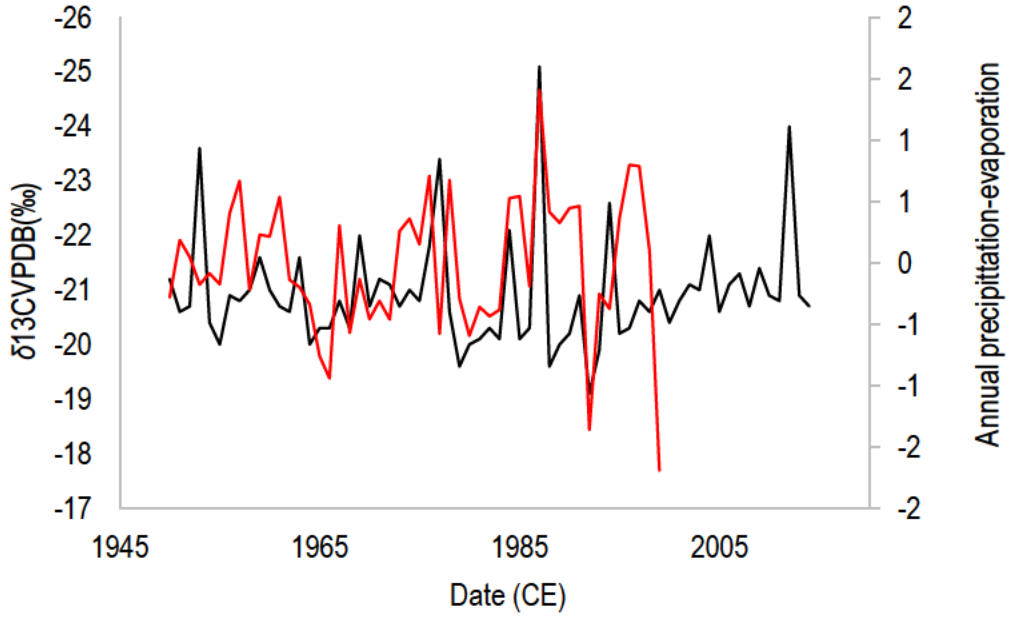

Figure 43: Mean ring $\delta^{13}C$ series (black) shown on the left y-axis and annual average p-e (red) shown on the right y-axis (CorrC -0.27).

Summer climate-growth relationships

The mean ring $\delta^{13}C$ series were compared to summer (October - March) climate records between 1950 and 1999 from climate data set OBSHIS4682. Correlation coefficients for rainfall, relative humidity, temperature, solar irradiance, evaporation, p-e and sun duration were calculated (Table 24).

Table 24: Correlation coefficients for the mean series and OBSHIS4682 (October –March) between 1950-1999 climate data

OBSHIS4682 summer (Oct-end Mar) climate records between 1950-1999	Mean atm corrected series	TTest
Total rainfall	0.06	0.4
Ave relative humidity	0.03	0.1
Average temperature	-0.29	2.0
Ave maximum temperature	-0.16	-1.1
Ave minimum temperature	-0.32	2.6
Ave solar irradiance	0.03	0.1
Evaporation	-0.06	-0.4

Precipitation – evaporation (p-e)	0.07	0.4
Sun duration	0.14	1.0

The covariance between the mean ring $\delta^{13}C$ series and summer minimum temperature was -0.32 (Figure 44).

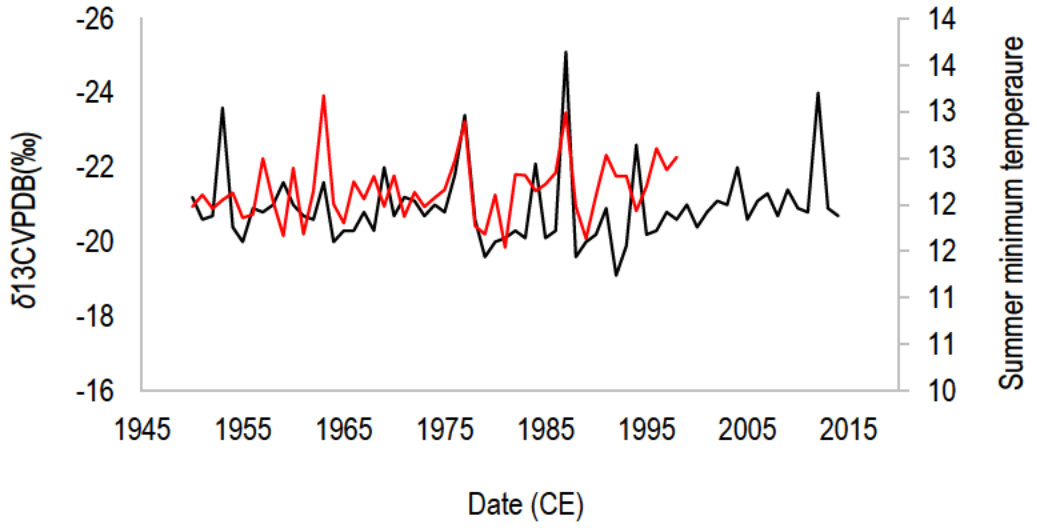

Figure 44: Mean ring $\delta^{13}C$ series (black) shown on the left y-axis and summer minimum temperature (red) shown on the right y-axis (CorrC -0.32)

Winter climate-growth relationships

The mean ring $\delta^{13}C$ series were compared to winter (April - September) climate records between 1950 and 1999 from climate data set OBSHIS4682. Correlation coefficients for winter rainfall, relative humidity, temperature, solar irradiance, evaporation, and p-e were calculated (Table 25).

Table 25: Correlation coefficients for the mean series and OBSHIS4682 winter (April - September) between 1950-1999 climate data

OBSHIS4682 winter (Apri-end Sep) climate records between 1950-1999	Mean atm corrected series	TTest
Total rainfall	-0.28	-2.2
Ave relative humidity	-0.12	-0.8
Average temperature	0.14	1.0
Ave maximum temperature	0.06	0.4

Ave minimum temperature	0.19	1.3
Ave solar irradiance	-0.03	-0.1
Evaporation	0.05	0.4
Precipitation – evaporation (p-e)	-0.25	-2.0
Sun duration	0.00	0

The covariance between the mean ring $\delta^{13}C$ series and winter rainfall was -0.28 (Figure 45). The covariance between the mean ring $\delta^{13}C$ series and p-e was -0.25 (Figure 46).

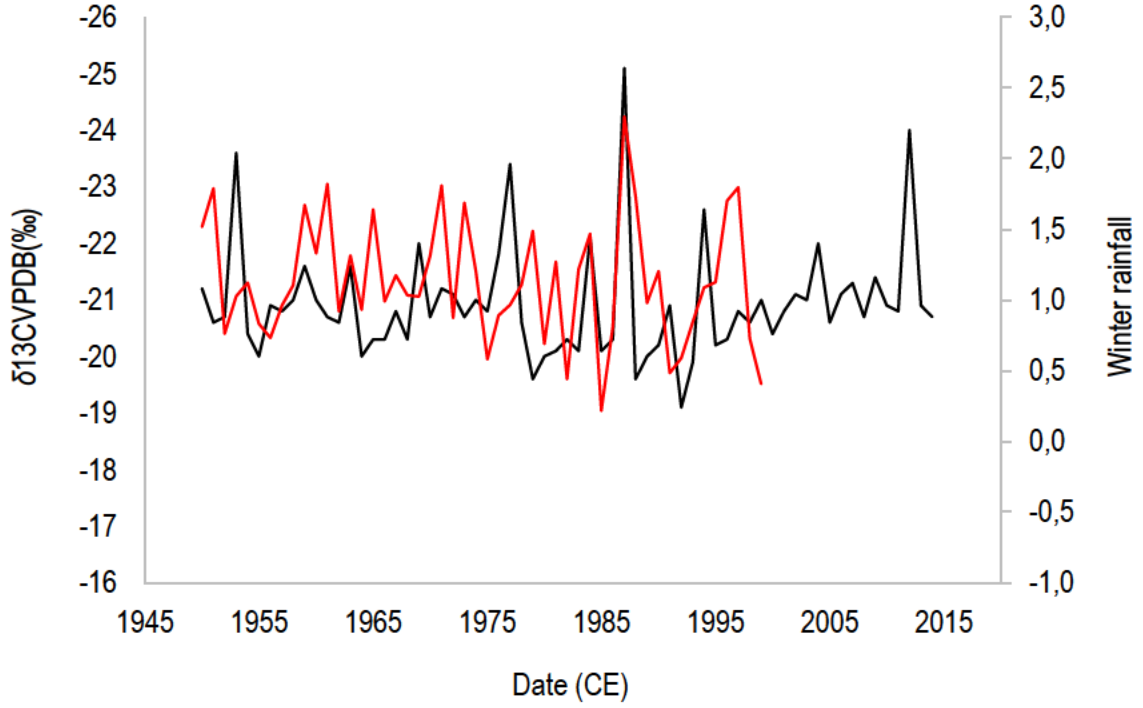

Figure 45: Mean ring $\delta^{13}C$ series (black) shown on the left y-axis and winter rainfall (red) shown on the right y-axis (CorrC -0.28)

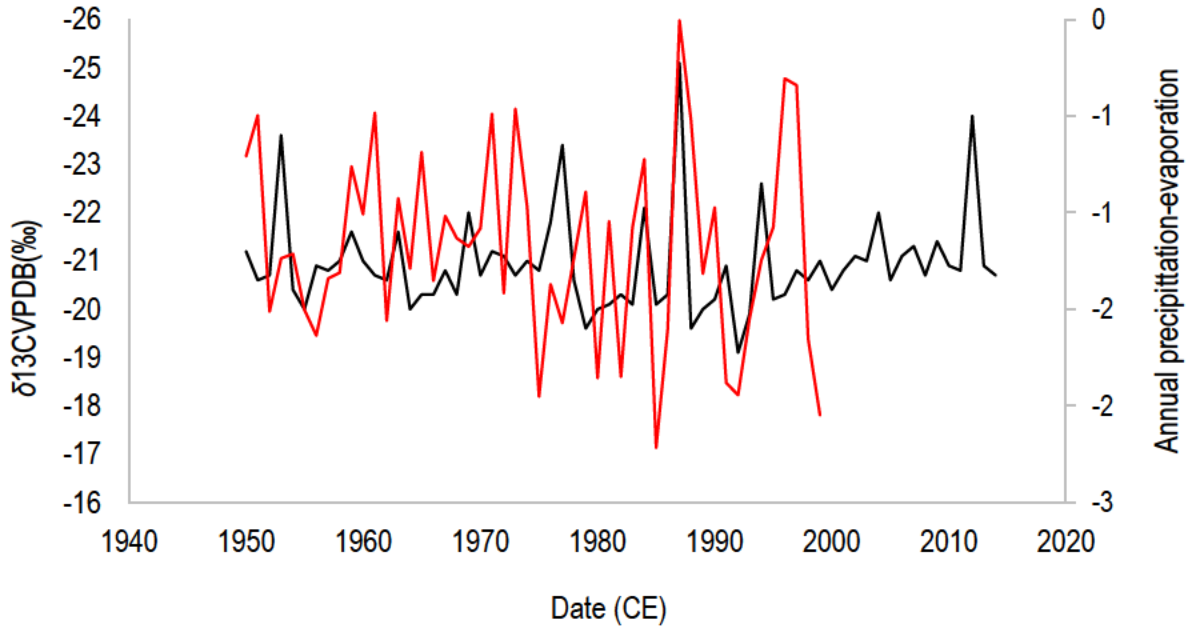

Figure 46: Mean ring $\delta^{13}C$ series (black) shown on the left y-axis and annual p-e (red) shown on the right y-axis (CorrC -0.25)

4.4 DISCUSSION

4.4.1 Tree developmental effects

$\delta^{13}C$ values within a closed canopy forest have been found to be less depleted with increasing forest canopy height (Jackson et al., 1993; Offermann et al., 2011; van der Merwe and Medina, 1991; West et al., 2000). The literature review explained that developmental effects include but are not limited to the canopy effect. The concentration of CO_2 in the understorey resulting from soil respiration influences the isotopic signal of the trees when they are young (Jackson et al., 1993; Offermann et al., 2011; van der Merwe and Medina, 1991). The increased availability of sunlight as the trees grow up to the canopy level increases CO_2 assimilation and photosynthetic rate, changing the c_i/c_a ratio and the isotopic signature recorded in wood (McDowell et al., 2011).

Four of the six ring $\delta^{13}C$ series from the Karkloof growing site showed a growth trend with more negative/less positive values in the earlier growing years. For these four ring $\delta^{13}C$ series, developmental effects are present within the $\delta^{13}C$ values of the oldest rings (Figure 36).

Two of the ring $\delta^{13}C$ series (PF1 and PF12) presented less negative $\delta^{13}C$ values in their younger years relative to the collection, and in contrast to the other four series, exhibit a more negative $\delta^{13}C$ value trend with age (Figure 37). The reason for this is not known. PF1 is the youngest tree at 67 years whilst PF12 is approximately 150 years old. PF12 is positioned at the margin of the forest and has grown over an old fence line (Figure 47). PF1 is located at the edge of a large forest gap. Their positions suggest that they may have had access to higher light levels in the earlier years and more mixed source air (less negative atmospheric air). As the trees grew up and the forest margin / gap became more densely populated, they may have encountered more stand competition and shade, and this might explain why the $\delta^{13}C$ values are becoming more negative.

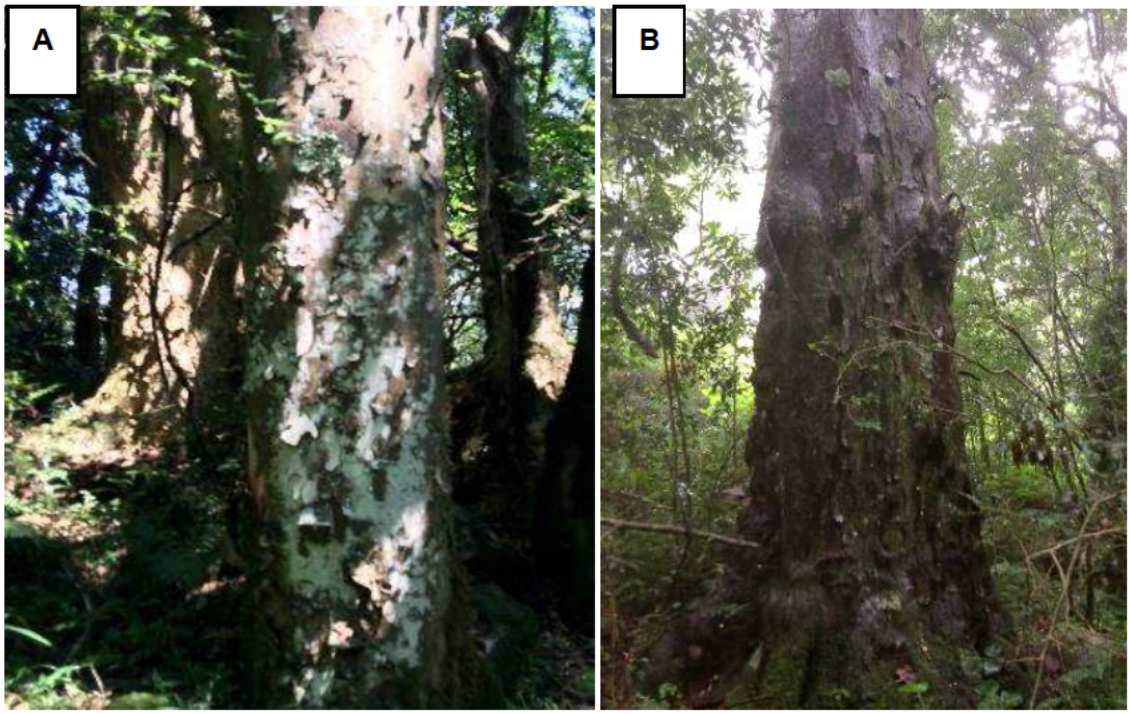

Figure 47: A:Sample PF1. B: Sample PF12

As the carbon isotope ratios in a ring $\delta^{13}C$ series change, they can provide an indication of when the tree has grown sufficiently high enough to penetrate the canopy, and in turn an indication of tree age. The point at which the trees generally converge in this study area was observed to be around 1950. However, the developmental trends were observed not to be halted by this convergence. The convergence feature could suggest that the trees are accessing the same atmospheric air, and that the $\delta^{13}C$ value of this source air aligns as the starting point for each series before plant discrimination begins. This common starting point may account for the general convergence in $\delta^{13}C$ values within the time series. However, trend in the ring $\delta^{13}C$ time series persists beyond the convergence year, and this is suggesting that developmental effects, or other effects like anthropological effects on $\delta^{13}C$ are active in the ring $\delta^{13}C$ series after the trees break through the canopy level.

Other developmental effects like CO_2 concentration in the understorey and increasing availability of sunlight would undoubtedly have influenced the $\delta^{13}C$ values of the series during the life of the sampled trees before they reached upper canopy level. These various non-stationary developmental trends within the ring $\delta^{13}C$ series can be both linear and non-linear in nature, and until they are isolated and removed from the ring $\delta^{13}C$ series, will cause temporal instability in the

mean $\delta^{13}C$ series with concomitant shifts in the observed relationship with climate over time (McDowell et al., 2011).

McDowell et al. (2011) used a combination of very old tree specimens and size stratified sampling to study developmental effects for various species from different growing sites. The same strategy may be available for the Karkloof growing site because of the existence of the *Afrocarpus falcatus* disc in the Natal Museum.

4.4.2 Crossdating and ring $\delta^{13}C$ variability

Verification of annual and missing rings

Sample PF3 had two radii sampled from it four years apart. Visual inspection of the core identified a mismatch between the bark ends of the core (Figure 48). Missing rings were confirmed when the within-tree variability was checked for ring $\delta^{13}C$ series from PF3 (Figure 49). Correlation between the radii was achieved when two missing rings were accounted for at the bark end of the 2017 core. It is not known exactly where on the bark end the missing rings should be, however ring eccentricity was identified before three years.

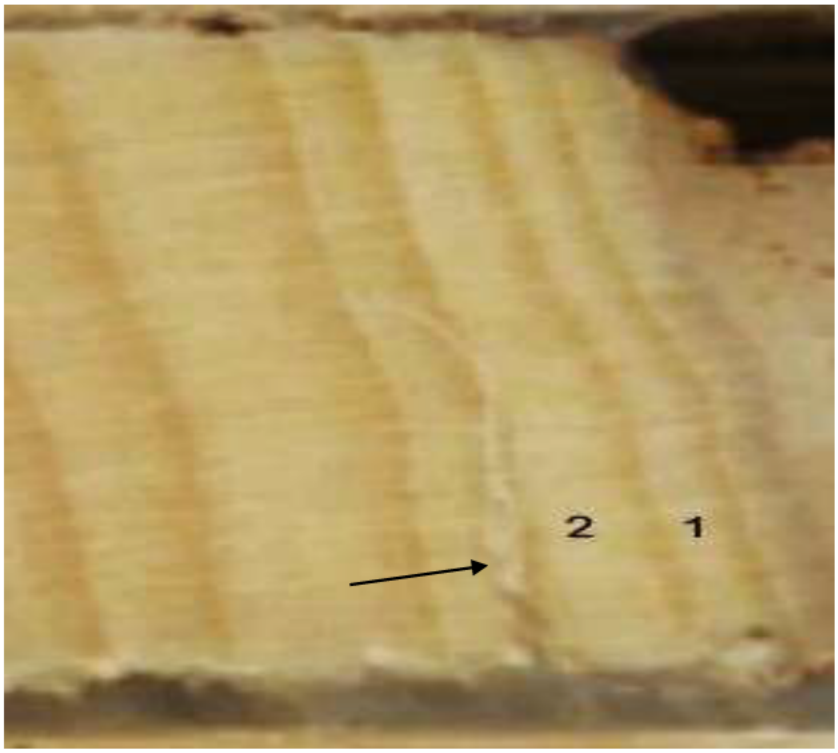

Figure 48: Sample PF3BJB (2017) cored four years after PFSW showing ring eccentricity at the location identified by the arrow.

When the two missing rings were accounted for, coherence of signal could be visually confirmed by graphically comparing the ring $\delta^{13}C$ series (Figure 49). The correlation was supported by a positive CorrC of 0.35 and T Test 2.9. This also confirmed that additional rings had been laid around the stem since the first core of 2013 and that *Afrocarpus falcatus* does produce annual rings.

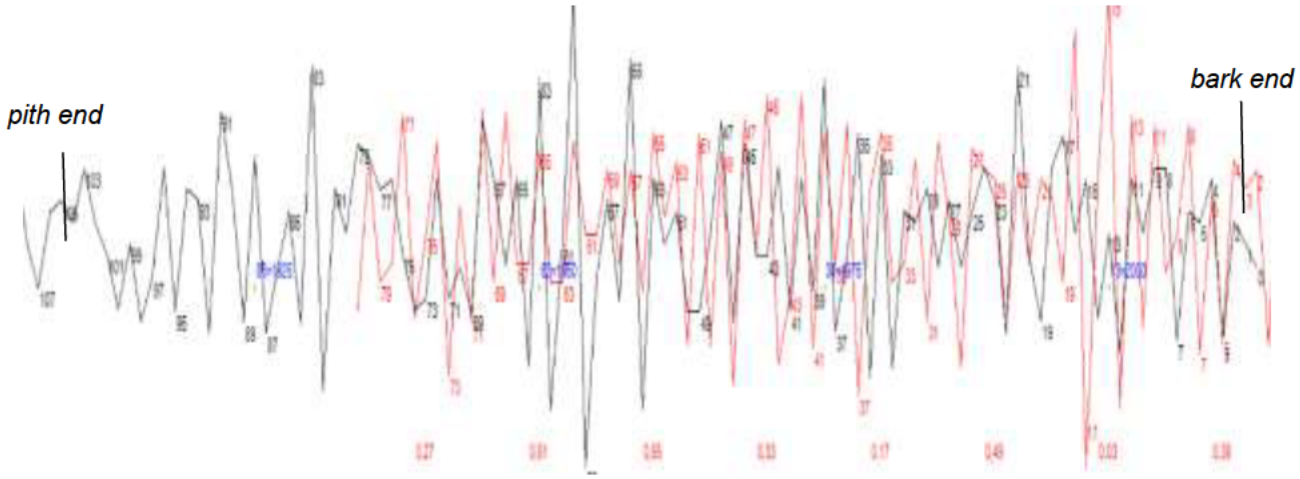

Figure 49: Time series of two cores from tree sample PF3. The normalised ring $\delta^{13}C$ series of the 2017 core (red, with red ring numbers) and the 2013 core (black, with black ring numbers) with two missing rings identified at the bark end. CorrC is shown in red for a running 10-year window, below the graphs.

Signal coherence

Of the six ring $\delta^{13}C$ measurement series, a level of signal coherence (rbar=0.35) was identified between samples PF1 and PF12. Although the other samples did show varying levels of coherence to the mean, they did not pass the correlation coefficient acceptance criteria of 0.328 without exceeding the maximum offset criteria of three rings.

4.4.3 Data corrections and averaging

In an open canopy forest, where developmental effects influencing trees are minimal relative to closed canopy environments (McDowell et al., 2011) the correction to W_i may be appropriate to ring $\delta^{13}C$ series. The open canopy tree has a more constant operating environment with less change in atmospheric source air, irradiance and the effects of stand level competition (Cook and Peters, 1981; Fritts, 1976; McDowell et al., 2011). In contrast, correcting W_i for closed canopy ring $\delta^{13}C$ series without first understanding and disentangling the developmental effects on the $\delta^{13}C$ values may be less appropriate and result in biased series (McDowell et al., 2011). This thesis investigated the effects of the correction to W_i on samples PF1 and PF12. It is acknowledged that the sample size analysed is not representative of the sample set, and thus any interpretations of the growth response to climate will be limited. Application of the correction was rejected for the revised ring $\delta^{13}C$ series before the data was averaged to produce a mean ring $\delta^{13}C$ series because the corrected values did not make the $\delta^{13}C$ values less negative as intended. This suggests that other unidentified developmental effects may be counteracting the correction factor. One such effect which may be responsible for this could be occurring from the height gravitational constraints imposed on water transport to leaves at canopy level (McDowell et al., 2011). The resulting effect on stomatal conductance with increased tree height could explain why the majority of the ring $\delta^{13}C$ series from the Karkloof growing site continue to register less negative $\delta^{13}C$ values after reaching upper canopy (Figure 50).

Figure 50: Pole shaped Afrocarpus falcatus stems from the Karkloof growing site influenced by the shady growing conditions of closed canopy forests

4.4.4 Growth-climate relationships

The mean ring $\delta^{13}C$ series was compared to climate records between 1950 and 1999, for annual, summer and winter months. Since the Karkloof growing site is situated within a mistbelt and experiences high rainfall, it was hypothesised in the literature review that the limiting environmental factor would theoretically be temperature related (Chapter 2). The result of this climate-growth analysis using $\delta^{13}C$ series has shown that temperature influences *Afrocarpus falcatus* growth at the Karkloof growing site during the summer growing season (October- end March). Minimum summer temperature is significantly negatively correlated with the mean $\delta^{13}C$ series (CorrC -0.32) during summer. Winter rainfall (CorrC -27) and p-e (CorrC -26) are negatively correlated to the mean ring $\delta^{13}C$ series.

The results suggest that the tree growth-climate relationship is seasonally driven with strong opposite responses in both summer and winter. In the growing season, between October and the end of March, the growing site receives 80% of its annual rainfall. The strong response of *Afrocarpus falcatus* to winter rainfall (CorrC -0.27) and its sensitivity to winter p-e (CorrC -0.25) suggests that *Afrocarpus falcatus* responds to rain during this drier period of the year. Krepkowski et al. (2011) found evidence for cambial dormancy for *Afrocarpus falcatus* during the Ethiopian dry season but when rain events occurred, a continuous increase of the stem diameter was recorded along with indistinct ring boundaries. It is possible that winter rainfall may also stimulate cambial activity at the Karkloof site and contribute to the formation of indistinct ring boundaries known as false rings. This could be investigated using the six samples from the Karkloof site together with winter rainfall records. The identification and removal of false rings within the ring $\delta^{13}C$ series would help to crossdate more samples, strengthen the mean $\delta^{13}C$ series and improve the understanding of the *Afrocarpus falcatus* growth-climate relationship at this site.

The reason for the strong covariance between the mean $\delta^{13}C$ series and summer minimum temperature is not fully understood. One explanation may be linked to the location of the trees on the steep south-east facing slopes, and their limited exposure to sunlight. The sun rises in the east and the forests receive early morning light before the sun passes overhead to warm the grassland covered north-facing slopes. Since the OBHIS4687 climate data set has been developed for the surrounding area, the level of irradiance and the sun duration records used in this analysis will not be fully representative of this forest microclimate. If they were, correlations

with the mean $\delta^{13}C$ series and irradiance and sun duration may have provided more insight into the level of light availability to these trees. Further studies at this site would benefit from recording sun duration on site to compare against the records contained within OBHIS4687 climate data set used for this analysis. Since summer is the season which experiences high rainfall and heavy mist, moisture availability is not limited, and access to warmer temperatures and sunlight control the photosynthetic rate. Stomatal conductance occurs in early daylight and the stoma close before maximum temperatures are reached. The tree has to transport water up the tall pole-like stems to the leaves at the upper canopy level for photosynthesis before the forest shades over and before the stoma close. This could explain why photosynthetic rate is increased by higher minimum temperatures.

Taking into consideration the impact of developmental effects on the ring $\delta^{13}C$ series, the relationship between micro-climate and ring $\delta^{13}C$ series is not anticipated to be linear. However, outliers within the mean ring $\delta^{13}C$ series that correlate with climate at high and low points in time will significantly affect the net correlation with climate, presenting a linear relationship that does not describe the growth-climate relationship well, but nevertheless is a starting point for the development of a more accurate characterisation of the biological model that drives the growth-climate relationships.

(Hall et al., 2008) developed a $\delta^{13}C$ modern analogue for *Afrocarpus falcatus* using $\delta^{13}C$ values of archaeological charcoal. However, the developmental effects on *Afrocarpus falcatus* isotope discrimination caused by the closed canopy environment cannot be accounted for in $\delta^{13}C$ values of archaeological charcoal. The ring $\delta^{13}C$ series from *Afrocarpus falcatus* museum specimens could be studied though, as they would have grown under more constant conditions and should be able to provide valuable information on the developmental effects from closed canopy environments.

4.5 CONCLUSION

This Chapter described how a ring-based $\delta^{13}C$ series was developed for the Karkloof growing site to achieve the second objective of this thesis. The mean series comprised two samples with an inter-series correlation of 0.35 and an EPS of 0.524. Additional crossdated samples are required to build up this tentative chronology to a higher level of species representation for *Afrocarpus falcatus* at the Karkloof site. The four $\delta^{13}C$ series that were not included within the mean series

did show coherence in signal and have the potential to be crossdated to the mean. The main challenge to increasing the sample depth of the mean series is the resolution of missing and false rings.

In meeting the third and last objective, the mean ring $\delta^{13}C$ series was tested against instrumental climate records of annual, summer, and winter rainfall, relative humidity, temperature, solar irradiance, evaporation, precipitation minus evaporation (p-e) and sun duration.

Developmental effects associated with the closed canopy environment were observed to be the main factors affecting ring $\delta^{13}C$ time series at this site, and trends in $\delta^{13}C$ were observed to continue after reaching upper canopy level. It was suggested that the constraint of hydraulic conductivity of water against gravity in long tree stems of high *Afrocarpus falcatus* trees is causing signals of lower stomatal conductance to be imprinted in the wood of the tree rings with increase in height and age. More research on the extent and duration of these development effects will be critical to improve the interpretation of the $\delta^{13}C$ series.

Ring $\delta^{13}C$ series were shown to potentially be driven by climate environmental forcing. It is possible that winter rainfall events are recorded in $\delta^{13}C$ series when cambial dormancy becomes temporarily active, and this response could lead to the development of false rings in the winter. Ring $\delta^{13}C$ series were also shown to covary with minimum temperature in the summer, implying that temperature was the limiting growth factor in the growing season. Although the conclusions reached within this thesis are based on a limited number of samples, the results could potentially be consistent with the growth-climate hypothesis described in the literature review. This would need to be verified with a larger crossdated ring $\delta^{13}C$ sample size in future work.

The hypotheses developed for this chapter was:

	Hypothesis	**Alternative**
Hypothesis 3	*Afrocarpus falcatus* tree-ring stable carbon isotopes are driven by climate environmental forcing - **TRUE**	Climate cannot be reconstructed from *Afrocarpus falcatus* using stable carbon isotopes - **FALSE**

This chapter has shown that *Afrocarpus falcatus* tree-ring stable carbon isotopes are driven by climate, and for this reason, the null hypothesis for the stable carbon isotopes shown above is proved true.

CHAPTER 5: SYNTHESIS

5.1 INTRODUCTION

This chapter presents a summary of the results from the application of two tree-ring environmental proxies that were used to investigate the growth-climate relationships of *Afrocarpus falcatus* at the Karkloof growing site. The extent to which these proxies met the thesis objectives and addressed the research question will be assessed. The chapter will conclude with a true or false statement for the hypotheses and discuss their implications for palaeoclimate reconstructions from *Afrocarpus falcatus* in the Karkloof, KwaZulu-Natal.

The aim of this research was to investigate tree-growth climate relationships and develop a modern analogue for *Afrocarpus falcatus* in the Karkloof. The objectives were:

1. To develop a mean tree-ring width-based chronology using classical methods;
2. To develop a mean stable carbon isotope tree-ring-based chronology; and
3. To test the mean ring-width and $\delta^{13}C$ series against instrumental climate records of rainfall, relative humidity, temperature, solar irradiance, evaporation, sun duration, and precipitation minus evaporation.

5.2 TREE-RING WIDTH CHRONOLOGY AND ASSOCIATED ENVIRONMENTAL FORCING

The literature review describes how classic ring-width methodology has evolved to address the challenges of closed canopy moist forests. Cook and Peters (1981) illustrate that non-climatic factors dominate the ring-width variations at closed canopy sites and result in a high noise-to-signal ratio, which, for ring-width analysis, can only be overcome through high sample replication and statistical detrending. The selected growing site is a steeply inclined mistbelt-mixed Podocarpus forest situated in the Karkloof, KwaZulu-Natal, on south-east facing slopes. The forest receives high rainfall relative to the rest of the country and is a closed canopy environment.

This thesis identified and crossdated 20 *Afrocarpus falcatus* ring-width series, confirming that the species produces annual rings at the Karkloof growing site. However, missing rings, potentially false rings, and high levels of ring-width eccentricity were identified. This was consistent with the

findings of earlier regional ring-width studies (Curtis et al., 1978; E. C. February and Stock, 1998; McNaughton and Tyson, 1979). Most ring-width series in this study (17) presented a positive linear growth trend with age which confirmed that the majority of trees were growth supressed at an earlier age within the canopy. Three samples (PF1, PF12, PF21) presented growth trends more typical of open canopy forest trees. These three trees may have grown in positions where they received more sunlight and their locations on the margin of the forest might support this explanation. Individual patterns of suppression and release events were identified in all the ring-width series and reflect the gap-phase dynamics of the closed canopy environment. Crossdating was achieved by accounting for missing rings and removing compressed ring segments from ring-width series. Coherence between five of the 20 samples was established (CorrC 0.43, EPS 0.740), resulting in a mean ring-width series for the Karkloof growing site, satisfying the first objective of the thesis.

The occurrence of compression, missing rings, ring-width eccentricity, patterns of suppression, release, and statistical outliers confirmed that the Hall (1976) ring-width chronology is not a reliable representation of the average ring-width variability of the *Afrocarpus falcatus* population that were growing at the Karkloof site before it was felled in 1916. This may explain why (Vogel et al., 2001) revealed growth hiatuses in the Karkloof *Afrocarpus falcatus* specimen studied by (Hall, 1976) through radiocarbon dating.

Tree growth-climate relationships were investigated using climate data sets developed by Schulze and Horan (2007; 2010) for rainfall, relative humidity, temperature, solar irradiance, sun duration and precipitation minus evaporation. In the literature review, the thesis established that mean chronologies from sites such as the Karkloof forest, which experience moist conditions, should theoretically correlate with temperature. The results of the climate correlation analysis showed that annual and summer (average, maximum and minimum) temperatures correlated positively with the mean ring-widths. The highest temperature correlation was for summer minimum temperature (CorrC 0.32, T Test 2.7) and the highest correlation with annual temperature was with average temperature (CorrC 0.30 T Test 2.6). No relationships with rainfall were recorded annually or for the summer or winter season. There were no correlations in winter for any of the climate factors.

Non-climatic factors (compression and ring-width eccentricity) were confirmed to be affecting ring-width at this site. This thesis showed that the development of a mean ring-width series at the Karkloof growing site was attainable for *Afrocarpus falcatus* growth-climate relationship

investigation, and this satisfied the second thesis objective and proved hypothesis one and two to be true. However, any application of this finding to palaeoclimate reconstruction would be constrained if it were limited to limited numbers of specimens.

	Hypothesis	**Alternative**
Hypothesis 1:	*Afrocarpus falcatus* tree rings from the Karkloof are annual - **TRUE**	*Afrocarpus falcatus* tree rings from the Karkloof are not annual - **FALSE**
Hypothesis 2:	*Afrocarpus falcatus* tree-ring widths are driven by climate environmental forcing - **TRUE**	Climate cannot be reconstructed from *Afrocarpus falcatus* using tree-ring widths - **FALSE**

Climate correlation with the mean ring-width series showed that mean ring-width variability was driven by temperature and not rainfall. This would suggest that the Hall (1976) ring-width measurement series is not a rainfall proxy record.

5.3 TREE-RING STABLE CARBON ISOTOPES AND ASSOCIATED CLIMATE ENVIRONMENTAL FORCING

Coherence between ring $\delta^{13}C$ series between trees is highly dependent on the correct identification of annual tree rings. Tree ring identification and crossdating of the series confirmed that *Afrocarpus falcatus* produces annual rings. However, missing rings and potentially false rings were identified. Four of the six ring $\delta^{13}C$ series witnessed more negative $\delta^{13}C$ values in their earlier growing years. This is evidence that developmental effects within the $\delta^{13}C$ values of the oldest rings of the series. This was consistent with the literature which shows that $\delta^{13}C$ values within a closed canopy forest are less depleted with increasing forest canopy height (Jackson et al., 1993; McDowell et al., 2011; Offermann et al., 2011; Van der Merwe and Medina, 1991; West et al., 2001). Developmental effects can originate from numerous sources including CO_2 soil respiration, changes in light availability and constraints in hydraulic conductivity with increased height (McDowell et al., 2011). Two samples (PF1, PF12) presented growth trends more typical of open canopy forest trees (less negative $\delta^{13}C$ values in the early years of the tree). This might suggest these two trees experienced greater light intensity and mixed atmospheric air in their early years.

The linear trend of less negative ring $\delta^{13}C$ values with age was observed to extend beyond the point at which the series convergence (in approximately 1950) and is ongoing. This suggests that developmental effects are still influencing $\delta^{13}C$ discrimination in the ring $\delta^{13}C$ series and the most plausible explanation, described in the literature review, may be related to the effects on stomatal conductance from increasing tree height and crown illumination (McDowell et al., 2011). These non-stationary developmental effects on the ring $\delta^{13}C$ values could not been removed in the analysis. However, the series were truncated at the point of convergence (1950) to remove as many non-stationary effects as possible. Since the climate dataset covers 1950 to 1999, the removal of the older ring $\delta^{13}C$ segments would not have affected the investigation into tree growth-climate relationships.

(Hall et al., 2008)) developed a $\delta^{13}C$ modern analogue for *Afrocarpus falcatus* to determine if the archaeological charcoal preserved an environmental signal. However, the developmental effects on *Afrocarpus falcatus* isotope discrimination caused by the closed canopy environment cannot be accounted for in $\delta^{13}C$ values of charcoal. The ring $\delta^{13}C$ series from *Afrocarpus falcatus* museum specimens could be studied though, as they would have grown under more constant conditions and should be able to provide valuable information on the developmental effects from closed canopy environments.

Crossdating was achieved by accounting for missing rings, removal of rings prior to 1950, and applying the Belmecheri and Lavergne (2020) atmospheric CO_2 correction. Coherence between two of the six samples was established (CorrC 0.35, EPS 0.524). This resulted in the development of a mean ring $\delta^{13}C$ width series for the Karkloof growing site, satisfying the second objective of the thesis.

Investigation of the tree growth-climate relationships was achieved using the same climate variables as those applied in the ring-width analysis. As with the ring-width growth-climate hypothesis, the $\delta^{13}C$ literature established that the mean ring $\delta^{13}C$ chronology from the Karkloof growing site should theoretically be more positively correlated with temperature related factors. The results of the climate correlation analysis showed that summer (average, maximum and minimum) temperatures correlated positively with the mean ring $\delta^{13}C$ series. The highest temperature correlation was for summer minimum temperature (CorrC -0.32, T Test 2.6). A strong covariance between mean ring $\delta^{13}C$ series was observed for winter rainfall (CorrC -0.28 T Test -2.2) and precipitation minus evaporation (CorrC -0.25 T Test -2.0).

Canopy related tree developmental effects (understorey soil respiration, availability of light, hydraulic conductivity) were confirmed to be the factors affecting ring $\delta^{13}C$ series at this site. These effects could not be removed from the series however a tentative mean ring $\delta^{13}C$ series was developed (CorrC 0.35, EPS 0.524) and showed that the growth-climate relationship of *Afrocarpus falcatus* is driven by environmental forcing. This satisfied the fourth thesis objective and proved hypothesis three to be true.

	Hypothesis	**Alternative**
Hypothesis 3	*Afrocarpus falcatus* tree ring stable carbon isotopes are driven by climate environmental forcing - **TRUE**	Climate cannot be reconstructed from *Afrocarpus falcatus* using stable carbon isotopes - **FALSE**

5.4 CONCLUSION

Limited understanding of southern Hemisphere's past climate is a limitation to global climate modelling which relies on a representation of the climate system beyond the time period covered by the instrumental record (Villalba, 2000). Since past climate is predominantly derived from the field of palaeoclimatology, scientists in this field need to focus resources on data deficient regions such as South Africa. Environmental proxies that extend climate reconstruction beyond the timescales of meteorological recordings include ice cores, marine sediments, pollen, corals and tree-rings (IPCC, 2013). Tree-ring proxies are valued for their potential to yield continuous, annually resolved climate reconstructions (Jones et al., 2009a) however contributions from South Africa remain sparse with stable carbon isotope ($\delta^{13}C$) studies in South Africa having had more success in the reconstruction of climate than ring-width studies (Woodborne et al., 2016).

Within the context of limited tree-ring studies in southern Africa, the aim of this thesis was to investigate tree-growth climate relationships and develop a modern analogue for *Afrocarpus falcatus* in the Karkloof. This was achieved through ring-width and ring $\delta^{13}C$ analysis. Investigation

into the growth-climate relationship of *Afrocarpus falcatus* showed that temperature was the most important driver in the Karkloof growing area. It is likely that the high moisture regime of the study area results in a low probability of rainfall ever being a limiting factor for growth, except in drier years, where the growth response, in those periods, may invert to follow moisture availability instead of temperature.

This thesis established that challenges exist for dendroclimatological research on trees from closed-canopy environments because these trees have unique experiences within the forest-interior. This thesis confirmed that an adequate number of samples is needed to counteract the high frequency growth responses from closed-canopy trees and to identify a common climate signal.

There is the opportunity to use the Karkloof *Afrocarpus falcatus* museum specimen to extend the temperature record of the study area beyond the available instrumental records. However, as this thesis has shown, a ring-width series from a closed-canopy environment is highly affected by non-climatic factors. It is thus anticipated that without other specimens of similar age, the Karkloof museum specimen ring-width series is not a representative chronology for the growing site, and that the reconstructed temperature record would be of low confidence. Since the ring $\delta^{13}C$ series were shown to be unaffected by compression and ring-width eccentricity and require a much smaller sample size, they would be the more reliable proxy to reconstruct minimum temperatures from the Karkloof museum specimen.

This thesis showed that tree developmental effects on modern ring $\delta^{13}C$ series are dynamic and not well understood. As the developmental effects from the canopy are better able to be accounted for in older specimens, a ring $\delta^{13}C$ series from the Karkloof museum specimen presents an opportunity to elucidate on the effects of factors like atmospheric source air and irradiance. This in turn could assist with a better understanding of the developmental effects in modern samples, and in the development of appropriate statistical methods to identify and isolate these trends.

Dendroclimatology in South Africa has been limited to rainfall reconstructions for the drier northern areas of the country. The Karkloof museum specimen presents a unique opportunity to develop a climate record for the moist temperate areas of KwaZulu-Natal, albeit with its limitations. It would be a start towards trying to extend our spatial records further south and in furthering our understanding of the regional climate system. Importantly, it would immediately assist in developing methods for studying long-lived trees from closed canopy environments in South

Africa, and this could encourage more interest and investment from others to this research. This thesis has highlighted the challenges with researching trees from closed-canopy environments and confirmed that dendroclimatology is more easily implemented on open canopy trees in South Africa. Where museum specimens (and potentially archaeological resources like wooden buildings) exist, canopy growing conditions should first be established. Future dendroclimatological research effort should ideally be redirected to long-lived trees from open canopy environments.

CHAPTER 6: REFERENCES

Adie, H., Lawes, M., 2011. Podocarps in Africa : Temperate Zone Relicts or Rainforest Survivors. Smithsonian Contributions to Botany 95, 79–100.

Ainsworth, E., Rogers, A., 2007. The response of photosynthesis and stomatal conductance to rising [CO2]: mechanisms and environmental interactions. Plant, Cell & Environment 30, 258–270. https://doi.org/10.1111/j.1365-3040.2007.01641.x

Belmecheri, S., Lavergne, A., 2020. Compiled records of atmospheric CO2 concentrations and stable carbon isotopes to reconstruct climate and derive plant ecophysiological indices from tree rings. Dendrochronologia 63, 125748. https://doi.org/10.1016/j.dendro.2020.125748

Bonnesoeur, V., Locatelli, B., Guariguata, M.R., Ochoa-Tocachi, B.F., Vanacker, V., Mao, Z., Stokes, A., Mathez-Stiefel, S.-L., 2019. Impacts of forests and forestation on hydrological services in the Andes: A systematic review. Forest Ecology and Management 433, 569–584. https://doi.org/10.1016/j.foreco.2018.11.033

Bradley, R.S., 2015. Chapter 13 - Tree Rings, in: Bradley, R.S. (Ed.), Paleoclimatology (Third Edition). Academic Press, San Diego, pp. 453–497. https://doi.org/10.1016/B978-0-12-386913-5.00013-2

Brienen, R.J.W., 2011. Stable carbon isotopes in tree rings indicate improved water use efficiency and drought responses of a tropical dry forest tree species. Trees 25, 103–113. https://doi.org/10.1007/s00468-010-0474-1

Briffa, K., Jones, P.D., 1990. Basic chronology statistics and assessment., in: Methods of Dendrochronology: Applications in the Environmental Sciences, In: Cook ER, Kairiukstis LA (Eds). Springer, Kluwer Acad Dordrecht, pp. 137–152.

Briffa, K.R., Melvin, T.M., 2011. A Closer Look at Regional Curve Standardization of Tree-Ring Records: Justification of the Need, a Warning of Some Pitfalls, and Suggested Improvements in Its Application, in: Hughes, M.K., Swetnam, T.W., Diaz, H.F. (Eds.), Dendroclimatology: Progress and Prospects. Springer Netherlands, Dordrecht, pp. 113–145. https://doi.org/10.1007/978-1-4020-5725-0_5

Buras, A., 2017. A comment on the expressed population signal. Dendrochronologia 44, 130–132. https://doi.org/10.1016/j.dendro.2017.03.005

Cook, E.R., 1987. The Decomposition of Tree-Ring Series for Environmental Studies.

Cook, E.R., 1985. A Time series approach to tree-ring standardisation. The University of Arizona.

Cook, E.R., Briffa, K.R., Meko, D.M., Graybill, D.A., Funkhouser, G., 1995. The “segment length curse” in long tree-ring chronology development for palaeoclimatic studies. The Holocene 5, 229–237. https://doi.org/10.1177/095968369500500211

Cook, E.R., Kairiukstis, L.A., 1990. Methods of Dendrochronology: Applications in the Environmental Sciences. Springer Science & Business Media.

Cook, E.R., Peters, K., 1997. Calculating unbiased tree-ring indices for the study of climatic and environmental change. The Holocene 7, 361–370. https://doi.org/10.1177/095968369700700314

Cook, E.R., Peters, K., 1981. The Smoothing Spline: A New Approach to Standardizing Forest Interior Tree-Ring Width Series for Dendroclimatic Studies.

Coplen, T.B., 2011. Guidelines and recommended terms for expression of stable-isotope-ratio and gas-ratio measurement results. Rapid Communications in Mass Spectrometry 25, 2538–2560. https://doi.org/10.1002/rcm.5129

Curtis, B.A., Tyson, P.D., Dyer, T.G.J., 1978. Dendrochronological age determination of Podocarpus falcatus. South African Journal of Science 74, 92–95.

Dale, V.H., Joyce, L.A., McNulty, S., Neilson, R.P., Ayres, M.P., Flannigan, M.D., Hanson, P.J., Irland, L.C., Lugo, A.E., Peterson, C.J., Simberloff, D., Swanson, F.J., Stocks, B.J., Wotton, B.M., 2001. Climate Change and Forest Disturbances: Climate change can affect forests by altering the frequency, intensity, duration, and timing of fire, drought, introduced species, insect and pathogen outbreaks, hurricanes, windstorms, ice storms, or landslides. BioScience 51, 723–734. https://doi.org/10.1641/0006-3568(2001)051[0723:CCAFD]2.0.CO;2

Dunwiddie, P.W., LaMarche, V.C., 1980. A climatically responsive tree-ring record from Widdringtonia cedarbergensis, Cape Province, South Africa. Nature 286, 796–797. https://doi.org/10.1038/286796a0

Ehleringer, J.R., 2017. Stable isotope geochemistry and ecology: Carbon in Plants.

Ehleringer, J.R., 1991. 13C/12C fractionation and its utility in terrestrial plant studies. Academic Press, Inc, United States.

Farquhar, G., O’Leary, M.H., Berry, J., 1982. On the Relationship Between Carbon Isotope Discrimination and the Intercellular Carbon Dioxide Concentration in Leaves. Australian Journal of Plant Physiology 13, 281–292. https://doi.org/10.1071/PP9820121

February, E.C., Stock, W., 1998. The relationship between ring width measures and precipitation for Widdringtonia cedarbergensis. South African Journal of Botany 64, 213–216. https://doi.org/10.1016/S0254-6299(15)30870-X

February, E.C., Stock, W.D., 1999. Declining Trend in the 13C/12C Ratio of Atmospheric Carbon Dioxide from Tree Rings of South African Widdringtonia cedarbergensis. Quaternary Research 52, 229–236. https://doi.org/10.1006/qres.1999.2057

February, Stock, 1998. An assessment of the dendrochronological potential of two Podocarpus species. The Holocene 8, 747–750. https://doi.org/10.1191/095968398674919061

Feng, X., 1999. Trends in intrinsic water-use efficiency of natural trees for the past 100–200 years: a response to atmospheric CO2 concentration. Geochimica et Cosmochimica Acta 63, 1891–1903. https://doi.org/10.1016/S0016-7037(99)00088-5

Fitchett, J.M., 2019. The Holocene Climates of South Africa, in: Knight, J., Rogerson, C.M. (Eds.), The Geography of South Africa : Contemporary Changes and New Directions. Springer International Publishing, Cham, pp. 47–55. https://doi.org/10.1007/978-3-319-94974-1_6

Francey, R.J., Allison, C.E., Etheridge, D.M., Trudinger, C.M., Enting, I.G., Leuenberger, M., Langenfelds, R.L., Michel, E., Steele, L.P., 1999. A 1000-year high precision record of δ13C in atmospheric CO2. Tellus B 51, 170–193. https://doi.org/10.1034/j.1600-0889.1999.t01-1-00005.x

Fritts, H.C., 1976. Tree Rings and Climate. Academic Press INC.

Fritts, H.C., 1966. Growth-Rings of Trees: Their Correlation with Climate. Science 154, 973–979.

Gebrekirstos, A., Bräuning, A., Sass-Klassen, U., Mbow, C., 2014. Opportunities and applications of dendrochronology in Africa. Current Opinion in Environmental Sustainability 6, 48–53. https://doi.org/10.1016/j.cosust.2013.10.011

Gillooly, J.F., 1975. A preliminary assessment of the potential offered by some indigenous tree species in the Rustenburg district, for dendrochronology in South Africa. Department of Geography and Environmental Studies, University of Witwatersrand, Johannesburg.

Grissino-Mayer, H.D., 2001. Evaluating Crossdating Accuracy: A Manual and Tutorial for the Computer Program COFECHA.

Hall, G., Woodborne, S., Pienaar, M., 2009. Rainfall control of the δ13C ratios of Mimusops caffra from KwaZulu-Natal, South Africa. The Holocene 19, 251–260. https://doi.org/10.1177/0959683608100569

Hall, G., Woodborne, S., Scholes, M., 2008. Stable carbon isotope ratios from archaeological charcoal as palaeoenvironmental indicators. Chemical Geology 247, 384–400. https://doi.org/10.1016/j.chemgeo.2007.11.001

Hall, M., 1976. Dendroclimatology, rainfall and human adaptation in the later Iron Age of Natal and Zululand. Annals of the Natal Museum 22, 693–703.

Helama, S., Arppe, L., Timonen, M., Mielikäinen, K., Oinonen, M., 2018. A 7.5 ka chronology of stable carbon isotopes from tree rings with implications for their use in palaeo-cloud reconstruction. Global and Planetary Change 170, 20–33. https://doi.org/10.1016/j.gloplacha.2018.08.002

Holmes, R., 1983. Computer-assisted quality control in tree-ring dating and measurement. Tree Ring Bulletin 43, 69–75.

Holmes, R.L., Adams, R.K., Fritts, H.C., 1986. Tree-Ring Chronologies of Western North America: California, Eastern Oregon and Northern Great Basin with Procedures Used in the Chronology Development Work Including Users Manuals for Computer Programs COFECHA and ARSTAN. Laboratory of Tree-Ring Research, University of Arizona (Tucson, AZ).

Holmgren, K., Karlén, W., Lauritzen, S.E., Lee-Thorp, J.A., Partridge, T.C., Piketh, S., Repinski, P., Stevenson, C., Svanered, O., Tyson, P.D., 1999. A 3000-year high-resolution stalagmite-based record of palaeoclimate for northeastern South Africa. The Holocene 9, 295–309. https://doi.org/10.1191/095968399672625464

Hughes, M.K., 2002. Dendrochronology in climatology – the state of the art. Dendrochronologia 20, 95–116. https://doi.org/10.1078/1125-7865-00011

IPCC, 2013. Climate Change 2013: The Physical Science Basis. Contribution of Working Group I to the Fifth Assessment Report of the Intergovernmental Panel on Climate Change . (No. [Stocker, T.F., D. Qin, G.-K. Plattner, M. Tignor, S.K. Allen, J. Boschung, A. Nauels, Y. Xia, V. Bex and P.M. Midgley (eds.)]). Cambridge University Press, Cambridge, United Kingdom and New York, NY, USA, 1535 pp.doi:10.1017/CBO9781107415324.

Jackson, P.C., Meinzer, F.C., Goldstein, G., Holbrook, N.M., Cavelier, J., Rada, F., 1993. 9 - Environmental and Physiological Influences on Carbon Isotope Composition of Gap and Understory Plants in a Lowland Tropical Forest, in: Ehleringer, J.R., Hall, A.E., Farquhar, G.D. (Eds.), Stable Isotopes and Plant Carbon-Water Relations. Academic Press, San Diego, pp. 131–140. https://doi.org/10.1016/B978-0-08-091801-3.50016-7

Jones, P.D., Briffa, K.R., Osborn, T.J., Lough, J.M., van Ommen, T.D., Vinther, B.M., Luterbacher, J., Wahl, E.R., Zwiers, F.W., Mann, M.E., Schmidt, G.A., Ammann, C.M., Buckley, B.M., Cobb, K.M., Esper, J., Goosse, H., Graham, N., Jansen, E., Kiefer, T., Kull, C., Küttel, M., Mosley-Thompson, E., Overpeck, J.T., Riedwyl, N., Schulz, M., Tudhope, A.W., Villalba, R., Wanner, H., Wolff, E., Xoplaki, E., 2009. High-resolution palaeoclimatology of the last millennium: a review of current status and future prospects. The Holocene 19, 3–49. https://doi.org/10.1177/0959683608098952

Kagawa, A., Sugimoto, A., Moaximov, T., 2006. 13CO2 pulse-labelling of photoassimilates reveals carbon allocation within and between tree rings. Plant, Cell & Environment 29, 1571–1584. https://doi.org/10.1111/j.1365-3040.2006.01533.x

Krepkowski, J., Bräuning, A., Gebrekirstos, A., Strobl, S., 2011. Cambial growth dynamics and climatic control of different tree life forms in tropical mountain forest in Ethiopia. Trees 25, 59–70. https://doi.org/10.1007/s00468-010-0460-7

Krepkowski, J., Gebrekirstos, A., Shibistova, O., Bräuning, A., 2013. Stable carbon isotope labeling reveals different carry-over effects between functional types of tropical trees in an Ethiopian mountain forest. New Phytologist 199, 431–440. https://doi.org/10.1111/nph.12266

Leavitt, S.W., 2010. Tree-ring C–H–O isotope variability and sampling. Science of The Total Environment 408, 5244–5253. https://doi.org/10.1016/j.scitotenv.2010.07.057

Leavitt, S.W., Danzer, S.R., 1993. Method for batch processing small wood samples to holocellulose for stable-carbon isotope analysis. Anal. Chem. 65, 87–89. https://doi.org/10.1021/ac00049a017

Lilly MA, 1977. An assessment of the dendrochronological potential of indigenous tree species in South Africa. Occ. Paper No. 18 (Dept Geogr. & envir. Stud., Univ. of Witwatersrand, Johannesburg).

Loader, N.J., McCarroll, D., Miles, D., Young, G.H.F., Davies, D., Ramsey, C.B., 2019. Tree ring dating using oxygen isotopes: a master chronology for central England. Journal of Quaternary Science 34, 475–490. https://doi.org/10.1002/jqs.3115

Loader, N.J., Robertson, I., Barker, A.C., Switsur, V.R., Waterhouse, J.S., 1997. An improved technique for the batch processing of small wholewood samples to α-cellulose. Chemical Geology 136, 313–317. https://doi.org/10.1016/S0009-2541(96)00133-7

Macfarlane, C., Warren, C.R., White, D.A., Adams, M.A., 1999. A rapid and simple method for processing wood to crude cellulose for analysis of stable carbon isotopes in tree rings. Tree Physiology 19, 831–835. https://doi.org/10.1093/treephys/19.12.831

Martinelli, N., 2004. Climate from dendrochronology: latest developments and results. Global and Planetary Change 40, 129–139. https://doi.org/10.1016/S0921-8181(03)00103-6

Maxwell, R.S., Wixom, J.A., Hessl, A.E., 2011. A comparison of two techniques for measuring and crossdating tree rings. Dendrochronologia 29, 237–243. https://doi.org/10.1016/j.dendro.2010.12.002

McCarroll, D., Loader, N.J., 2006. Isotopes in Tree Rings, in: Leng, M.J. (Ed.), Isotopes in Palaeoenvironmental Research. Springer Netherlands, Dordrecht, pp. 67–116. https://doi.org/10.1007/1-4020-2504-1_02

McCarroll, D., Loader, N.J., 2004. Stable isotopes in tree rings. Quaternary Science Reviews 23, 771–801. https://doi.org/10.1016/j.quascirev.2003.06.017

McDowell, N.G., Bond, B.J., Dickman, L.T., Ryan, M.G., Whitehead, D., 2011. Relationships Between Tree Height and Carbon Isotope Discrimination, in: Meinzer, F.C., Lachenbruch, B., Dawson, T.E. (Eds.), Size- and Age-Related Changes in Tree Structure and Function. Springer Netherlands, Dordrecht, pp. 255–286. https://doi.org/10.1007/978-94-007-1242-3_10

McNaughton, J., Tyson, P.O., 1979. A Preliminary Assessment of Podocarpus falcatus In Dendrochronological and Dendroclimatological Studies in the Witelsbos Forest Reserve. South African Forestry Journal 111, 29–33. https://doi.org/10.1080/00382167.1979.9630201

Monserud, R.A., Marshall, J.D., 2001. Time-series analysis of δ13C from tree rings. I. Time trends and autocorrelation. Tree Physiology 21, 1087–1102. https://doi.org/10.1093/treephys/21.15.1087

Mosteller, F., Tukey, J., 1977. Data analysis and regression. Reading, MA: Addison-Wesley.

Neukom, R., Nash, D.J., Endfield, G.H., Grab, S.W., Grove, C.A., Kelso, C., Vogel, C.H., Zinke, J., 2014. Multi-proxy summer and winter precipitation reconstruction for southern Africa over the last 200 years. Climate Dynamics 42, 2713–2726. https://doi.org/10.1007/s00382-013-1886-6

Norström, E., Holmgren, K., Mörth, C.-M., 2008. A 600-year-long δ18O record from cellulose of Breonadia salicina trees, South Africa. Dendrochronologia 26, 21–33. https://doi.org/10.1016/j.dendro.2007.08.001

Norström, E., Holmgren, K., Morth, C.-M., 2005. Rainfall-driven variations in δ13C composition and wood anatomy of Breonadia salicina trees from South Africa between AD 1375 and 1995 : research article. South African Journal of Science 101, 162–168.

Offermann, C., Ferrio, J.P., Holst, J., Grote, R., Siegwolf, R., Kayler, Z., Gessler, A., 2011. The long way down—are carbon and oxygen isotope signals in the tree ring uncoupled from canopy physiological processes? Tree Physiology 31, 1088–1102. https://doi.org/10.1093/treephys/tpr093

O'Leary, M.H., 1988. Carbon Isotopes in Photosynthesis. BioScience 38, 328–336. https://doi.org/10.2307/1310735

Osborn, T.J., Briffa, K.R., 2000. Revisiting timescale-dependent reconstruction of climate from tree-ring chronologies. Dendrochronologia 18, 9–25.

Pearl, J., Keck, J., Tintor, W., Siekacz, L., Herrick, H., Meko, D., Pearson, C., 2020. New frontiers in tree-ring research. The Holocene 30, 095968362090223. https://doi.org/10.1177/0959683620902230

Peel, M.C., Finlayson, B.L., McMahon, T.A., 2007. Updated world map of the Köppen-Geiger climate classification. Hydrology and Earth System Sciences Discussions 4, 439–473. https://doi.org/10.5194/hessd-4-439-2007

Preston-Whyte, R.A., Tyson, P.D., 1988. The atmosphere and weather of southern Africa. Oxford University Press, Cape Town.

Rezaie, N., D'Andrea, E., Bräuning, A., Matteucci, G., Bombi, P., Lauteri, M., 2018. Do atmospheric CO2 concentration increase, climate and forest management affect iWUE of common beech? Evidences from carbon isotope analyses in tree rings. Tree Physiology 38, 1110–1126. https://doi.org/10.1093/treephys/tpy025

Rinntech, 2011. LINTAB. Precision Ring by Ring. Available at: http://www.rinntech.de/content/view/16/47/lang,english/.

Robertson, I., Leavitt, S., 2008. Progress in isotope dendroclimatology. Chemical Geology 252, EX1–EX4.

Rutherford, M. C, Mucina, L, Mucina, Ladislav, Rutherford, Michael C, 2006. The vegetation of South Africa, Lesotho and Swaziland.

Saurer, M., Siegwolf, R.T.W., Schweingruber, F.H., 2004. Carbon isotope discrimination indicates improving water-use efficiency of trees in northern Eurasia over the last 100 years. Global Change Biology 10, 2109–2120. https://doi.org/10.1111/j.1365-2486.2004.00869.x

Savard, M.M., Daux, V., 2020. An overview on isotopic divergences – causes for instability of tree-ring isotopes and climate correlations. Climate of the Past 16, 1223–1243. https://doi.org/10.5194/cp-16-1223-2020

Schweingruber, F.H., 1988. Tree Rings: Basics and Applications of Dendrochronology. Kluwer Academic Publishers.

Seifert, T., Seifert, S., Seydack, A., Durrheim, G., Gadow, K. von, 2014. Competition effects in an afrotemperate forest. Forest Ecosystems 1, 13. https://doi.org/10.1186/s40663-014-0013-4

Siyum, Z.G., Ayoade, J.O., Onilude, M.A., Feyissa, M.T., 2019. Climate forcing of tree growth in dry Afromontane forest fragments of Northern Ethiopia: evidence from multi-species responses. Forest Ecosystems 6, 15. https://doi.org/10.1186/s40663-019-0178-y

Speer, J.H., 2010. Fundamentals of Tree-ring Research. University Of Arizon Press.

Stokes, Smiley, 1968. An Introduction to Tree-Ring Dating, University of Chicago, Chicago.

Thackeray, J.F., 1996. Ring width variation in a specimen of south African Podocarpus, circa 1350-1937 A.D. Palaeoecology of Africa 24, 223–240.

Thackeray, J.F., Potze, S., 2000. A sectioned yellowwood tree trunk housed at the Transvaal Museum, Pretoria. Annals of the Transvaal Museum.

Therrell, M., Stahle, D., Ries, L., Schugart, H., 2006. Tree-ring reconstructed rainfall variability in Zimbabwe. Clim Dyn. 26, 677–685.

Tyson, P.D., Dyer, T.G.J., 1975. Mean Annual Fluctuations Of Precipitation In The Summer Rainfall Region Of South Africa. null 57, 105–110. https://doi.org/10.1080/03736245.1974.10559553

Van der Merwe, N.J., Medina, E., 1991. The canopy effect, carbon isotope ratios and foodwebs in amazonia. Journal of Archaeological Science 18, 249–259. https://doi.org/10.1016/0305-4403(91)90064-V

Van der Sleen, P., Zuidema, P.A., Pons, T.L., 2017. Stable isotopes in tropical tree rings: theory, methods and applications. Functional Ecology 31, 1674–1689. https://doi.org/10.1111/1365-2435.12889

Villalba, R., 2000. Dendroclimatology: A Southern Hemisphere Perspective, in: Smolka, P., Volkheimer, W. (Eds.), Southern Hemisphere Paleo- and Neoclimates: Key Sites, Methods, Data and Models. Springer Berlin Heidelberg, Berlin, Heidelberg, pp. 27–57.

Vogel, J.C., Fuls, A., Visser, E., 2001. Radiocarbon adjustments to the dendrochronology of a yellowwood tree : research letter. South African Journal of Science 97, 164–166.

West, A.G., Midgley, J.J., Bond, W.J., 2001. The evaluation of δ13C isotopes of trees to determine past regeneration environments. Forest Ecology and Management 147, 139–149. https://doi.org/10.1016/S0378-1127(00)00474-6

Wigley, T.M.L., Jones, P.D., Briffa, K.R., 1987. Cross-dating methods in dendrochronology. Journal of Archaeological Science 14, 51–64. https://doi.org/10.1016/S0305-4403(87)80005-5

Woodborne, S., Gandiwa, P., Hall, G., Patrut, A., Finch, J., 2016. A Regional Stable Carbon Isotope Dendro-Climatology from the South African Summer Rainfall Area. PLOS ONE 11, 1–15. https://doi.org/10.1371/journal.pone.0159361

Woodborne, S., Hall, G., Robertson, I., Patrut, A., Rouault, M., Loader, N.J., Hofmeyr, M., 2015. A 1000-Year Carbon Isotope Rainfall Proxy Record from South African Baobab Trees

(Adansonia digitata L.). PLOS ONE 10, e0124202. https://doi.org/10.1371/journal.pone.0124202

APPENDICES

Appendix A: Field sampling records

Study area	Description
Names of collectors	UKZN: J. Baverstock, Dr. J.M Finch, Prof. T.R Hill, Prof. S. Woodborne
Tree species	*Afrocarpus falcatus*
No. of trees sampled in total	20
Permit details	DAFF KZN0023/06/14-15/17
Sampling date(s)	7 November 2014 23 November 2014 September 2015 15 September 2015
Place	Karkloof, KwaZulu-Natal, South Africa
Nearby town and local authority District	Howick, Umngeni Local Municipality Mshwati District Municipality
Properties permissions	Mbona Private Nature Reserve (Richard Booth, Conservation Director, mbona@iuncapped.co.za) UCL Company (Pty) Ltd 'The Forest' (Edward Naidoo, Agricultural Manager, naidooe@ucl.co.za)
Latitude and longitude	2km extent of study area between 29°18'19.00"S 30°21'5.00"E and
Height a.s.l (m)	1200 - 1500
Slope inclination	South east facing slope (shaded from between 14h00-16h00) Average 23% (tilted stems)
Summer rainfall season and MAP	October – March, 1271 mm (OBSHIS4682 1950-1999) 80% of rainfall in summer season (Tyson and Dyer, 1975)
Temperature	annual mean max 22°C, annual mean min 10°C
Known disturbances in area	Felling between 1850 and 1950
Climate (Köppen-Geiger)	Warm, temperate, warm summer
Aridity (De Martonne)	Moist sub-humid
Forest type	Dominant trees as %
Surface layer	organic layer with decomposition
Nearby water sources (distance)	Head streams, main head Mpolweni
Forest type Dominant species Canopy	Mist-belt mixed Podocarpus forest (Rutherford et al., 2006) *Podocarpus latifolius* closed stand
Afrocarpus falcatus leaves	Slightly sickle shaped Mature leaves twisted at base Small (3-5 x 0.3-0.5 cm) Leaf apex: Narrowly tapering and sharply pointed
Bark	Dark purplish brown Flaking in rough round to rectangular patches

UCL Property- ‘The Forest’

Mbona Nature Reserve

Location of samples in study area

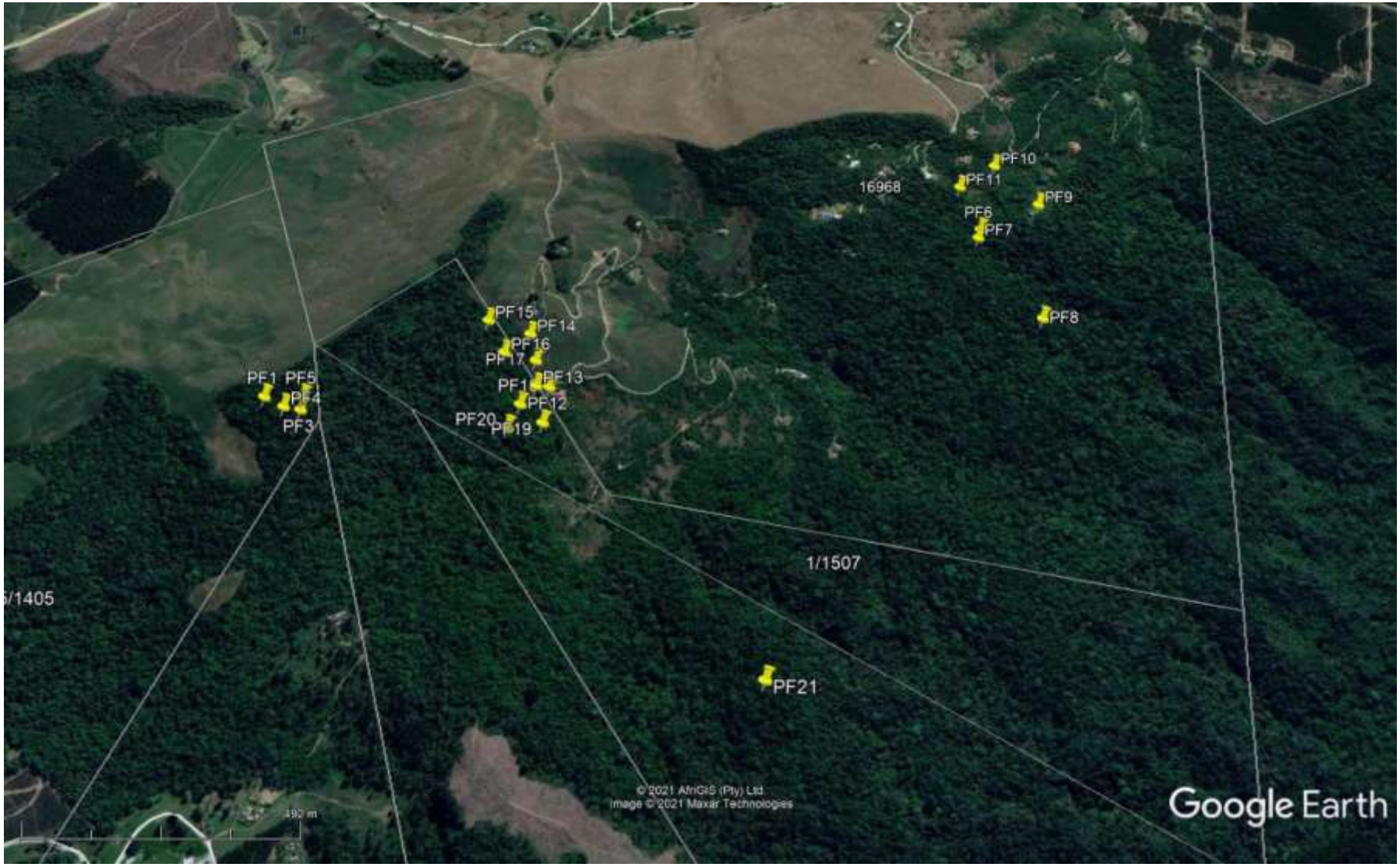

Sampled trees

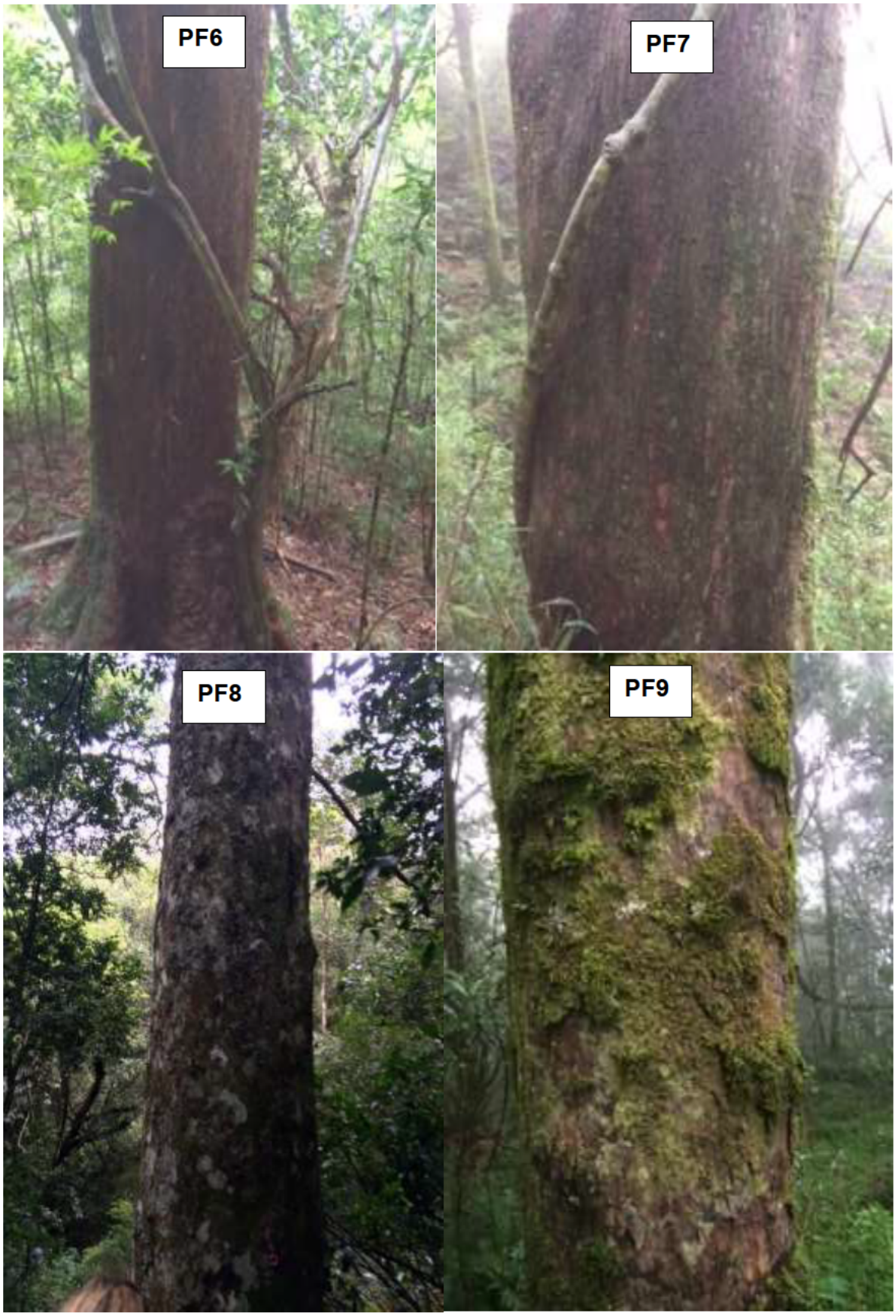
PF6
PF7
PF8
PF9


PF10


PF11


PF12


PF13


PF14
PF15
PF16
PF17


PF18


PF19


PF20


PF21

Sampling records							
ID	**GPS coordinates**	**masl**	**Circumference / diameter (cm)**	**Height / crown (m)**	**Locality**	**Cored date**	**Comment**
PF1	29°18'19.00"S, 30°21'5.00"E	1469	120/19.1	13/3	The Forest	11/07/14	
PF3	29°18'20.00"S, 30°21'8.00" E	1455	115/18.1	10/3	The Forest	11/07/14	
PF4	29°18'19.77"S, 30°21'6.65"E	1463	101/16.08	11/4	The Forest	11/07/14	
PF5	29°18'19.00"S, 30°21'8.00"E	1465	100/15.92	10/5	The Forest	11/07/2014	
PF6	29°18'04" S,30°22'03"E	1305	112/17.83	11/4	The Forest	06/04/2015	Quite deformed
PF7	29°18'4.77"S 30°22'2.74"E	1301	113/17.99	13/5	Yellowwood Walk (right)	06/04/2015	
PF8	29°18'11.96"S 30°22'7.13"E	1233	118/18.78	13/5	Yellowwood Walk (right)	06/04/2015	
PF9	29°18'1.56"S 30°22'8.39"E	1288	121/19.26	13/6	Below Mbona, Residence	06/04/2015	Treehouse above Yellowwood Walk
PF10	29°17'57.76"S 30°22'5.07"E	1313	150/23.88	14/7	Mbona, Zebra Walk	06/04/2015	
PF11	29°17'59.92"S 30°22'1.74"E	1322	120/19.1	13/6	Mbona, Zebra Walk	06/04/2015	labelled tree
PF12	29°18'18"S, 30°21'26"E	1349	200 / 31.84	20/10	Mbona, western Mbona / UCL border	06/04/2015	Entangled in barbed wire, not pole
PF13	29°18'17.88"S 30°21'26.09"E	1355	142/22.6	11/4	Mbona, Roadside	06/04/2015	
PF14	29°18'13.65"S, 30°21'25.3"E	1370	160/25.47	14/8	Mbona, western Mbona / UCL border	10/09/2015	pole
PF15	29°18'12.54"S 30°21'21.82"E	1426	80/12.73	12/5	Mbona, western Mbona / UCL border	10/09/2015	steep
PF16	29°18'15.20"S 30°21'23.34"E	1393	114/18.15	10/3	Mbona, western Mbona / UCL border	10/09/2015	Very steep
PF17	29°18'15.85"S, 30°21'25.9"E	1370	111/17.67	10 10/4	Mbona, western Mbona / UCL border	10/09/2015	buttressy, steep
PF18	29°18'19.37"S 30°21'24.95"E	1351	133/21.17	20/8	Mbona, western Mbona / UCL border	10/09/2015	small lobate shape but minimal
PF19	29°18'20.8" S, 30°21'26.8"E	1333	98/15.6	10 / 3	Mbona, western Mbona / UCL border	10/09/2015	pole
PF20	29°18'21.2"S, 30°21'24.1"E	1344	157/24.99	25/10	Mbona, western Mbona / UCL border	10/09/2015	pole
PF21	29°18'21.2"S, 30°21'24.1"E	1207	120/19.10	15/5	UCL property, not the Forest	28/09/2015	

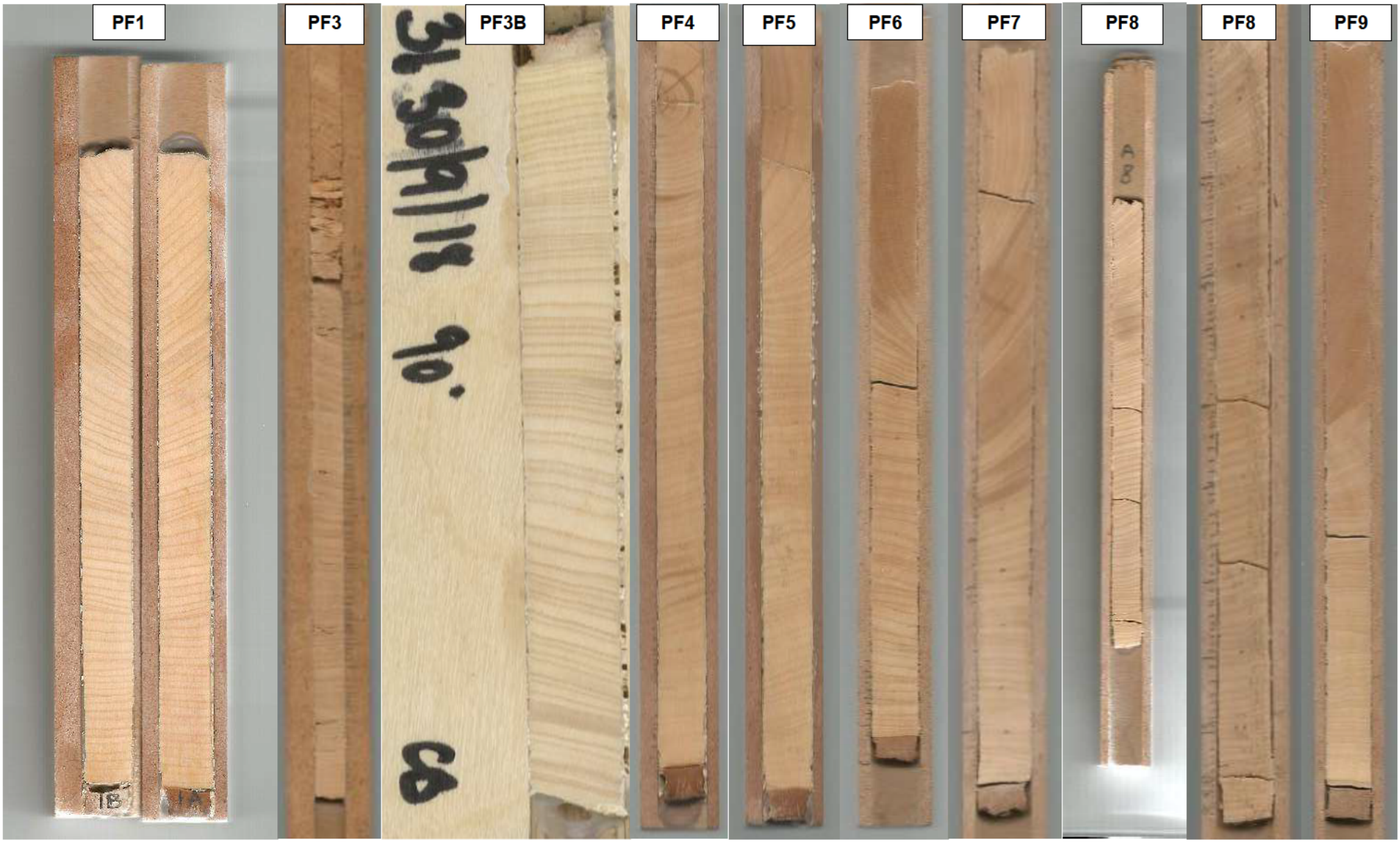
PF1
PF3
PF3B
PF4
PF5
PF6
PF7
PF8
PF8
PF9


PF10
PF11
PF12
PF13
PF14
PF15
PF16
PF17
PF18
PF19
PF20
PF21

Appendix B: Climate records

UKZN OBSHIS4682 year average annual climate records											
Year	start	end	rainfall	T max	T min	Ave T	Evap	Radiation	Rel hum	Sun dur	p-e
1950	>=1950/01/01	<=1950/12/31	2,9	21,6	10,0	15,8	3,2	17,1	93,1	52,4	-0,3
1951	>=1951/01/01	<=1951/12/31	3,4	21,5	9,3	15,4	3,2	17,5	93,8	51,8	0,2
1952	>=1952/01/01	<=1952/12/31	3,2	21,5	9,7	15,6	3,1	17,3	93,8	52,7	0,0
1953	>=1953/01/01	<=1953/12/31	2,9	21,2	9,2	15,2	3,1	17,2	93,9	52,8	-0,2
1954	>=1954/01/01	<=1954/12/31	3,1	21,7	9,5	15,6	3,2	17,7	94,4	50,7	-0,1
1955	>=1955/01/01	<=1955/12/31	3,0	21,6	9,3	15,4	3,2	17,8	94,3	51,0	-0,2
1956	>=1956/01/01	<=1956/12/31	3,6	21,7	9,5	15,6	3,2	17,6	93,5	51,3	0,4
1957	>=1957/01/01	<=1957/12/31	3,9	21,9	9,9	15,9	3,2	17,5	93,5	50,8	0,7
1958	>=1958/01/01	<=1958/12/31	3,1	22,4	9,7	16,0	3,3	17,9	93,1	48,7	-0,2
1959	>=1959/01/01	<=1959/12/31	3,5	22,1	9,4	15,8	3,3	17,9	93,4	49,7	0,2
1960	>=1960/01/01	<=1960/12/31	3,4	21,9	9,5	15,7	3,2	17,4	92,3	51,3	0,2
1961	>=1961/01/01	<=1961/12/31	3,8	22,1	9,8	15,9	3,3	17,5	92,4	50,9	0,5
1962	>=1962/01/01	<=1962/12/31	3,2	22,5	9,7	16,1	3,3	17,7	91,7	48,9	-0,1
1963	>=1963/01/01	<=1963/12/31	3,0	22,0	9,9	15,9	3,2	17,3	92,3	51,7	-0,2
1964	>=1964/01/01	<=1964/12/31	2,8	21,5	10,0	15,8	3,1	16,9	92,6	53,4	-0,3
1965	>=1965/01/01	<=1965/12/31	2,5	21,8	9,4	15,6	3,2	17,5	92,3	52,1	-0,8
1966	>=1966/01/01	<=1966/12/31	2,3	22,1	9,9	16,0	3,2	17,2	92,0	51,3	-0,9
1967	>=1967/01/01	<=1967/12/31	3,4	21,4	9,6	15,5	3,1	16,9	92,9	53,6	0,3
1968	>=1968/01/01	<=1968/12/31	2,6	21,2	9,4	15,3	3,1	16,9	92,8	54,2	-0,6
1969	>=1969/01/01	<=1969/12/31	3,1	21,8	10,2	16,0	3,2	16,8	92,3	52,7	-0,1
1970	>=1970/01/01	<=1970/12/31	2,8	22,2	9,8	16,0	3,3	17,8	92,5	50,3	-0,5
1971	>=1971/01/01	<=1971/12/31	2,9	21,6	9,6	15,6	3,2	17,5	93,8	51,9	-0,3
1972	>=1972/01/01	<=1972/12/31	2,8	21,9	9,7	15,8	3,3	17,8	93,7	50,6	-0,5
1973	>=1973/01/01	<=1973/12/31	3,3	21,0	9,5	15,2	3,0	16,7	93,4	54,9	0,3
1974	>=1974/01/01	<=1974/12/31	3,5	21,3	9,9	15,6	3,1	16,7	92,1	54,2	0,4
1975	>=1975/01/01	<=1975/12/31	3,4	22,1	9,8	15,9	3,2	17,2	91,3	51,4	0,1
1976	>=1976/01/01	<=1976/12/31	4,0	22,0	9,8	15,9	3,3	17,4	91,9	51,1	0,7

1977	>=1977/01/01	<=1977/12/31	2,9	23,1	9,7	16,4	3,5	18,0	90,8	47,0	-0,6
1978	>=1978/01/01	<=1978/12/31	3,9	22,2	9,8	16,0	3,3	17,2	91,6	50,9	0,7
1979	>=1979/01/01	<=1979/12/31	3,1	22,4	9,7	16,0	3,4	17,9	91,8	50,1	-0,3
1980	>=1980/01/01	<=1980/12/31	2,9	22,8	9,3	16,1	3,5	18,1	91,7	47,8	-0,6
1981	>=1981/01/01	<=1981/12/31	2,9	21,7	9,2	15,4	3,2	17,5	92,5	52,2	-0,4
1982	>=1982/01/01	<=1982/12/31	2,8	22,0	9,9	15,9	3,3	17,3	91,4	51,6	-0,4
1983	>=1983/01/01	<=1983/12/31	2,8	22,0	10,3	16,1	3,2	16,9	91,0	52,3	-0,4
1984	>=1984/01/01	<=1984/12/31	3,6	21,1	9,5	15,3	3,1	16,9	92,7	54,8	0,5
1985	>=1985/01/01	<=1985/12/31	3,9	22,4	10,1	16,2	3,3	17,5	91,4	49,8	0,5
1986	>=1986/01/01	<=1986/12/31	3,1	22,1	9,9	16,0	3,3	17,5	92,0	50,8	-0,2
1987	>=1987/01/01	<=1987/12/31	4,5	21,6	10,4	16,0	3,1	16,4	91,5	53,9	1,4
1988	>=1988/01/01	<=1988/12/31	3,5	21,4	10,1	15,7	3,1	16,4	91,1	54,4	0,4
1989	>=1989/01/01	<=1989/12/31	3,4	21,2	9,7	15,5	3,1	16,6	91,8	55,1	0,3
1990	>=1990/01/01	<=1990/12/31	3,5	20,8	9,6	15,2	3,0	16,4	92,3	56,3	0,4
1991	>=1991/01/01	<=1991/12/31	3,6	21,7	10,2	15,9	3,1	16,7	92,1	53,4	0,5
1992	>=1992/01/01	<=1992/12/31	2,1	23,2	9,9	16,5	3,5	18,2	90,7	46,9	-1,4
1993	>=1993/01/01	<=1993/12/31	3,0	22,2	10,2	16,2	3,3	17,2	91,1	50,6	-0,3
1994	>=1994/01/01	<=1994/12/31	2,9	22,0	9,2	15,6	3,3	17,7	91,7	50,9	-0,4
1995	>=1995/01/01	<=1995/12/31	3,6	21,7	10,0	15,9	3,2	16,9	91,4	53,0	0,4
1996	>=1996/01/01	<=1996/12/31	3,8	20,9	9,9	15,4	3,0	16,4	92,1	56,6	0,8
1997	>=1997/01/01	<=1997/12/31	3,8	20,7	9,9	15,3	3,0	16,1	92,1	57,3	0,8
1998	>=1998/01/01	<=1998/12/31	3,3	21,9	10,0	16,0	3,2	16,9	91,2	52,2	0,1
1999	>=1999/01/01	<=1999/12/31	1,7	22,8	10,5	16,6	3,4	17,4	91,0	48,9	-1,7

UKZN OBSHIS4682 average summer climate records											
Year	start	end	rainfall	T max	T min	Ave T	Evap	Radiation	Rel hum	Sun dur	p-e
1950	>=1950/09/01	<=1951/03/31	4,2	23,0	11,98	17,5	3,8	20,0	93,8	57,6	0,4
1951	>=1951/09/01	<=1952/03/31	4,7	23,2	12,11	17,6	3,8	20,0	94,2	57,3	0,9
1952	>=1952/09/01	<=1953/03/31	4,8	22,9	11,96	17,4	3,8	19,8	94,2	58,3	1,1
1953	>=1953/09/01	<=1954/03/31	4,0	22,9	12,05	17,5	3,8	19,9	94,4	57,8	0,2
1954	>=1954/09/01	<=1955/03/31	4,9	23,1	12,12	17,6	3,8	20,3	94,5	56,3	1,1
1955	>=1955/09/01	<=1956/03/31	4,4	23,3	11,86	17,6	3,9	20,6	94,6	55,5	0,5
1956	>=1956/09/01	<=1957/03/31	6,1	22,9	11,90	17,4	3,8	20,1	94,5	57,6	2,4
1957	>=1957/09/01	<=1958/03/31	5,4	23,7	12,50	18,1	3,9	20,4	94,1	54,9	1,4
1958	>=1958/09/01	<=1959/03/31	5,0	23,7	12,04	17,9	4,0	20,7	93,9	54,9	1,1
1959	>=1959/09/01	<=1960/03/31	4,0	23,4	11,66	17,5	3,9	20,4	93,9	55,8	0,1
1960	>=1960/09/01	<=1961/03/31	5,5	23,7	12,39	18,0	3,9	20,1	92,9	55,3	1,6
1961	>=1961/09/01	<=1962/03/31	5,5	23,4	11,68	17,5	3,9	20,2	93,1	57,0	1,6
1962	>=1962/09/01	<=1963/03/31	5,1	23,7	12,15	17,9	3,9	20,2	92,9	55,8	1,2
1963	>=1963/09/01	<=1964/03/31	3,5	24,7	13,17	18,9	4,1	20,2	91,6	52,5	-0,6
1964	>=1964/09/01	<=1965/03/31	3,5	23,3	12,01	17,7	3,9	20,0	93,2	57,1	-0,4
1965	>=1965/09/01	<=1966/03/31	3,3	23,1	11,80	17,5	3,8	19,9	93,1	58,2	-0,5
1966	>=1966/09/01	<=1967/03/31	4,9	23,0	12,25	17,6	3,7	19,3	93,2	58,7	1,2
1967	>=1967/09/01	<=1968/03/31	3,7	23,4	12,06	17,7	3,9	19,8	93,3	56,4	-0,2
1968	>=1968/09/01	<=1969/03/31	4,1	23,8	12,31	18,1	4,0	20,0	92,7	55,5	0,1
1969	>=1969/09/01	<=1970/03/31	3,3	23,3	11,98	17,6	3,9	20,1	93,6	57,2	-0,6
1970	>=1970/09/01	<=1971/03/31	4,6	23,4	12,31	17,9	3,9	20,3	93,5	56,0	0,7
1971	>=1971/09/01	<=1972/03/31	4,7	23,0	11,87	17,5	3,8	20,3	94,5	57,2	0,9
1972	>=1972/09/01	<=1973/03/31	4,1	23,6	12,13	17,9	3,9	20,4	94,0	55,0	0,1
1973	>=1973/09/01	<=1974/03/31	5,2	22,3	11,98	17,1	3,6	18,8	93,7	60,8	1,6
1974	>=1974/09/01	<=1975/03/31	4,0	23,1	12,07	17,6	3,8	19,6	92,5	58,3	0,2
1975	>=1975/09/01	<=1976/03/31	7,4	23,2	12,16	17,7	3,8	19,7	93,1	57,7	3,6

1976	>=1976/09/01	<=1977/03/31	4,0	24,1	12,47	18,3	4,0	20,3	92,0	54,6	0,0
1977	>=1977/09/01	<=1978/03/31	4,8	24,9	12,89	18,9	4,1	20,4	91,3	51,7	0,6
1978	>=1978/09/01	<=1979/03/31	5,6	23,9	11,77	17,8	4,0	20,7	93,2	54,6	1,5
1979	>=1979/09/01	<=1980/03/31	3,8	24,1	11,68	17,9	4,1	21,0	93,6	53,5	-0,3
1980	>=1980/09/01	<=1981/03/31	4,7	23,4	12,10	17,8	3,9	19,9	93,0	57,4	0,8
1981	>=1981/09/01	<=1982/03/31	4,2	23,6	11,54	17,6	4,0	20,4	92,8	55,8	0,2
1982	>=1982/09/01	<=1983/03/31	3,7	24,0	12,33	18,2	4,0	20,4	91,8	54,6	-0,4
1983	>=1983/09/01	<=1984/03/31	5,5	22,7	12,31	17,5	3,6	18,6	92,3	60,3	1,9
1984	>=1984/09/01	<=1985/03/31	6,0	23,5	12,15	17,8	3,9	20,2	92,6	55,9	2,1
1985	>=1985/09/01	<=1986/03/31	4,8	23,7	12,22	18,0	4,0	20,4	92,5	55,6	0,9
1986	>=1986/09/01	<=1987/03/31	6,2	23,2	12,34	17,8	3,8	19,7	92,9	57,2	2,4
1987	>=1987/09/01	<=1988/03/31	5,1	22,9	12,99	17,9	3,6	18,3	92,9	59,9	1,5
1988	>=1988/09/01	<=1989/03/31	4,7	22,2	11,98	17,1	3,6	18,7	92,3	61,6	1,1
1989	>=1989/09/01	<=1990/03/31	5,5	22,4	11,64	17,0	3,6	19,2	93,4	60,8	1,9
1990	>=1990/09/01	<=1991/03/31	5,4	22,6	12,10	17,3	3,7	18,8	92,9	60,3	1,7
1991	>=1991/09/01	<=1992/03/31	4,5	23,7	12,53	18,1	3,9	20,0	92,7	56,1	0,6
1992	>=1992/09/01	<=1993/03/31	3,4	24,4	12,30	18,4	4,1	20,8	92,1	53,1	-0,8
1993	>=1993/09/01	<=1994/03/31	5,3	23,2	12,31	17,7	3,8	19,4	92,5	57,9	1,6
1994	>=1994/09/01	<=1995/03/31	3,4	24,4	11,93	18,1	4,1	20,9	92,0	53,1	-0,7
1995	>=1995/09/01	<=1996/03/31	6,7	23,0	12,20	17,6	3,7	19,1	92,3	58,8	3,0
1996	>=1996/09/01	<=1997/03/31	4,8	23,1	12,60	17,8	3,7	19,1	92,1	58,7	1,1
1997	>=1997/09/01	<=1998/03/31	5,4	22,7	12,37	17,5	3,6	18,6	92,8	60,4	1,7
1998	>=1998/09/01	<=1999/03/31	4,0	23,6	12,51	18,1	3,9	19,8	92,5	56,5	0,1

UKZN OBSHIS4682 average winter climate records											
Year	start	end	Rainfall	T max	T min	Ave T	Evap	Radiation	Rel Hum	Sun dur	p-e
1950	>=1950/04/01	<=1950/08/30	1,5	19,3	6,78	13,0	2,2	13,2	92,4	46,5	-0,7
1951	>=1951/04/01	<=1951/08/30	1,8	19,3	5,68	12,5	2,3	13,9	93,3	44,3	-0,5
1952	>=1952/04/01	<=1952/08/30	0,8	19,4	6,38	12,9	2,3	13,6	93,1	45,5	-1,5
1953	>=1953/04/01	<=1953/08/30	1,0	19,2	5,33	12,3	2,3	13,8	93,2	44,6	-1,2
1954	>=1954/04/01	<=1954/08/30	1,1	19,6	5,72	12,7	2,3	14,1	94,4	42,9	-1,2
1955	>=1955/04/01	<=1955/08/30	0,8	19,6	5,95	12,8	2,3	14,1	93,8	43,0	-1,5
1956	>=1956/04/01	<=1956/08/30	0,7	20,0	6,42	13,2	2,4	13,9	92,0	42,9	-1,6
1957	>=1957/04/01	<=1957/08/30	1,0	19,6	6,22	12,9	2,3	13,7	93,0	44,8	-1,3
1958	>=1958/04/01	<=1958/08/30	1,1	20,2	6,11	13,2	2,4	14,1	92,2	41,3	-1,3
1959	>=1959/04/01	<=1959/08/30	1,7	20,3	6,23	13,3	2,4	14,2	92,7	41,0	-0,8
1960	>=1960/04/01	<=1960/08/30	1,3	19,7	5,75	12,7	2,3	13,8	91,3	43,7	-1,0
1961	>=1961/04/01	<=1961/08/30	1,8	19,8	6,96	13,4	2,3	13,4	91,8	45,2	-0,5
1962	>=1962/04/01	<=1962/08/30	0,9	20,6	6,09	13,4	2,5	14,2	90,0	40,5	-1,6
1963	>=1963/04/01	<=1963/08/30	1,3	19,1	6,13	12,6	2,2	13,5	93,1	47,4	-0,9
1964	>=1964/04/01	<=1964/08/30	0,9	19,2	6,70	13,0	2,2	13,1	91,8	47,1	-1,3
1965	>=1965/04/01	<=1965/08/30	1,6	19,7	6,24	13,0	2,3	13,4	91,2	45,6	-0,7
1966	>=1966/04/01	<=1966/08/30	1,0	19,9	6,43	13,2	2,3	13,5	90,5	44,3	-1,4
1967	>=1967/04/01	<=1967/08/30	1,2	18,9	6,12	12,5	2,2	13,1	92,6	47,9	-1,0
1968	>=1968/04/01	<=1968/08/30	1,0	18,6	5,88	12,3	2,2	13,2	92,2	49,1	-1,1
1969	>=1969/04/01	<=1969/08/30	1,0	19,1	6,93	13,0	2,2	12,8	91,4	48,1	-1,2
1970	>=1970/04/01	<=1970/08/30	1,3	20,2	6,74	13,5	2,4	13,8	91,2	43,6	-1,1
1971	>=1971/04/01	<=1971/08/30	1,8	19,5	6,43	13,0	2,3	13,7	93,0	44,6	-0,5
1972	>=1972/04/01	<=1972/08/30	0,9	19,4	6,43	12,9	2,3	13,7	93,0	45,1	-1,4
1973	>=1973/04/01	<=1973/08/30	1,7	18,8	6,21	12,5	2,2	12,9	92,9	48,4	-0,5
1974	>=1974/04/01	<=1974/08/30	1,2	18,8	6,50	12,6	2,2	13,0	91,5	49,2	-1,0
1975	>=1975/04/01	<=1975/08/30	0,6	21,1	6,67	13,9	2,5	14,2	88,7	39,9	-2,0

1976	>=1976/04/01	<=1976/08/30	0,9	19,3	6,20	12,8	2,3	13,5	91,8	46,1	-1,4
1977	>=1977/04/01	<=1977/08/30	1,0	21,0	5,75	13,4	2,5	14,4	89,6	39,3	-1,6
1978	>=1978/04/01	<=1978/08/30	1,1	20,0	6,20	13,1	2,3	13,5	90,2	44,4	-1,2
1979	>=1979/04/01	<=1979/08/30	1,5	20,1	6,85	13,5	2,4	13,5	89,7	44,8	-0,9
1980	>=1980/04/01	<=1980/08/30	0,7	21,0	5,81	13,4	2,5	14,5	90,0	39,0	-1,9
1981	>=1981/04/01	<=1981/08/30	1,3	19,4	5,87	12,7	2,3	13,7	91,7	45,7	-1,0
1982	>=1982/04/01	<=1982/08/30	0,4	19,6	6,53	13,0	2,3	13,5	91,2	45,8	-1,9
1983	>=1983/04/01	<=1983/08/30	1,2	19,6	7,12	13,4	2,3	13,2	89,8	47,1	-1,1
1984	>=1984/04/01	<=1984/08/30	1,5	18,8	6,16	12,5	2,2	13,3	92,4	48,8	-0,7
1985	>=1985/04/01	<=1985/08/30	0,2	20,3	6,48	13,4	2,4	14,1	90,2	42,2	-2,2
1986	>=1986/04/01	<=1986/08/30	0,8	20,7	7,28	14,0	2,4	13,6	90,4	41,8	-1,6
1987	>=1987/04/01	<=1987/08/30	2,3	19,7	7,04	13,4	2,3	13,1	89,7	46,5	0,0
1988	>=1988/04/01	<=1988/08/30	1,7	19,4	6,80	13,1	2,3	13,1	90,0	47,6	-0,5
1989	>=1989/04/01	<=1989/08/30	1,0	19,4	6,79	13,1	2,3	13,2	89,8	47,5	-1,3
1990	>=1990/04/01	<=1990/08/30	1,2	18,9	6,87	12,9	2,2	12,8	91,1	49,2	-1,0
1991	>=1991/04/01	<=1991/08/30	0,5	19,9	6,60	13,2	2,4	13,8	91,1	45,2	-1,9
1992	>=1992/04/01	<=1992/08/30	0,6	21,1	6,45	13,8	2,5	14,3	88,7	39,5	-1,9
1993	>=1993/04/01	<=1993/08/30	0,8	20,3	7,03	13,7	2,4	13,7	89,8	43,2	-1,5
1994	>=1994/04/01	<=1994/08/30	1,1	19,6	5,94	12,8	2,3	13,7	90,9	44,5	-1,2
1995	>=1995/04/01	<=1995/08/30	1,1	19,0	6,58	12,8	2,2	13,0	90,5	49,0	-1,1
1996	>=1996/04/01	<=1996/08/30	1,7	17,6	6,35	12,0	2,0	12,3	91,9	54,3	-0,3
1997	>=1997/04/01	<=1997/08/30	1,8	18,4	6,58	12,5	2,1	12,9	91,3	51,2	-0,3
1998	>=1998/04/01	<=1998/08/30	0,7	20,2	6,71	13,4	2,4	13,6	89,4	43,5	-1,7
1999	>=1999/04/01	<=1999/08/30	0,4	20,8	7,61	14,2	2,5	13,6	88,4	41,9	-2,0

Appendix C: Tree-ring width raw measurements

PF1	1947	112	185	177							
PF1	1950	153	212	139	146	218	154	194	153	134	129
PF1	1960	131	130	203	149	247	150	200	176	112	133
PF1	1970	178	214	174	206	238	252	223	-999	-999	294
PF1	1980	100	80	203	135	236	324	100	217	158	142
PF1	1990	-999	-999	184	241	352	120	132	156	256	201
PF1	2000	258	124	-999	170	124	202	170	300	222	147
PF1	2010	204	237	181	500	999					
PF3BJB	1938	95	79								
PF3BJB	1940	159	309	142	187	520	502	431	629	918	393
PF3BJB	1950	520	344	712	385	469	418	636	444	687	404
PF3BJB	1960	502	418	603	167	912	909	1323	909	584	161
PF3BJB	1970	423	958	477	903	451	379	291	240	244	371
PF3BJB	1980	344	768	583	503	344	476	741	1164	608	688
PF3BJB	1990	344	318	159	265	317	159	345	109	397	291
PF3BJB	2000	265	266	187	431	640	427	374	400	348	374
PF3BJB	2010	212	483	611	483	693	348	374	270	999	
PF3SW	1913	47	92	48	46	61	81	57			
PF3SW	1920	101	127	132	95	144	52	176	214	335	167
PF3SW	1930	167	194	303	216	335	283	61	106	127	47
PF3SW	1940	92	212	209	142	231	39	272	81	266	210
PF3SW	1950	120	158	102	90	219	136	332	166	243	161
PF3SW	1960	267	68	288	220	402	275	246	81	152	335
PF3SW	1970	246	339	220	233	131	102	89	203	89	369
PF3SW	1980	174	161	161	208	267	433	267	237	136	119
PF3SW	1990	102	107	204	212	68	191	153	153	116	111
PF3SW	2000	175	179	142	143	55	131	102	127	47	148
PF3SW	2010	153	107	123	161	999					
PF4	1895	171	79	93	74	90					
PF4	1900	67	68	34	123	85	77	92	74	78	127
PF4	1910	87	120	92	131	137	119	169	133	108	123
PF4	1920	93	88	206	161	124	121	165	94	84	53
PF4	1930	108	188	142	132	40	53	54	72	49	139
PF4	1940	55	143	81	125	58	59	96	135	141	131
PF4	1950	70	92	63	29	54	123	196	151	126	101
PF4	1960	54	89	235	167	68	114	227	78	170	144
PF4	1970	123	35	86	46	111	72	231	288	138	236
PF4	1980	69	173	173	126	133	136	176	95	119	154
PF4	1990	61	64	137	84	76	182	211	213	211	266
PF4	2000	232	92	191	155	175	241	299	402	150	120
PF4	2010	183	173	230	233	999					
PF5	1930	288	337	400	382	257	188	103	158	184	65
PF5	1940	56	164	67	151	101	140	59	98	172	228
PF5	1950	126	172	124	55	164	54	74	67	183	150
PF5	1960	92	235	122	285	184	165	135	243	219	213
PF5	1970	175	104	85	59	62	125	461	244	72	446
PF5	1980	201	248	506	153	87	40	69	121	60	338
PF5	1990	166	145	112	260	250	201	286	422	137	142
PF5	2000	121	85	73	21	189	200	83	102	70	50
PF5	2010	115	52	85	99	999					
PF6	1944	131	69	142	142	211	273				
PF6	1950	103	130	87	61	179	82	94	176	186	123
PF6	1960	97	36	99	59	65	69	71	46	115	107
PF6	1970	77	43	184	134	197	163	473	80	295	91
PF6	1980	301	113	261	140	180	335	274	303	125	78
PF6	1990	311	180	73	127	229	169	297	306	209	158
PF6	2000	134	261	248	94	85	195	221	110	296	119

PF6 2010 131 81 43 52 56 999
PF7 1916 1 44 25 20
PF7 1920 18 44 125 115 123 53 82 142 127 39
PF7 1930 38 184 202 130 105 342 262 296 184 126
PF7 1940 141 79 145 69 148 171 304 83 97 71
PF7 1950 113 144 249 262 196 117 116 38 54 63
PF7 1960 46 170 64 127 91 36 60 39 149 123
PF7 1970 56 78 88 133 141 201 50 233 168 143
PF7 1980 74 194 56 120 39 85 97 168 278 53
PF7 1990 100 115 129 192 127 108 141 169 96 144
PF7 2000 203 150 51 223 46 646 132 164 66 125
PF7 2010 131 50 75 111 175 999
PF8 1890 125 84 180 139 178 138 192 62 98 98
PF8 1900 121 126 164 106 178 100 180 109 108 106
PF8 1910 77 60 90 31 93 57 93 86 175 118
PF8 1920 102 143 154 107 60 115 134 100 76 97
PF8 1930 115 -999 88 112 132 131 109 65 167 182
PF8 1940 154 134 114 156 130 169 199 235 172 102
PF8 1950 52 110 108 194 247 267 180 -999 238 62
PF8 1960 181 147 215 178 272 218 175 155 135 134
PF8 1970 153 26 161 52 283 311 183 151 133 155
PF8 1980 117 317 255 161 151 128 97 -999 153 127
PF8 1990 76 99 167 99 146 76 36 102 68 -999
PF8 2000 -999 40 80 20 -999 -999 30 35 124 110
PF8 2010 -999 -999 -999 80 122 999
PF9 1936 50 16 73 126
PF9 1940 27 28 174 34 12 25 75 28 17 25
PF9 1950 28 139 16 23 37 785 966 192 275 219
PF9 1960 63 294 213 226 336 574 275 252 103 117
PF9 1970 417 74 255 170 32 138 230 196 94 166
PF9 1980 119 167 147 449 106 82 464 92 243 78
PF9 1990 85 473 90 169 150 95 188 213 230 311
PF9 2000 137 134 132 128 59 83 89 68 83 148
PF9 2010 195 109 120 423 140 999
PF10 1940 88 86 113 105 52 89 73 252 162 146
PF10 1950 140 202 204 237 213 123 159 134 446 272
PF10 1960 139 181 411 233 223 207 254 116 157 191
PF10 1970 345 423 330 311 378 238 221 162 126 307
PF10 1980 262 188 167 195 191 271 147 147 288 190
PF10 1990 114 221 158 131 185 505 226 55 142 305
PF10 2000 292 245 155 220 86 147 71 176 122 35
PF10 2010 42 42 45 93 140 999
PF11 1921 233 66 157 153 103 184 69 174 205
PF11 1930 116 385 182 97 137 200 228 157 64 292
PF11 1940 239 148 169 195 360 259 234 250 42 293
PF11 1950 307 203 154 133 163 76 124 293 102 73
PF11 1960 199 136 132 81 34 112 62 150 105 144
PF11 1970 241 306 288 330 311 179 238 221 137 220
PF11 1980 115 107 178 144 331 314 254 89 411 279
PF11 1990 275 89 232 74 257 194 138 212 135 148
PF11 2000 124 94 115 110 185 196 128 217 156 179
PF11 2010 159 93 170 127 121 999
PF12 1883 218 195 190 249 66 87 236
PF12 1890 84 142 179 213 108 247 80 160 61 242
PF12 1900 156 359 112 224 164 505 196 315 176 246
PF12 1910 225 251 92 155 231 69 69 36 23 11
PF12 1920 12 23 27 37 237 329 240 336 213 239
PF12 1930 196 165 297 270 365 215 325 212 519 10
PF12 1940 129 148 86 92 73 100 38 64 92 96
PF12 1950 114 62 71 169 98 54 134 126 292 141

PF12 1960 69 105 55 149 270 73 67 182 36 29
PF12 1970 33 29 14 470 49 53 58 72 66 67
PF12 1980 62 82 167 26 23 21 24 20 20 35
PF12 1990 52 66 228 116 148 23 30 69 102 89
PF12 2000 31 38 67 30 221 89 113 187 211 37
PF12 2010 102 154 169 216 146 999
PF13 1945 2 2 8 48 33
PF13 1950 23 11 28 75 23 52 116 103 152 380
PF13 1960 458 361 476 141 291 54 184 72 276 191
PF13 1970 432 182 119 329 163 86 42 369 123 172
PF13 1980 154 233 157 138 188 62 237 55 273 158
PF13 1990 225 176 148 407 339 184 226 257 332 329
PF13 2000 590 397 387 269 97 320 90 270 125 125
PF13 2010 167 107 84 109 999
PF14 1870 149 28 194 155 65 26 50 78 131 278
PF14 1880 176 145 108 15 188 176 180 166 180 184
PF14 1890 99 282 148 38 86 19 130 70 137 170
PF14 1900 74 57 80 65 97 174 92 60 179 229
PF14 1910 181 128 179 137 186 2 77 2 110 244
PF14 1920 78 141 173 106 2 256 99 150 221 191
PF14 1930 64 29 142 418 50 266 327 238 92 97
PF14 1940 394 462 311 74 56 362 355 51 220 467
PF14 1950 57 147 124 41 117 126 334 147 78 240
PF14 1960 308 2 71 134 198 51 172 182 102 55
PF14 1970 10 120 2 310 83 119 311 62 62 149
PF14 1980 2 243 121 2 157 245 79 2 258 2
PF14 1990 203 44 44 109 49 120 165 71 76 137
PF14 2000 187 134 2 87 104 2 86 168 98 89
PF14 2010 67 61 51 123 74 999
PF15 1942 30 47 40 97 109 94 44 24
PF15 1950 199 139 99 87 81 119 106 141 122 46
PF15 1960 35 126 16 120 29 145 47 21 177 152
PF15 1970 139 93 44 159 178 40 23 169 213 212
PF15 1980 43 115 258 198 219 91 184 187 145 231
PF15 1990 147 165 108 181 123 146 165 243 85 97
PF15 2000 53 155 101 224 191 214 321 1 123 136
PF15 2010 187 96 115 120 181 999
PF16 1923 43 28 189 160 93 110 130
PF16 1930 94 70 345 162 178 161 217 297 123 201
PF16 1940 215 284 245 355 344 226 197 146 170 177
PF16 1950 184 213 270 133 80 272 252 280 291 350
PF16 1960 303 259 129 321 203 178 241 228 172 167
PF16 1970 225 80 170 207 219 287 229 156 165 257
PF16 1980 169 154 166 140 118 166 157 52 233 81
PF16 1990 125 201 206 251 253 177 206 81 168 133
PF16 2000 167 133 60 142 129 228 55 156 187 188
PF16 2010 51 50 165 232 212 999
PF17 1918 146 147
PF17 1920 219 109 61 184 136 132 456 290 100 271
PF17 1930 186 128 156 187 225 219 121 266 264 142
PF17 1940 201 323 156 381 158 315 170 61 50 289
PF17 1950 405 290 212 177 303 380 91 132 142 279
PF17 1960 202 196 234 309 376 208 145 216 252 262
PF17 1970 139 220 275 306 210 154 172 313 229 248
PF17 1980 153 213 229 328 254 345 249 297 184 96
PF17 1990 62 262 299 120 274 291 266 134 177 198
PF17 2000 215 223 277 274 263 223 175 85 161 169
PF17 2010 125 165 242 316 120 999
PF18 1934 335 247 266 368 310 282
PF18 1940 178 312 209 229 170 259 310 256 182 293

PF18 1950 230 264 22 196 23 4 148 16 15 157
PF18 1960 118 23 114 240 117 135 12 209 19 116
PF18 1970 66 152 117 92 11 104 62 120 174 169
PF18 1980 123 230 273 303 147 243 169 113 114 108
PF18 1990 65 196 200 199 137 197 87 34 61 78
PF18 2000 113 191 200 192 87 143 129 151 97 122
PF18 2010 66 115 83 69 65 999
PF19 1873 104 124 55 17 20 9 26
PF19 1880 33 38 50 38 50 23 38 19 28 15
PF19 1890 33 16 11 49 126 83 97 96 147 60
PF19 1900 53 111 61 87 50 80 29 52 48 21
PF19 1910 54 51 38 26 20 72 13 51 38 36
PF19 1920 69 50 96 31 44 27 104 25 22 36
PF19 1930 27 10 40 36 22 37 31 13 19 24
PF19 1940 136 82 169 415 102 28 12 14 175 122
PF19 1950 156 150 131 79 179 140 108 103 44 24
PF19 1960 116 42 113 85 116 128 100 87 143 92
PF19 1970 168 52 209 165 152 26 86 52 154 54
PF19 1980 194 163 132 6 410 228 195 175 183 108
PF19 1990 197 51 129 172 170 346 126 23 197 46
PF19 2000 95 82 59 109 44 81 64 155 62 112
PF19 2010 61 111 117 137 42 999
PF20 1906 91 205 202 143
PF20 1910 106 172 257 204 199 216 210 187 22 190
PF20 1920 190 9 171 179 137 8 150 16 208 268
PF20 1930 267 183 184 161 35 111 122 47 263 184
PF20 1940 243 171 140 138 100 97 153 164 207 247
PF20 1950 28 115 162 202 141 17 121 87 95 88
PF20 1960 379 275 513 133 106 148 838 434 435 336
PF20 1970 219 487 317 321 536 643 301 197 167 168
PF20 1980 165 266 216 249 156 38 163 12 154 207
PF20 1990 173 249 307 380 343 448 378 308 269 125
PF20 2000 304 483 320 312 455 19 20 333 284 256
PF20 2010 249 328 329 336 222 999
PF21 1877 200 148 171
PF21 1880 129 148 97 138 56 137 51 173 135 80
PF21 1890 145 96 215 131 115 105 167 109 109 54
PF21 1900 52 92 82 132 60 124 138 63 113 185
PF21 1910 106 78 66 188 132 100 182 59 155 104
PF21 1920 136 73 80 102 188 98 188 120 144 40
PF21 1930 82 199 120 182 109 96 130 116 116 126
PF21 1940 76 130 204 144 159 31 147 38 64 57
PF21 1950 118 31 116 16 153 22 65 95 50 85
PF21 1960 177 82 142 134 108 120 62 22 72 182
PF21 1970 101 189 98 191 92 38 84 88 86 85
PF21 1980 84 51 59 115 136 103 83 121 44 53
PF21 1990 148 178 124 128 30 127 58 40 18 9
PF21 2000 14 18 26 38 36 37 14 16 6 74
PF21 2010 33 34 33 30 23 999

Appendix D: Stable carbon isotope raw measurements

PF1bJB1	-23,16	PF3 1	-22,48	PF3 1	-22,48	PF3bJB1	-23,94	PF 8B - 1	-23,71	PF 12G - 1	-23,39	PF 14B - 1	-21,69	PF 21 - 1	-23,56
PF1bJB2	-22,38	1a		1a		PF3bJB2	-22,55	PF 8B - 2	-24,74	PF 12G - 2	-22,95	No sample		PF 21 - 2	-22,79
PF1bJB3	-22,65	PF3 2	-22,84	PF3 2	-22,84	PF3bJB3	-23,88	PF 8B - 3	-23,88	PF 12G - 3	-22,80	PF 14B - 3	-20,50	PF 21 - 3	-22,70
PF1bJB4	-27,56	PF3 3	-22,88	PF3 3	-22,88	PF3bJB4	-23,32	PF 8B - 4	-25,17	PF 12G - 4	-23,43	PF 14B - 4	-20,45	PF 21 - 4	-23,10
PF1bJB5	-22,35	PF3 4	-22,76	PF3 4	-22,76	PF3bJB5	-22,93	PF 8B - 5	-24,40	PF 12G - 5	-22,25	PF 14B - 5	-20,88	PF 21 - 5	-22,84
PF1bJB6	-21,68	PF3 5	-23,81	PF3 5	-23,81	PF3bJB6	-22,20	PF 8B - 6	-24,48	PF 12G - 6	-22,03	PF 14B - 6	-21,03	PF 21 - 6	-22,54
PF1bJB7	-22,68	PF3 6	-23,27	PF3 6	-23,27	PF3bJB7	-23,42	PF 8B - 7	-24,69	PF 12G - 7	-22,80	PF 14B - 7	-21,27	PF 21 - 7	-24,56
PF1bJB8	-23,14	PF3 7	-23,18	PF3 7	-23,18	PF3bJB8	-23,08	PF 8B - 8	-23,44	PF 12G - 8A	-22,13	PF 14B - 8	-21,13	PF 21 - 8	-22,46
PF1bJB9	-23,45	PF3 8	-23,05	PF3 8	-23,05	PF3bJB9	-24,50	PF 8B - 9	-23,47	PF 12G - 8B	-22,18	PF 14B - 9	-21,61	PF 21 - 9	-23,92
PF1bJB10	-24,30	PF3 9	-24,04	PF3 9	-24,04	PF3bJB10	-23,44	PF 8B - 10	-23,69	PF 12G 8C	-22,33	PF 14B - 10	-20,38	PF 21 - 10	-23,46
PF1bJB11	-23,32	PF3 10	-23,44	PF3 10	-23,44	PF3bJB11	-23,48	PF 8B - 11	-22,20	PF 12G 8D	-22,24	PF 14B - 11	-21,26	PF 21 - 11	-23,14
PF1bJB12		PF3 11	-22,80	PF3 11	-22,80	PF3bJB12	-23,95	PF 8B - 12	-22,72	PF 12G - 12	-22,21	PF 14B - W12	-21,17	PF 21 - 12	-23,62
PF1bJB13	-22,77	PF3 12	-22,80	PF3 12	-22,80	PF3bJB13	-22,86	PF 8B - 13	-21,71	PF 12G - 13	-22,91	PF 14B - 13	-21,61	PF 21 - 13	-24,18
PF1bJB14	-21,79	PF3 13	-22,27	PF3 13	-22,27	PF3bJB14	-24,00	PF 8B - 14	-22,87	PF 12G - 14	-22,69	PF 14B - 14	-20,92	PF 21 - 14	-23,95
PF1bJB15	-23,96	13a		13a		PF3bJB15	-22,84	PF 8B - 15	-22,47	PF 12G - 15	-21,88	PF 14B - 15	-20,78	PF 21 - 15	-24,35
PF1bJB16	-21,26	PF3 14	-23,35	PF3 14	-23,35	PF3bJB16	-24,80	PF 8B - 16	-22,84	PF 12G - 16	-22,64	PF 14B - 16	-21,25	PF 21 - 16	-23,14
PF1bJB17	-21,31	14a		14a		PF3bJB17	-22,27	PF 8B - 17	-22,90	PF 12G - 17	-22,80	PF 14B - 17	-21,01	PF 21 - 17	-25,30
PF1bJB18	-21,19	PF3 15	-23,36	PF3 15	-23,36	PF3bJB18	-21,83	PF 8B - 18	-21,50	PF 12G - 18	-22,67	PF 14B - 18	-20,79	PF 21 - 18	-24,82
PF1bJB19	-22,20	PF3 16	-24,21	PF3 16	-24,21	PF3bJB19	-24,38	PF 8B - 19	-25,56	PF 12G - 19	-22,18	PF 14B - 19	-21,46	PF 21 - 19	-24,96
PF1bJB20	-21,61	PF3 17	-23,66	PF3 17	-23,66	PF3bJB20	-22,32	PF 8B - 20	-21,95	PF 12G - 20	-23,94	No sample		PF 21 - 20	-24,23
PF1bJB21	-23,29	PF3 18	-23,74	PF3 18	-23,74	PF3bJB21	-22,87	PF 8B - 21	-21,36	PF 12G - 21	-22,63	PF 14B - 21	-21,39	PF 21 - 21	-23,42
PF1bJB22	-21,76	PF3 19	-22,79	PF3 19	-22,79	PF3bJB22	-22,62	PF 8B - 22	-23,45	PF 12G - 22	-23,14	PF 14B - 22	-21,21	PF 21 - 22	-23,22
PF1bJB23	-22,10	PF3 20	-22,18	PF3 20	-22,18	PF3bJB23	-22,12	PF 8B - 23	-21,51	PF 12G - 23	-23,20	PF 14B - 23	-21,69	PF 21 - 23	-22,77
PF1bJB24	-21,94	PF3 21	-23,18	PF3 21	-23,18	PF3bJB24	-22,47	PF 8B - 24	-22,03	PF 12G - 24	-22,80	PF 14B - 24	-20,80	PF 21 - 24	-24,40
PF1bJB25	-21,45	PF3 21a	-23,02	PF3 21a	-23,02	PF3bJB25	-21,92	PF 8B - 25	-27,82	PF 12G - 25	-22,66	PF 14B - 25	-21,32	PF 21 - 25	-24,68
PF1bJB26	-22,02	PF3 22	-23,16	PF3 22	-23,16	PF3bJB26	-23,01	PF 8B - 26	-23,22	PF 12G - 26	-22,38	PF 14B - 26	-21,05	PF 21 - 26	-24,41
PF1bJB27	-22,06	PF3 22a	-22,02	PF3 22a	-22,02	PF3bJB27	-22,47	PF 8B - 27	-24,65	PF 12G - 27	-22,70	PF 14B - 27	-21,23	PF 21 - 27	-23,68
PF1bJB28	-23,48	PF3 23	-21,72	PF3 23	-21,72	PF3bJB28	-21,94	PF 8B - 28	-23,05	PF 12G - 28	-23,75	PF 14B - 28	-21,45	PF 21 - 28	-24,69
PF1bJB29	-25,62	PF3 24	-22,58	PF3 24	-22,58	PF3bJB29	-21,14	PF 8B - 29	-22,78	PF 12G - 29	-21,85	PF 14B - 29	-21,01	PF 21 - 29	-24,68

PF1bJB30	-20,79	25a		25a		PF3bJB30	-22,55	PF 8B - 30	-22,00	PF 12G - 30	-21,00	PF 14B - 30	-20,48	PF 21 - 30	-23,57
PF1bJB31	-21,71	PF3 25	-22,30	PF3 25	-22,30	PF3bJB31	-22,46	PF 8B - 31	-22,46	PF 12G - 31	-20,75	PF 14B - 31	-21,24	PF 21 - 31	-22,92
PF1bJB32	-21,41	PF3 26	-21,68	PF3 26	-21,68	PF3bJB32	-21,62	PF 8B - 32	-21,58	PF 12G - 32	-21,24	PF 14B - 32	-21,39	PF 21 - 32	-22,63
PF1bJB33	-21,40	PF3 27	-21,47	PF3 27	-21,47	PF3bJB33	-22,63	PF 8B - 33	-23,76	PF 12G - 33	-21,69	PF 14B - 33	-21,13	PF 21 - 33	-21,16
PF1bJB34	-20,88	28a		28a		PF3bJB34	-21,91	PF 8B - 34	-22,07	PF 12G - 34	-21,60	PF 14B - 34	-21,34	PF 21 - 34	-23,17
PF1bJB35	-23,68	PF3 28	-21,80	PF3 28	-21,80	PF3bJB35	-22,34	PF 8B - 35	-23,72	PF 12G - 35	-22,76	PF 14B - 35	-21,13	PF 21 - 35	-23,31
PF1bJB36	-21,40	PF3 29	-21,46	PF3 29	-21,46	PF3bJB36	-22,92	PF 8B - 36	-21,54	PF 12G - 36	-21,17	PF 14B - 36	-21,14	PF 21 - 36	-22,77
PF1bJB37	-20,94	30a		30a		PF3bJB37	-21,90	PF 8B - 37	-22,18	PF 12G - 37	-21,80	PF 14B - 37	-20,14	PF 21 - 37	-23,00
PF1bJB38	-21,30	30b		30b		PF3bJB38	-21,53	PF 8B - 38	-23,13	PF 12G - 38	-21,91	PF 14B - 38	-21,03	PF 21 - 38	-24,19
PF1bJB39	-30,46	30c		30c		PF3bJB39	-23,26	PF 8B - 39	-21,78	PF 12G - 39	-20,44	PF 14B - 39	-20,04	PF 21 - 39	-22,97
PF1bJB40	-20,90	PF3 30	-21,77	PF3 30	-21,77	PF3bJB40	-22,18	PF 8B - 40	-21,89	PF 12G - 40	-21,14	PF 14B - 40	-20,10	PF 21 - 40	-23,45
PF1bJB41	-20,85	PF3 31	-21,44	PF3 31	-21,44	PF3bJB41	-22,60	PF 8B - 41	-21,66	PF 12G - 41	-21,12	PF 14B - 41	-20,35	PF 21 - 41	-23,36
PF1bJB42	-21,27	31a		31a		PF3bJB42	-21,62	PF 8B - 42	-21,66	PF 12G - 42	-21,55	PF 14B - 42	-20,83	PF 21 - 42	-23,29
PF1bJB43	-22,23	31b		31b		PF3bJB43	-22,89	PF 8B - 43	-21,14	PF 12G - 43	-19,44	PF 14B - 43	-19,93	PF 21 - 43	-23,61
PF1bJB44	-20,68	PF3 32	-21,30	PF3 32	-21,30	PF3bJB44	-21,48	PF 8B - 44	-21,36	PF 12G - 44	-20,79	PF 14B - 44	-21,43	PF 21 - 44	-22,84
PF1bJB45	-20,91	PF3 33	-21,14	PF3 33	-21,14	PF3bJB45	-22,24	PF 8B - 45	-23,70	PF 12G - 45	-21,97	PF 14B - 45	-20,18	PF 21 - 45	-23,53
PF1bJB46	-24,98	PF3 34	-22,31	PF3 34	-22,31	PF3bJB46	-23,67	PF 8B - 46	-24,23	PF 12G - 46	-21,09	PF 14B - 46	-20,84	PF 21 - 46	-22,25
PF1bJB47	-21,03	PF3 35	-21,61	PF3 35	-21,61	PF3bJB47	-22,34	PF 8B - 47	-23,36	PF 12G - 47	-20,78	PF 14B - 47	-24,64	PF 21 - 47	-22,60
PF1bJB48	-21,60	PF3 36	-22,91	PF3 36	-22,91	PF3bJB48	-22,61	PF 8B - 48	-22,25	PF 12G - 48	-21,98	PF 14B - 48	-20,43	PF 21 - 48	-22,74
PF1bJB49	-21,42	PF3 37	-22,05	PF3 37	-22,05	PF3bJB49	-21,51	PF 8B - 49	-21,95	PF 12G - 49	-20,47	PF 14B - 49	-20,41	PF 21 - 49	-22,91
PF1bJB50	-22,22	PF3 38	-22,25	PF3 38	-22,25	PF3bJB50	-23,16	PF 8B - 50	-21,28	PF 12G - 50	-21,56	PF 14B - 50	-20,82	PF 21 - 50	-24,43
PF1bJB51	-22,02	39a		39a		PF3bJB51	-22,43	PF 8B - 51	-21,35	PF 12G - 51	-20,54	PF 14B - 51	-21,18	PF 21 - 51	-22,15
PF1bJB52	-21,89	PF3 39	-23,06	PF3 39	-23,06	PF3bJB52	-23,68	PF 8B - 52	-20,88	PF 12G - 52	-20,52	PF 14B - 52	-21,14	PF 21 - 52	-22,72
PF1bJB53	-22,51	PF3 40	-21,72	PF3 40	-21,72	PF3bJB53	-22,67	PF 8B - 53	-21,89	PF 12G - 53	-20,94	PF 14B - 53	-19,97	PF 21 - 53	-22,39
PF1bJB54	-22,62	PF3 41	-22,24	PF3 41	-22,24	PF3bJB54	-23,99	PF 8B - 54	-24,97	PF 12G - 54	-21,25	PF 14B - 54	-20,74	PF 21 - 54	-23,39
PF1bJB55	-22,16	PF3 42	-21,68	PF3 42	-21,68	PF3bJB55	-23,30	PF 8B - 55	-21,87	PF 12G - 55	-22,04	PF 14B - 55	-21,18	PF 21 - 55	-22,56
PF1bJB56	-23,24	PF3 43	-22,37	PF3 43	-22,37	PF3bJB56	-23,21	PF 8B - 56	-22,04	PF 12G - 56	-21,07	PF 14B - 56	-20,09	PF 21 - 56	-23,09
PF1bJB57	-21,40	43a		43a		PF3bJB57	-22,25	PF 8B - 57	-22,23	PF 12G - 57	-21,19	PF 14B - 57B	-20,39	PF 21 - 57	-25,05
PF1bJB58	-22,26	PF3 44	-21,84	PF3 44	-21,84	PF3bJB58	-22,91	PF 8B - 58	-23,09	PF 12G - 58	-21,52	PF 14B - 58	-21,64	PF 21 - 58	-23,30
PF1bJB59	-22,26	PF3 45	-21,99	PF3 45	-21,99	PF3bJB59	-22,30	PF 8B - 59	-22,88	PF 12G - 59	-20,85	PF 14B - B59	-21,39	PF 21 - 59	-22,33
PF1bJB60	-21,83	PF3 46	-22,17	PF3 46	-22,17	PF3bJB60	-22,70	PF 8B - 60	-22,58	No sample		PF 14B - 60	-20,08	PF 21 - 60	-24,53

PF1bJB61	-21,93	PF3 47	-21,40	PF3 47	-21,40	PF3bJB61	-22,06	PF 8B - 61	-22,17	PF 12G - 61	-22,04	PF 14B - 61	-21,17	PF 21 - 61	-22,74
PF1bJB62	-21,37	48a		48a		PF3bJB62	-22,24	PF 8B - 62	-22,22	PF 12G - 62	-21,57	PF 14B - 62	-19,89	PF 21 - 62	-22,82
PF1bJB63	-21,05	PF3 48	-22,25	PF3 48	-22,25	PF3bJB63	-22,32	PF 8B - 63	-22,48	PF 12G - 63	-21,73	PF 14B - 63	-20,52	PF 21 - 63	-23,46
PF1bJB64	-27,38	PF3 49	-21,17	PF3 49	-21,17	PF3bJB64	-21,36	PF 8B - 64	-22,83	PF 12G - 64	-21,78	PF 14B - 64	-20,36	PF 21 - 64	-23,24
PF1bJB65	-21,58	PF3 50	-21,23	PF3 50	-21,23	PF3bJB65	-22,05	PF 8B - 65	-22,14	PF 12G - 65	-21,29	PF 14B - 65	-20,42	PF 21 - 65	-23,44
PF1bJB66	-21,61	51a		51a		PF3bJB66	-22,60	PF 8B - 66	-23,86	No sample		PF 14B - 66	-20,32	PF 21 - 66	-23,00
		51b		51b		PF3bJB67	-21,83	PF 8B - 67	-23,99	PF 12G - 67	-20,86	PF 14B - 67	-20,36	PF 21 - 67	-22,70
		PF3 51	-21,92	PF3 51	-21,92	PF3bJB68	-22,18	PF 8B - 68	-23,17	PF 12G - 68	-23,03	PF 14B - 68	-20,47	PF 21 - 68	-22,03
		52a		52a		PF3bJB69	-22,64	PF 8B - 69	-22,14			PF 14B - 69	-21,61	PF 21 - 69	-23,37
		PF3 52	-22,64	PF3 52	-22,64	PF3bJB70	-21,42	PF 8B - 70	-21,78	PF 12G - 69	-19,38	PF 14B - 70	-20,64	PF 21 - 70	-23,45
		PF3 53	-22,36	PF3 53	-22,36	PF3bJB71	-21,99	PF 8B - 71	-21,23	PF 12G - 70	-19,11	PF 14B - 71	-22,15	PF 21 - 71	-22,42
		PF3 54	-22,47	PF3 54	-22,47	PF3bJB72	-20,80	PF 8B - 72	-21,33	PF 12G - 71	-20,03	PF 14B - 72	-21,31	PF 21 - 72	-24,19
		55a		55a		PF3bJB73	-21,79	PF 8B - 73	-22,94	PF 12G - 72	-20,09	PF 14B - 73	-21,88	PF 21 - 73	-23,51
		55b		55b		PF3bJB74	-21,60	PF 8B - 74	-24,50	No sample		PF 14B - 74	-19,99	PF 21 - 74	-23,63
		PF3 55	-21,97	PF3 55	-21,97	PF3bJB75	-23,15	PF 8B - 75	-22,76	No sample		PF 14B - 75	-20,59	PF 21 - 75	-22,32
		PF3 56	-23,57	PF3 56	-23,57	PF3bJB76	-22,28	PF 8B - 76	-23,54	PF 12G - 75	-19,69	PF 14B - 76	-21,52	PF 21 - 76	-25,32
		PF3 57	-21,96	PF3 57	-21,96	PF3bJB77	-22,44	PF 8B - 77	-23,70	PF 12G - 76	-19,33	PF 14B - 77	-20,93	PF 21 - 77	-23,63
		58a		58a		PF3bJB78	-23,43	PF 8B - 78	-23,92	PF 12G - 77	-19,33	PF 14B - 78	-22,10	PF 21 - 78	-23,65
		PF3 58	-22,59	PF3 58	-22,59	PF3bJB79	-22,15	PF 8B - 79	-24,03	PF 12G - 78	-20,21	PF 14B - 79	-20,50	PF 21 - 79	-23,46
		PF3 59	-22,34	PF3 59	-22,34	PF3bJB80	-22,59	PF 8B - 80	-24,23	No sample		PF 14B - 80	-22,85	PF 21 - 80	-23,48
		PF3 60	-22,73	PF3 60	-22,73	PF3bJB81	-23,17	PF 8B - 81	-24,12	PF 12G - 78	-20,06	PF 14B - 81	-20,41	PF 21 - 81	-23,69
		PF3 61	-25,43	PF3 61	-25,43	PF3bJB82	-22,52	PF 8B - 82	-23,84	PF 12G - 80	-20,46	PF 14B - 82	-20,72	PF 21 - 82	-23,68
		PF3 62	-21,52	PF3 62	-21,52	PF3bJB83	-23,42	PF 8B - 83	-24,51	PF 12G - 81	-19,23	PF 14B - 83	-19,96	PF 21 - 83	-23,90
		PF3 63	-21,60	PF3 63	-21,60			No sample		PF 12G - 82	-20,37	PF 14B - 84	-20,00	PF 21 - 84	-23,56
		PF3 64	-23,24	PF3 64	-23,24			PF 8B - 85	-24,22	PF 12G - 83	-19,90	PF 14B - 85	-20,82	PF 21 - 85	-23,24
		PF3 65	-21,80	PF3 65	-21,80			PF 8B - 86	-23,19	PF 12G - 84	-19,71	PF 14B - 86	-20,16	PF 21 - 86	-23,29
		PF3 66	-23,03	PF3 66	-23,03			PF 8B - 87	-24,97	PF 12G - 85	-20,08	PF 14B - 87	-20,23	PF 21 - 87	-22,18
		PF3 67a	-22,52	PF3 67a	-22,52			PF 8B - 88	-23,82	No sample		PF 14B - 88	-20,61	PF 21 - 88	-21,40
		PF3 67b	-21,75	PF3 67b	-21,75			PF 8B - 89	-23,38	PF 12G - 87	-20,72	PF 14B - 89	-20,38	PF 21 - 89	-22,06
		PF3 67c	-24,09	PF3 67c	-24,09			PF 8B - 90	-24,66	PF 12G - 88	-19,88	PF 14B - 90	-21,07	No sample	
		PF3 68	-22,77	PF3 68	-22,77			PF 8B - 91	-24,64	PF 12G - 89	-20,60	PF 14B - 91	-21,00	PF 21 - 91	-21,93

		PF3 69	-22,31	PF3 69	-22,31			PF 8B - 92	-23,58	PF 12G - 90	-20,02	PF 14B - 92	-20,88	No sample	
		PF3 70	-21,27	PF3 70	-21,27			PF 8B - 93	-21,45	PF 12G - 91	-19,97	PF 14B - 93	-22,31	PF 21 - 93	-22,70
		PF3 71	-21,97	PF3 71	-21,97			PF 8B - 94	-23,08	PF 12G - 92	-20,58	PF 14B - 94	-20,80	PF 21 - 94	-23,21
		PF3 72	-22,29	PF3 72	-22,29			PF 8B - 95	-24,03	PF 12G - 93	-20,87	PF 14B - 95	-21,18	PF 21 - 95	-22,51
		PF3 73	-22,88	PF3 73	-22,88			PF 8B - 96	-22,69	PF 12G - 94	-21,06	PF 14B - 96	-21,42	PF 21 - 96	-21,23
		PF3 74	-22,41	PF3 74	-22,41			PF 8B - 97	-24,36	PF 12G - 95	-19,44	PF 14B - 97	-21,53	PF 21 - 97	-20,93
		PF3 75	-22,96	PF3 75	-22,96			PF 8B - 98	-24,11	PF 12G - 96	-19,80	PF 14B - 98	-21,43	PF 21 - 98	-21,67
		PF3 76	-23,68	PF3 76	-23,68			PF 8B - 99	-23,03	PF 12G - 97	-20,52	No sample		PF 21 - 99	-21,39
		PF3 77	-23,88	PF3 77	-23,88			No sample		PF 12G - 98	-19,93	PF 14B - 100	-21,26	PF 21 - 100	-20,89
		PF3 77a	-23,67	PF3 77a	-23,67			PF 8B - 10	-24,27	PF 12G - 99	-20,76	PF 14B - 101	-21,45	PF 21 - 101	-20,93
		PF3 78	-23,45	PF3 78	-23,45			PF 8B - 102	-24,31	PF 12G - 100	-19,55	PF 14B - 102?	-20,70	PF 21 - 102	-21,15
		PF3 79	-23,01	PF3 79	-23,01			PF 8B - 103	-25,34	PF 12G - 101	-20,13	PF 14B - 103	-20,98	PF 21 - 103	-20,58
		PF3 80	-22,34	PF3 80	-22,34			PF 8B - 104	-23,20	PF 12G - 102	-20,18	PF 14B - 104	-20,86	PF 21 - 104	-20,45
		PF3 81	-21,49	PF3 81	-21,49			PF 8B - 105	-24,84	PF 12G - 103	-19,57	PF 14B - 105	-21,09	PF 21 - 105	-21,24
		PF3 82	-21,48	PF3 82	-21,48			PF 8B - 106	-24,73	No sample		PF 14B - 106	-20,47	PF 21 - 106	-21,08
		82a		82a				PF 8B - 107	-23,25	No sample		PF 14B - 107	-21,50	PF 21 - 107	-21,11
		PF3 83	-21,07	PF3 83	-21,07			PF 8B - 108	-24,44	PF 12G - 106	-19,15	PF 14B - 108	-21,11	PF 21 - 108	-21,09
		PF3 84	-22,46	PF3 84	-22,46			PF 8B - 109	-23,67	PF 12G - 107	-19,51	PF 14B - 109	-20,74	PF 21 - 109	-20,73
		PF3 85	-20,95	PF3 85	-20,95			PF 8B - 110	-24,21	No sample		PF 14B - 110	-22,30	PF 21 - 110	-21,60
		PF3 86	-21,76	PF3 86	-21,76			PF 8B - 111	-23,33	PF 12G - 109	-20,75	PF 14B - 111	-21,48	PF 21 - 111	-21,78
		PF3 87	-21,57	PF3 87	-21,57			PF 8B - 112	-23,99	PF 12G - 110	-19,18	PF 14B - 112	-21,82	PF 21 - 112	-21,97
		PF3 88	-21,94	PF3 88	-21,94			PF 8B - 113	-23,29	PF 12G - 111	-20,31	PF 14B - 113	-21,27	PF 21 - 113	-21,34
		PF3 89	-22,79	PF3 89	-22,79			PF 8B - 114	-23,01	PF 12G - 112	-19,47	PF 14B - 114	-21,76	PF 21 - 114	-20,68
		PF3 90	-22,14	PF3 90	-22,14			PF 8B - 115	-27,66	PF 12G - 113	-19,86	PF 14B - 115	-21,63	PF 21 - 115	-19,95
		PF3 91	-22,93	PF3 91	-22,93			PF 8B - 116	-24,13	PF 12G - 114	-20,15	PF 14B - 116	-20,38	PF 21 - 116	-21,51
		PF3 92	-22,54	PF3 92	-22,54			PF 8B - 117	-23,23	PF 12G - 115	-19,66	PF 14B - 117	-20,50	PF 21 - 117	-21,06
		PF3 93	-21,41	PF3 93	-21,41			PF 8B - 118	-24,10	PF 12G - 116	-20,18	PF 14B - 118	-21,80	PF 21 - 118	-22,19
		PF3 94	-22,32	PF3 94	-22,32			PF 8B - 119	-24,42	PF 12G - 117	-20,57	PF 14B - 119	-20,98	PF 21 - 119	-22,60
		PF3 95	-22,03	PF3 95	-22,03			PF 8B - 120	-23,61	PF 12G - 118	-19,99	PF 14B - 120	-21,39	PF 21 - 120	-23,10
		PF3 96	-21,55	PF3 96	-21,55			PF 8B - 121	-23,82	PF 12G - 119	-20,24	PF 14B - 121	-21,90	PF 21 - 121	-23,73
		PF3 97	-22,29	PF3 97	-22,29			PF 8B - 122	-22,76	PF 12G - 120	-19,58	PF 14B - 122	-22,57	No sample	

		PF3 98	-21,66	PF3 98	-21,66			PF 8B - 123	-23,46	PF 12G - 121	-19,77	PF 14B - 123	-21,44	PF 21 - 123	-24,09
		PF3 99	-22,14	PF3 99	-22,14			PF 8B - 124	-23,01	PF 12G - 122	-20,28	PF 14B - 124	-21,74	No sample	
		PF3 99a	-22,08	PF3 99a	-22,08			PF 8B - 125	-22,52	PF 12G - 123	-21,20	PF 14B - 125	-21,87	PF 21 - 125	-22,88
		PF3 100	-22,89	PF3 100	-22,89			PF 8B - 126	-22,93	PF 12G - 124	-21,05	PF 14B - 126	-21,19	PF 21 - 126	-23,29
		PF3 101	-22,99	PF3 101	-22,99			PF 8B - 127	-23,68	PF 12G - 125	-20,38	PF 14B - 127	-20,94	PF 21 - 127	-22,39
		PF3 102	-23,68	PF3 102	-23,68			PF 8B - 128	-23,87	PF 12G - 126	-21,63	PF 14B - 128	-22,67	PF 21 - 128	-21,94
		PF3 103	-23,90	PF3 103	-23,90			PF 8B - 129	-23,84	PF 12G - 127	-19,92	PF 14B - 129	-20,93	PF 21 - 129	-22,74
		PF3 104	-23,84	PF3 104	-23,84			PF 8B - 130	-22,84	PF 12G - 128	-20,13	PF 14B - 130	-21,90	PF 21 - 130	-24,24
		PF3 105	-23,23	PF3 105	-23,23					PF 12G - 129	-20,15	PF 14B - 131	-20,50	There is no 131	
		PF3 106	-23,08	PF3 106	-23,08					PF 12G - 130	-21,74	PF 14B - 132	-21,54	PF 21 - 132	-24,87
		PF3 107	-22,80	PF3 107	-22,80					PF 12G - 131	-20,44	PF 14B - 133	-21,84	PF 21 - 133	-24,82
		PF3 108	-22,57	PF3 108	-22,57					PF 12G - 132	-20,28	PF 14B - 134	-22,71	No sample	
		PF3 109	-23,12	PF3 109	-23,12					PF 12G - 133	-20,46	PF 14B - 135	-22,28	PF 21 - 135	-24,22
		PF3 110	-23,21	PF3 110	-23,21					PF 12G - 134	-20,92	PF 14B - 136	-20,67	PF 21 - 136	-23,77
		PF3 111	-22,46	PF3 111	-22,46					PF 12G - 135	-20,57	PF 14B - 137	-21,37	PF 21 - 137	-23,91
		PF3 112	-23,29	PF3 112	-23,29					PF 12G - 136	-20,47	PF 14B - 138	-21,32	PF 21 - 138	-24,08
		PF3 113	-23,36	PF3 113	-23,36					PF 12G - 137	-21,10	PF 14B - 139	-21,20	PF 21 - 144	-24,32
		PF3 114	-24,25	PF3 114	-24,25					PF 12G - 138	-20,94	PF 14B - 140	-20,82		
										PF 12G - 139	-21,19	PF 14B - 141	-21,00		
										PF 12G - 140	-19,74	PF 14B - 142	-21,82		
										PF 12G - 141	-20,97	PF 14B - 143	-20,84		
										PF 12G - 142	-20,49	PF 14B - 144	-21,91		
										PF 12G - 143	-20,35	PF 14B - 145	-23,38		
										PF 12G - 144	-20,24	PF 14B - 146	-22,61		
										PF 12G - 145	-20,95	PF 14B - 147	-22,89		
										PF 12G - 146	-19,88	PF 14B - 148	-22,59		
										No sample		PF 14B - 149	-23,22		
										PF 12G - 148	-20,28	PF 14B - 150	-22,61		
										PF 12G - 149	-20,29	PF 14B - 151	-22,81		
										PF 12G - 150	-19,62	PF 14B - 152	-22,22		
										PF 12G - 151	-20,03	PF 14B - 153	-21,98		

										PF 12G - 152	-20,02	PF 14B - 154	-23,12		
										PF 12G - 153	-21,27	PF 14B - 155	-22,52		
										PF 12G - 154	-21,76	PF 14B - 156	-22,47		
										PF 12G - 155	-20,43	PF 14B - 157	-22,30		
										PF 12G - 156	-21,19	PF 14B - 158	-23,01		
										PF 12G - 157	-20,82	PF 14B - 159	-21,78		
										PF 12G - 158	-20,70	PF 14B - 160	-21,81		
										PF 12G - 159	-20,74	PF 14B - 161	-23,06		
												PF 14B - 162	-22,35		
												PF 14B - 163	-22,37		
												PF 14B - 164	-22,74		
												PF 14B - 165	-22,18		
												PF 14B - 166	-23,79		
												PF 14B - 167	-23,33		
												PF 14B - 168	-22,80		
												PF 14B - 169	-23,10		
												PF 14B - 170	-23,24		
												PF 14B - 171	-21,85		
												PF 14B - 172	-24,27		
												PF 14B - 173	-24,47		
												PF 14B - 174	-23,82		
												PF 14B - 175	-23,83		
												PF 14B - 176	-24,31		
												PF 14B - 177	-25,33		
												PF 14B - 178	-25,27		
												PF 14B - 179	-24,99		
												PF 14B - 180	-24,75		
												PF 14B - 181	-24,37		
												No sample			
												PF 14B - 183	-25,14		
												PF 14B - 184	-24,16		

												PF 14B - 185	-24,08		
												PF 14B - 186	-24,49		
												PF 14B - 187	-24,60		
												PF 14B - 88	-25,54		
												PF 14B - 189	-25,16		
												PF 14B - 190	-23,86		
												PF 14B - 191	-25,12		
												No sample			
												PF 14B - 193?	-23,75		
												PF 14B - 194	-24,16		
												PF 14B - 195	-24,48		
												No sample			
												PF 14B - 197	-23,99		
												PF 14B - 198	-24,04		
												PF 14B - 199	-23,47		
												PF 14B - 200	-23,79		
												PF 14B - 201	-24,34		
												PF 14B - 202	-24,14		
												PF 14B - 203	-24,42		
												PF 14B - 204	-24,24		
												PF 14B - 205	-24,19		
												PF 14B - 206	-24,54		
												PF 14B - 207	-24,16		
												PF 14B - 208	-23,99		
												PF 14B - 209	-21,44		